

NRC Publications Archive Archives des publications du CNRC

Measurements of the sound insulation of a wood frame house exposed to aircraft noise

Bradley, J. S.; Lay, K.; Norcross, S. G.

For the publisher's version, please access the DOI link below. / Pour consulter la version de l'éditeur, utilisez le lien DOI ci-dessous.

Publisher's version / Version de l'éditeur:

<https://doi.org/10.4224/20386147>

Internal Report (National Research Council of Canada. Institute for Research in Construction), 2002-03-01

NRC Publications Archive Record / Notice des Archives des publications du CNRC :

<https://nrc-publications.canada.ca/eng/view/object/?id=0457f1a7-6c4b-49f2-b14f-fa8f822a4568>

<https://publications-cnrc.canada.ca/fra/voir/objet/?id=0457f1a7-6c4b-49f2-b14f-fa8f822a4568>

Access and use of this website and the material on it are subject to the Terms and Conditions set forth at

<https://nrc-publications.canada.ca/eng/copyright>

READ THESE TERMS AND CONDITIONS CAREFULLY BEFORE USING THIS WEBSITE.

L'accès à ce site Web et l'utilisation de son contenu sont assujettis aux conditions présentées dans le site

<https://publications-cnrc.canada.ca/fra/droits>

LISEZ CES CONDITIONS ATTENTIVEMENT AVANT D'UTILISER CE SITE WEB.

Questions? Contact the NRC Publications Archive team at

PublicationsArchive-ArchivesPublications@nrc-cnrc.gc.ca. If you wish to email the authors directly, please see the first page of the publication for their contact information.

Vous avez des questions? Nous pouvons vous aider. Pour communiquer directement avec un auteur, consultez la première page de la revue dans laquelle son article a été publié afin de trouver ses coordonnées. Si vous n'arrivez pas à les repérer, communiquez avec nous à PublicationsArchive-ArchivesPublications@nrc-cnrc.gc.ca.



National Research
Council Canada

Conseil national
de recherches Canada

NRC - CNRC

Measurements of the Sound Insulation of a Wood Frame House Exposed to Aircraft Noise

Bradley, J.S.; Lay, K.; Norcross, S.G.

IRC IR-831

www.nrc.ca/irc/ircpubs

Measurements of the Sound Insulation of a Wood Frame House Exposed to Aircraft Noise

J.S. Bradley, K. Lay and S.G. Norcross

IRC Internal Report, IRC IR-831

November 2001 (revised February 2002)

Acknowledgements

Primary financial support for the IBANA project was provided by Transport Canada, the Department of National Defence and the National Research Council. Additional funding has been received from Vancouver International Airport Authority. The helpful cooperation of the staff at Ottawa, Toronto and Vancouver airports in making arrangements for the various field measurements was very much appreciated.

Disclaimer

The contents of this report are the results of tests and analyses carried out by the acoustics laboratory of the Institute for Research in Construction at the National Research Council of Canada. While they are thought to be the best interpretation of the available data, other interpretations are possible and these results may not reflect the policies of either Transport Canada or the Department of National Defence.

Summary

This report compares measurements of the sound insulation of various constructions of a test house, exposed to aircraft noise at Ottawa Airport, with predictions from laboratory measurements of the same constructions. Further analyses investigated the major sources of the differences between laboratory and field measurements and corrections were developed for the IBANA-Calc sound insulation software. Source spectrum shapes for modern aircraft types were also developed for this software.

The Ottawa Airport Test Structure (OATS) was a simple wood frame structure, representative of typical Canadian construction techniques, with two main rooms exposed to the noise from passing aircraft. The construction was systematically changed to include differences in wall and ceiling constructions, the addition of windows, and also the addition of various vents. In some tests, additional masking walls were added inside each room to simplify the situation so that sound transmission was predominantly through one of the outside walls. For each construction, the noise of departing aircraft was recorded outside in the free field and at the building façade as well as inside at 3 positions in each of the 2 test rooms.

Main Comparisons

There were 3 groups of comparisons of overall sound insulation measurements. The first group considered cases for sound transmission through only one or two simple walls of the test house. The second group included walls with windows and the third group included constructions with various vents.

(1) Walls

For these 4 constructions, the overall A-weighted Noise Reduction (NR) was predicted with a mean error of -6.4 dBA (varying from -8.7 to -4.3 dBA). When additional corrections were added to account for ground reflected sound and for structural flanking paths, the mean error was reduced to -3.1 dBA (varying from -5.4 to -1.1 dBA). Measured NR values were greater (better) than predicted values. Differences in sound transmission at the primary structural resonance, and the reduced incident sound on the approach side of the building were the major causes of the remaining prediction errors.

(2) Windows

The cases with windows were more accurately predicted because indoor transmitted sound levels were dominated by mid-frequency sound and hence less influenced by the complicating effects of low frequency ground reflections and low frequency aircraft directionality. The overall A-weighted NR values for the window cases were predicted with an average error of only 0.5 dBA (varying from -2.4 to +1.6 dBA). Significant differences in NR at the mass-air-mass resonance of the window occurred with variations in orientation of the façade relative to the aircraft flight path.

(3) Vents

Roof vents, ridge vents, and soffit vents usually had quite small effects while through-the-wall vents had quite large effects on measured sound insulation. Laboratory tests of the roof and ridge vents showed less effect on sound insulation when there was adequate fibrous insulation in the attic space, when there was a double layer of gypsum board, and

when there were a smaller number of roof vents. For numbers of vents likely to be installed in houses and with R40 fibrous insulation in the attic space, the effect of roof vents is about a 1 dBA reduction in the overall A-weighted NR value.

Tests of through-the-wall vents, that connected the outside directly to indoor spaces, led to 8 and 9 dBA reductions in the overall A-weighted NR values. At mid-frequencies, they had an effective transmission loss of 0 dBA. Such vents should include acoustical treatment and if possible be located on the quiet side of the building.

Investigations of Differences between Laboratory and Field Results

Ground reflected sound decreased incident low frequency sound levels by up to 8 dB. Calculations, using simulated aircraft flybys, indicated that this effect would vary with the height and distance of the aircraft from the building façade and that the effects would be insignificant for receivers above the ground floor level.

Façade orientation affects sound insulation because it influences the angular view of the complete flyby and because sound transmission varies with the angle of incidence of the sound. Attempts to quantify these effects may be practically adequate but were less precise than desired because results were complicated by unexpectedly large effects of ground reflections, aircraft directionality, and structural flanking paths.

Measurements of the effect of the vertical angle of the aircraft led to the expected small variations in measured NR values within the limits of the accuracy of the measurements.

Flanking paths in the wood frame building had large effects at higher frequencies but they did not result in large effects on the overall A-weighted indoor sound levels. They were assumed to be structural flanking paths and were seen to effectively bypass any benefits from using resilient channels to mount the gypsum board on the walls of the test house.

Measurements of incident sound levels using façade mounted microphones, as recommended in various standards, were found to produce large errors of up to 12 dB. Incident sound levels measured at the building façade are strongly influenced by ground reflections and diffraction effects that vary with the vertical angle of the aircraft.

New average spectrum shapes were derived for 4 aircraft categories. Because helicopter noise measurements were not possible, a helicopter spectrum shape was derived from published FAA data. The FAA data is based on single point maximum levels, which underestimate the actual low frequency sound produced over a complete aircraft passby. The other new spectrum shapes were derived from measurements at Ottawa, Toronto and Vancouver airports. Use of inappropriate older spectrum shapes was demonstrated to produce errors of up to 10 dB in calculated NR values.

Corrections to the source spectrum shapes to account for air absorption can further adjust these new spectrum shapes. Other corrections for the effects of ground reflections, façade orientation and vertical angle of the aircraft were derived to improve the calculation of building sound insulation in the IBANA-Calc software.

Table of Contents

	page
Acknowledgements	1
Summary	2
Table of Contents	4
1. Introduction	5
2. Ottawa Airport Test Structure and Measurement Procedures	7
2.1 OATS - The Ottawa Airport Test Structure	7
2.2 Experimental Plan	8
2.3 Measurement Procedures	14
2.4 Data Analysis	16
2.5 Calculations	16
3. Average Measured Noise Reductions for Each Configuration	18
3.1 Wall Configurations	18
3.1.1 Comparisons with Simple Predictions	18
3.1.2 Ground Reflection and Flanking Path Effects	25
3.2 Walls with Windows	31
3.3 Vents	40
3.3.1 Roof, Ridge and Soffit Vents	40
3.3.2 Wall Vents	44
4 Angle of Incidence Effects	53
4.1 Loudspeaker Source Tests	53
4.2 Variation of Façade Effects	56
4.3 Variation of Noise Reductions	64
5 Façade Orientation Effects	70
5.1 The Problem	70
5.2 The Proposed Approach and Complications	71
5.3 Measurement Results	72
6 Aircraft Source Spectra	78
6.1 Average Measured Spectra	78
6.2 Air Absorption and Distance Corrections	79
6.3 Helicopter Source Spectra	81
6.4 Comparisons of New Average Spectra with Other Spectra	82
7 Sound Insulation Calculations for IBANA-Calc	86
7.1 Basic Sound Insulation Calculations	86
7.2 NEF to Leq24 Conversions	86
7.3 Corrections to Field Conditions	87
8. Conclusions	91
8.1 The Main Comparisons	91
8.2 Exploration of Details	92
8.3 Future Research	93
References	95
Appendix I. Measured Average NR for Each Configuration	97
Appendix II. The Effect of Aircraft Directionality on Sound Insulation Measurements	99
Appendix III. Interference between Direct and Ground Reflected Aircraft Noise	107

1. Introduction

This report gives the results of an extensive series of sound insulation measurements in a test house built at Ottawa International Airport. Measured noise reductions were obtained for various modifications of the construction of the test house using actual aircraft noise as the test signal. The measured noise reductions were compared with calculated noise reductions based on previous laboratory measurements of the sound transmission loss of the same façade components such as walls and roofs [1].

The purpose of this work was to better understand the differences between laboratory measurements of sound insulation and the effective sound insulation of the same constructions when part of a complete building exposed to actual aircraft flybys.

There are many differences between conditions for laboratory tests and those for real buildings exposed to aircraft noise. Standard laboratory tests of the sound insulation of façade elements such as walls, windows, or roof-ceilings are carried out by building the test specimen between two reverberation chambers [2,3]. These reverberant test chambers are designed so that sound is incident on the test specimen equally from all directions and so that all other sound paths other than directly through the specimen are insignificant.

In the field, sound from an aircraft is incident on a particular building façade from a limited range of angles and the façade will be at a particular angle relative to the flight path. Aircraft are directional sound sources and do not radiate sound equally in all directions. This variation of incident aircraft noise with direction from the aircraft is further complicated by the variation of the sound level with distance to the aircraft as it flies by a building. Although the aircraft noise will travel directly from the aircraft to the building, in some cases a significant amount of sound energy may be incident on the building after reflecting from the ground or other large surfaces. We know that theory predicts that the transmission loss of simple limp panels varies with the angle of incidence of the sound. However, it is not clear how transmission loss varies with angle of incidence for the more complex constructions found in building façades.

In actual buildings there are also a number of other sound paths that are deliberately eliminated in the standard laboratory tests. There are structural flanking paths whereby sound propagates through the building structure from one exterior surface to a non-adjacent interior surface. There are several types of roof and soffit vents that are required to prevent moisture accumulation in attic spaces but which may act as effective sound paths. Similarly there are various other vents that penetrate the building façade and hence potentially modify the total sound insulation.

This work attempted to determine the importance of these various differences between laboratory and field conditions and to develop improved procedures for calculating the expected sound insulation of buildings exposed to aircraft noise. Noise reductions were measured in the two rooms of the test house for a systematic series of construction changes. In the initial tests sound was constrained to predominantly enter the test house by a single wall by adding masking walls in front of the other exposed walls. The façade constructions were identical to walls included in previous laboratory tests. The modifications systematically increased the complexity of the measured system and eventually included windows and various vents.

This work is a major component of the IBANA project (Insulating Buildings Against Noise from Aircraft). The complete IBANA project included both laboratory and field measurements of building façade sound insulation as well as the creation of computer software to permit the convenient use of these data to design the exterior sound insulation of buildings against aircraft noise.

The IBANA project is a result of an earlier comprehensive review of the NEF aircraft noise measure and various aspects of predicting aircraft noise and its effects in Canada [4-6]. One of the conclusions of that review was that improved building sound insulation was a key remedial measure for minimising the impact of aircraft noise. It was further concluded that, in Canada, available technical information and guidelines [7] for achieving improved sound insulation were out of date and in need of a new approach. A more specific review of current knowledge of building façade sound insulation issues was also completed [8]. This study found, that although the basic principles were generally well understood, there was almost no available data representative of the sound insulation of modern Canadian building constructions. Further, there was only a rough understanding of the relationship between laboratory and field sound insulation data, and existing Canadian guidelines were based on aircraft noise spectra that are not representative of modern aircraft types.

The IBANA project includes the following key components:

- Laboratory measurements of the sound insulation of various building façade components including various wall and roof constructions as well as windows and the effects of vents [1].
- Field measurements of the sound insulation of various configurations of a simple wood frame test house at Ottawa Airport.
- Development of procedures for conversion between laboratory and field measurements of sound insulation.
- Development of software to enable the more accurate and convenient design of the required sound insulation for buildings exposed to aircraft noise.
- Field validation of the new design procedure.

This report first presents the principal noise reduction measurement results and then the various analyses to consider particular effects in more detail. Chapter 2 describes the experimental design and measurement and analysis procedures. The third chapter compares the average measured noise reductions with noise reductions predicted from laboratory results. Chapters 4 and 5 consider vertical and horizontal angle of incidence effects respectively. Chapter 6 describes the development of standard source spectrum shapes for modern aircraft types and Chapter 7 discusses the corrections to laboratory measurements of sound transmission loss that can be included in the calculations of the IBANA-Calc software. There are also several appendices that include the results of more extensive calculations on particular topics.

2. Ottawa Airport Test Structure and Measurement Procedures

2.1 OATS - The Ottawa Airport Test Structure

The Ottawa Airport Test Structure (OATS) was intended to be the simplest wood frame structure that would be representative of modern Canadian home construction. The structure had two main rooms facing the passing aircraft and a small storage area on the side away from the aircraft. Figure 1 includes a plan of the structure and a sketch of its external appearance. The plan includes masking walls that were added to further block the direct sound propagation through one of the two exterior walls for each room. These were added and removed as part of the experimental changes described below.

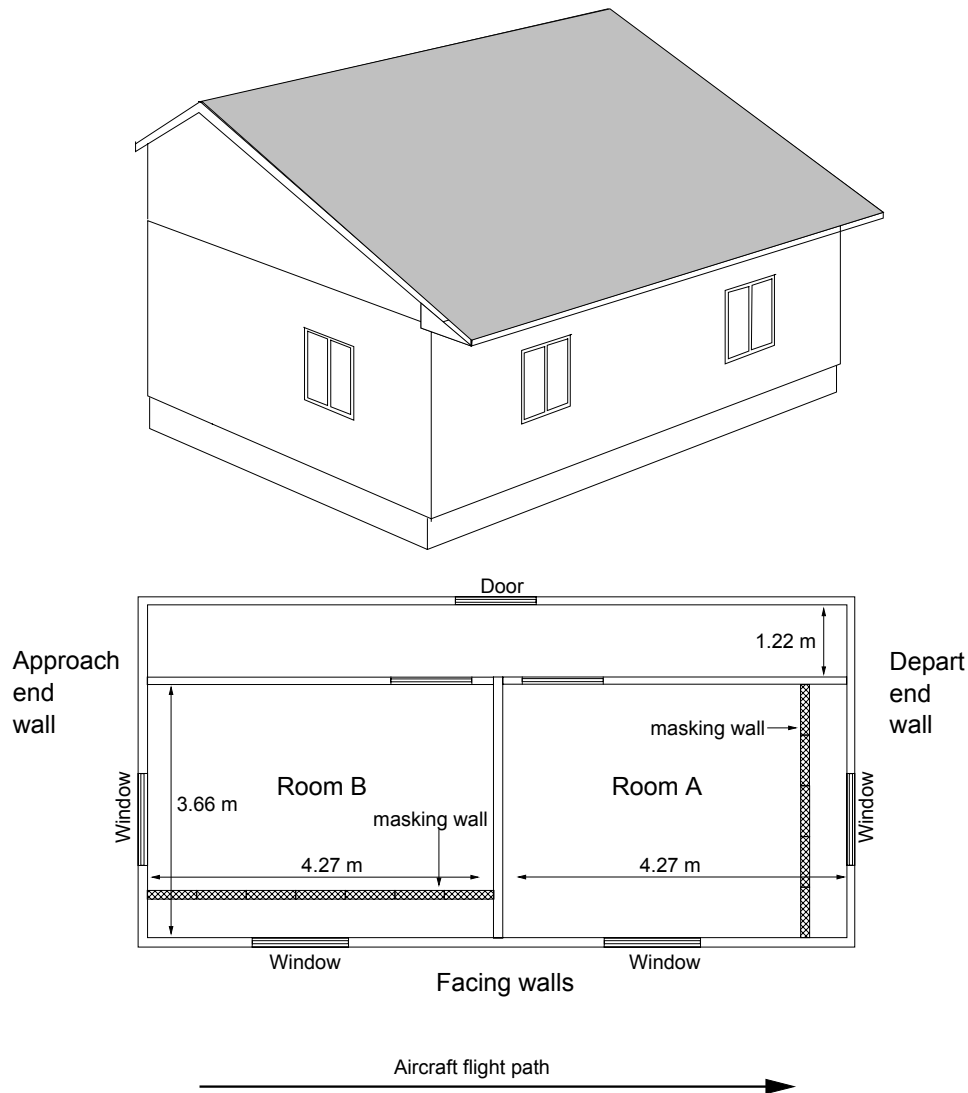


Figure 1. Sketch and floor plan of the OATS.

Many of the construction details were not varied during the tests. The floor was constructed of 16 mm plywood on wood I-joists. These were supported by a concrete block foundation. The walls were constructed of 140 mm wood studs (2 by 6) spaced at

406 mm (16 inches). There was vinyl siding on the exterior 11 mm OSB sheathing and the wall cavity was filled with glass fibre thermal insulation.

The interior surfaces of the two exterior walls in each room were initially a single layer of regular 13 mm gypsum board directly attached to the studs. The surfaces on the interior walls (i.e. between rooms) were always a double layer of gypsum board mounted on resilient channels to minimize sound propagation between the internal spaces. During the series of tests, the interior surfaces of the exterior walls were changed from a single layer of gypsum board attached directly to the studs, to a double layer attached via resilient channels.

The roof was constructed using wood trusses and with asphalt shingles on 11 mm OSB sheathing. There was 264 mm of glass fibre insulation (R40) in the attic space. During the initial tests the ceiling consisted of a double layer of regular 13 mm gypsum board attached via resilient channels. Later in the test series this was changed to a single layer of gypsum board directly attached to the roof framing. Other changes to the structure included the addition of various vents and the addition of windows. The details of each construction are given in the section below.

The OATS was located close to the flight track of aircraft departing from runway 25 at Ottawa airport. Specifically, it was located 240 m from the flight track at a point 1000 m from the west end of this runway and on airport property. The main façade of the building was parallel to the length of runway 25. The average vertical angle of the aircraft taking off past the structure was 55 degrees above horizontal.

2.2 Experimental Plan

The experimental plan was to test a series of constructions that were systematically increased in complexity to finally approach that of a complete building. For the initial tests, the roof-ceiling sound insulation was increased by using a double layer of gypsum board on resilient channels for the ceiling. For these cases the dominant sound path would be through the exterior walls. To further simplify the situation, tests were performed with a masking wall constructed in front of one of the exterior walls so that the dominant sound path was reduced to that through a single exterior wall. This was intended to help identify effects related to the orientation of the façade relative to the aircraft flight path. In all tests the same conditions were created in both rooms of the test structure but differences would be expected because one was more exposed to approaching aircraft and the other was more exposed to departing aircraft. The masking wall was constructed of prefabricated panels consisting of a double layer of 13 mm gypsum board on a light weight steel stud frame and with sound absorbing material in the cavity. All joints were taped to provide an air tight seal. The masking wall was located 300 mm from the inside surface of the exterior wall of the room.

The first three test configurations consisted of: (1) only the wall facing the passing aircraft exposed, (2) only the end walls perpendicular to the flight path exposed and (3) both exterior walls of each room exposed. (There was no configuration (4)). For configuration (5), the exterior walls were changed from directly attached single gypsum board to a double layer attached via resilient channels. The ceiling was changed from a double layer attached via resilient channels to a directly attached single layer. This configuration served as a base case or reference case for the subsequent changes where windows or vents were added.

It was intended that adding double gypsum board and resilient channels to the walls would make it easier to identify changes to the transmission path thorough the roof-ceiling due to the addition of vents. For test case (6) six roof vents were added to the roof. These were the same as used in previous laboratory tests of a similar roof construction and represent approximately double the roof vent area required by the National Building Code. For test case (7) the 11 mm OSB sheathing that had been installed on the soffit of the roof overhang was replaced with perforated metal soffit vents and so the roof included both soffit and roof vents. For test case (8) the roof vents were removed and the holes sealed and a ridge vent was added along the entire length of the ridge of the roof. The ridge and soffit vents remained for all subsequent tests including those with various added windows.

Test case (9) included vents in the walls of each test room (in addition to the ridge and soffit vents). Test cases (10), (11) and (12) correspond to adding windows, first to the end walls (10), then to the facing walls (11) and finally for both walls (12). Both windows were installed in each room for all tests but sound transmission via the other window was minimized by constructing masking walls in front of them.

Two further tests were carried out on the configuration with both windows exposed and are referred to as tests (13) and (14). For test (13) additional recordings were made with microphones at each exterior façade of the building. In test (14) a loudspeaker source was used and its position was systematically varied.

Table I summarises the various configurations for each test case. The complete details of each test case are given in the various parts of Table II below.

Case	Ceiling		Walls		Facing walls		End walls		Roof vents	Soffit vents
	Gyp	RCs	Gyp	RCs	Window	Masked	Window	Masked		
1	2	yes	1	no	no	yes	no	no	No	no
2	2	yes	1	no	no	no	no	yes	No	no
3	2	yes	1	no	no	no	no	no	No	no
4										
5	1	no	2	yes	no	no	no	no	No	no
6	1	no	2	yes	no	no	no	no	roof	no
7	1	no	2	yes	no	no	no	no	roof soffit	yes
8	1	no	2	yes	no	no	no	no	ridge	yes
9	1	no	2	yes	vent	no	no	no	ridge	yes
10	1	no	2	yes	yes	yes	yes	No	ridge	yes
11	1	no	2	yes	yes	no	yes	Yes	ridge	yes
12	1	no	2	Yes	yes	no	yes	No	ridge	yes
13	1	no	2	Yes	yes	no	yes	Yes	ridge	yes
14	1	no	2	Yes	yes	no	yes	Yes	ridge	yes

Table I. Summary of details of each of the measurement cases at OATS.

Gyp = number of layers of 13 mm gypsum board

RC = resilient channels

Masked: refers to presence of masking wall.

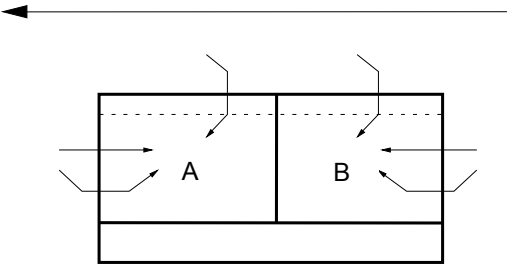
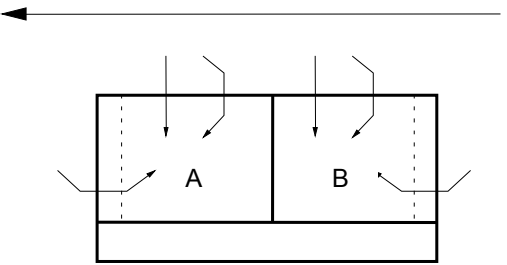
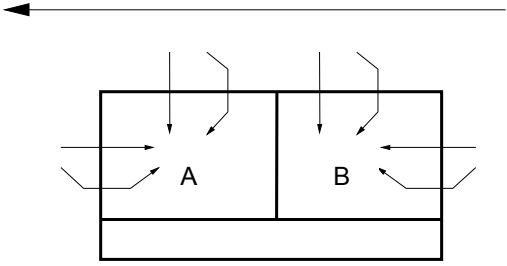
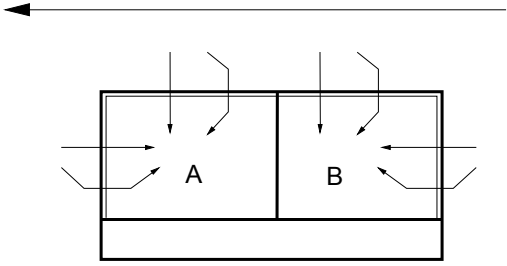
Test Case: #1	Test Case: #2
Purpose: to evaluate sound transmission via only the end walls of the test rooms.	Purpose: to evaluate sound transmission via only the facing walls of the test rooms.
	
Construction Walls: -directly attached single 13 mm gypsum board. Ceiling -double 13 mm gypsum board attached via resilient channels. Vents -none. Masking: -located in front of facing walls. (dotted lines)	Construction Walls: -directly attached single 13 mm gypsum board. Ceiling -double 13 mm gypsum board attached via resilient channels. Vents -none. Masking: -located in front of end walls. (dotted lines)
Test Case: #3	Test Case: #5
Purpose: to evaluate sound transmission via end and facing walls of the test rooms.	Purpose: base or reference case for tests with added vents and windows.
	
Construction Walls: -directly attached single 13 mm gypsum board. Ceiling -double 13 mm gypsum board attached via resilient channels. Vents -none. Masking: -none.	Construction Walls: -double 13 mm gypsum board attached via resilient channels. Ceiling: -directly attached single 13 mm gypsum board. Vents -none. Masking: -none.

Table II. Description of test cases 1, 2, 3, and 5. The long arrow indicates the direction of aircraft passing the test house. The straight arrows through a wall indicate direct transmission paths and the bent arrows indicate structural flanking paths.

Test Case: #6	Test Case: #7
Purpose: effect of added roof vents.	Purpose: effect of added roof and soffit vents.
(see Case #5 figure)	(see Case #5 figure)
Construction	Construction
Walls: -double 13 mm gypsum board attached via resilient channels.	Walls: -double 13 mm gypsum board attached via resilient channels.
Ceiling: -directly attached single 13 mm gypsum board.	Ceiling: -directly attached single 13 mm gypsum board.
Vents -6 roof vents.	Vents -6 roof vents plus soffit vents.
Masking: -none.	Masking: -none.

Test Case: #8	Test Case: #9
Purpose: effect of ridge and soffit vents.	Purpose: effect of wall vents.
(see Case #5 figure)	(see Case #5 figure)
Construction	Construction
Walls: -double 13 mm gypsum board attached via resilient channels.	Walls: -double 13 mm gypsum board attached via resilient channels.
Ceiling: -directly attached single 13 mm gypsum board.	Ceiling: -directly attached single 13 mm gypsum board.
Vents -roof ridge vent plus soffit vents.	Vents -wall vents in addition to ridge and soffit vents.
Masking: -none.	Masking: -none.

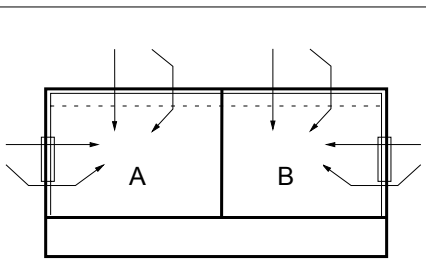
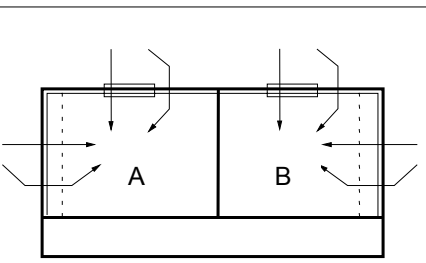
Test Case: #10	Test Case: #11
Purpose: effect of end windows.	Purpose: effect of facing windows.
	
Construction	Construction
Walls: -double 13 mm gypsum board attached via resilient channels.	Walls: -double 13 mm gypsum board attached via resilient channels.
Ceiling: -directly attached single 13 mm gypsum board.	Ceiling: -directly attached single 13 mm gypsum board.
Vents -roof ridge vent plus soffit vents.	Vents -roof ridge vent plus soffit vents.
Masking: -located in front of facing walls. (dotted lines)	Masking: -located in front of end walls. (dotted lines)

Table II. Description of test cases 6, 7, 8, 9, 10, and 11. The long arrow indicates the direction of aircraft passing the test house. The straight arrows through a wall indicate direct transmission paths and the bent arrows indicate structural flanking paths.

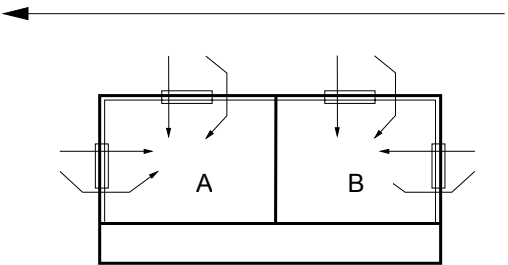
Test Case: #12	Test Case: #13
Purpose: effect of end and facing windows.	Purpose compare outdoor levels at each façade.
	(see figure for Case #12)
	Construction (same as Case #12)
Construction Walls: -double 13 mm gypsum board attached via resilient channels. Ceiling: -directly attached single 13 mm gypsum board. Vents -roof ridge vent plus soffit vents. Masking: -none.	Test Case: #14
	Purpose: measure effects of angle of incidence with loudspeaker source. (see figure for Case #12)
	Construction (same as Case #12)

Table II, Description of test cases 12, 13, and 14. The long arrow indicates the direction of aircraft passing the test house. The straight arrows through a wall indicate direct transmission paths and the bent arrows indicate structural flanking paths.

2.3 Measurement Procedures

The field measurements of noise reductions at OATS were made by simultaneously recording aircraft flybys both outdoors and indoors using a total of 8 microphones. Two microphones were outdoors and there were 3 microphones in each of the test rooms. The principal outdoor microphone was mounted on a mast 8.5 m above ground level near the test structure. It recorded the free-field incident aircraft sound levels. The second outdoor microphone was attached to the centre of the building façade facing the passing aircraft. It was approximately 1.65 m above ground level which corresponded to 1.2 m above the floor level of the test rooms. In each room the microphones were distributed to sample room positions more than 1 m from room surfaces. They were returned to the same locations for all recordings.

The outdoor microphone (on the mast) was a Bruel and Kjaer type 4921 outdoor microphone system. All of the other microphones were Bruel and Kjaer type 4190, 12 mm condenser microphones attached to Bruel and Kjaer type 4921 impedance matching preamplifiers. These 7 microphones were powered by ACO Pacifico battery powered microphone power supplies that were also used to amplify the microphone signals. Five channels of the signals were connected to the Tascam DA38 8-track digital audio tape recorder via X-Wire digital transmitters and receivers. The other three channels were directly connected by cable to the tape recorder. All of the equipment was battery powered. Figure 2 below shows a symbolic block diagram of the measurement equipment.

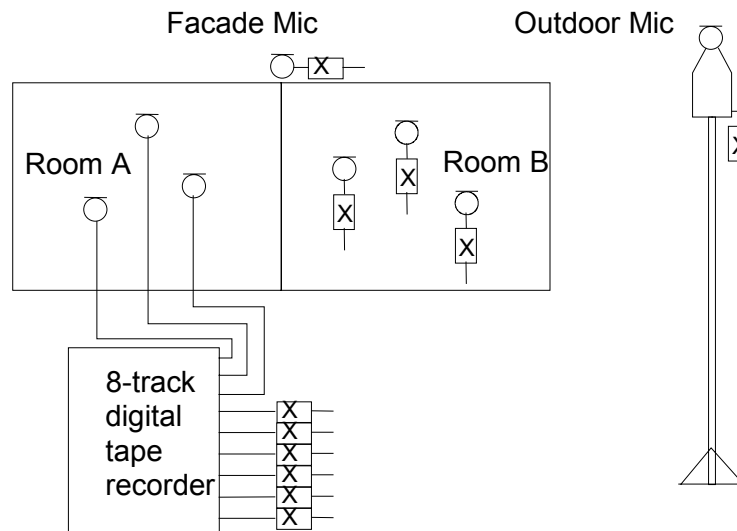


Figure 2. Block diagram of field recording system.

(X = X-Wire digital transmitter or receiver).

Continuous recordings were made to include all of the aircraft events over an approximately 2 hour period. Calibration tones were recorded on each track at both the beginning and the end of the two hour period. The operator stood outside the test house during the recordings and recorded the vertical elevation and type of each passing aircraft. The operator was able to listen to the radio communication between the airport control tower and the aircraft to warn him of imminent events and to help confirm the types of each aircraft. The picture in Figure 3 shows the operator recording the vertical

elevation of a passing aircraft. This was done by lining up the passing aircraft with markers protruding from the end of the roof from a fixed observation position. The angles of each marker as seen from the operator's position were known and hence the vertical



angles of each passing aircraft could be determined.

Figure 3. Operator recording vertical angle of passing aircraft during sound recordings.

Reverberation times were also measured in each room of the test structure on several occasions. A standard pink noise test signal was radiated into each room using large loudspeakers so that results could be obtained over the same 50 to 5000 Hz range as the aircraft noise reductions. Five decays were recorded at each of the 3 microphone positions in each room. A Norwegian Electronics type 830 1/3 octave band real time analyzer was used to determine the reverberation times over the first 15 dB of each decay. Values were averaged over data from all 3 microphone positions and from both rooms. Although the low frequency decays were extremely irregular these estimates are thought to be adequate for use in the noise reduction calculations.

2.4 Data Analysis

The first step in processing the recordings was to listen to them and identify significantly loud aircraft events that were not contaminated with other types of noise. When the acceptable events had been located on the tape, it was processed to give 1/3 octave band spectra at 0.1 s intervals for each of the 8 microphone signals and for a total of 30 s for each aircraft event. This was done by computer controlled playback of the tapes, 2 channels at a time, into a Bruel and Kjaer type 2144 real time analyser. The resulting mulit-spectra for each of the 8 tracks were stored in a single spreadsheet file and included all 1/3 octave bands from 50 to 5000 Hz.

Further processing was done using computer spreadsheet software. The results for the 3 microphones in each room were first averaged to get a single room average result. The data was reduced to 1 s time intervals by summing the values at 0.1 s time increments over each 1 s period. The data was further reduced by summing the levels in each band that were within 10 dB of the maximum to calculate Sound Exposure Levels (SEL) in each frequency band and for each microphone location. That is, SEL spectra were obtained for the Outdoor microphone recording, the Façade microphone recording, and for the averages of the microphone recordings in each room. The difference between the outdoor and indoor spectra were used to determine the noise reductions of the particular construction for each aircraft event. These final SEL spectra were saved with information giving the aircraft type and the vertical angle of the particular flyby.

2.5 Calculations

Most comparisons are made in terms of noise reductions between the outdoor (free field) microphone results and the average indoor levels in each room. As described above, for each room an energy average of the recordings at the 3 microphones was first performed to obtain a room average result. The differences between the outdoor microphone levels and the room average indoor levels in 1/3 octave bands gives the noise reductions for a particular aircraft event. Average noise reduction (NR) spectra were then determined by an energy average of all recorded aircraft events for each construction.

Simple calculations were made to estimate these noise reductions from the laboratory measurements of the sound transmission loss of the façade components. Where there was more than one component to be considered, the effective total transmission loss was determined as follows from the area-weighted sum of the transmission coefficients of each component.

$$\tau = \frac{\sum_i \tau_i S_i}{\sum_i S_i} \quad (2.1)$$

where τ_i and S_i are the transmission coefficient and area of the i th component.

The transmission coefficient τ describes the fraction of the incident sound energy that is transmitted through the construction. It is related to the sound transmission loss (TL) in decibels as follows,

$$TL = 10 \log [1/\tau], \text{ dB} \quad (2.2)$$

The sound transmission loss (TL) is related to indoor and outdoor sound levels as well as to the area of the façade element (S) and the sound absorption (A) in the receiving room. For the ideal case of plane waves incident from a particular angle θ ,

$$TL = L_1 - L_2 + 10 \log[4S \cos(\theta) / A], \text{ dB} \quad (2.3)$$

In this case L_1 is the free-field, outdoor, incident sound level and L_2 is the room average, indoor, received level. The noise reduction (NR), between the free field, outdoor, levels and the indoor room average levels, is given by $L_1 - L_2$. The angle of incidence relative to the normal to the façade is given by θ .

Between two rooms, in which there is an approximate diffuse field, and where there is an approximate average over all angles of incidence the following equation applies,

$$TL = L_1 - L_2 + 10 \log[S / A], \text{ dB} \quad (2.4)$$

In this case L_1 is the incident sound in the diffuse sound field of the source room. This can be thought of as approximately the same as averaging equation (2.3) over all θ .

In determining these equations the incident sound intensity is related to the measured sound pressure for each situation. The relationship between measured sound pressure and the incident intensity is different by a factor of 4 between the case of plane waves and that of a diffuse field. In a diffuse field, sound is incident on an object equally from all directions. Averaging over a complete aircraft flyby is not quite the same as a diffuse field in that sound can only arrive from angles within one hemisphere or less. Thus the relationship between pressure and intensity, averaged over a complete aircraft flyby, is expected to be intermediate between that for the plane wave case and that for a diffuse field.

Averaging over a complete aircraft flyby was expected to be approximately represented by an equation similar to (2.4) but where L_1 is the measured incident free field sound level. This last equation was used for all calculations because it was found to provide reasonable agreement with measurements. This is most importantly true for the simple construction cases in Section 3.1.1. In this report other possible effects such as, the influence of angle of incidence are considered later as further corrections to the simple application of equation (2.4).

3. Average Measured Noise Reductions for Each Configuration

The results and analyses in this section consider average measured noise reductions versus frequency results. That is, they are the averages over a number of aircraft events for each construction configuration of the test house. These average measured noise reductions are compared with calculated noise reductions from laboratory measurements of the same façade elements. Subsequent sections consider the results in more detail rather than just as average values.

3.1 Wall Configurations

This section considers results for Cases #1 to #5 that are for complete walls exposed to aircraft noise. The cases including windows will be presented in section 3.2 and those including vents in section 3.3. The wall results are first compared with simple predictions in section 3.1.1. Then in section 3.1.2 various corrections are introduced to improve the predictions of the field measurements.

3.1.1 Comparisons with Simple Predictions from Laboratory Measurements

Test cases 1, 2, 3, and 5 corresponding to walls without vents or windows are first considered. The average noise reductions between the outdoor (free field) microphone measurements and the average indoor levels in each room are compared with simple calculations from laboratory transmission loss measurements. Simple predictions of the expected noise reductions were made as described in section 2.5. These calculations are based on the laboratory transmission loss measurements, receiving room reverberation,

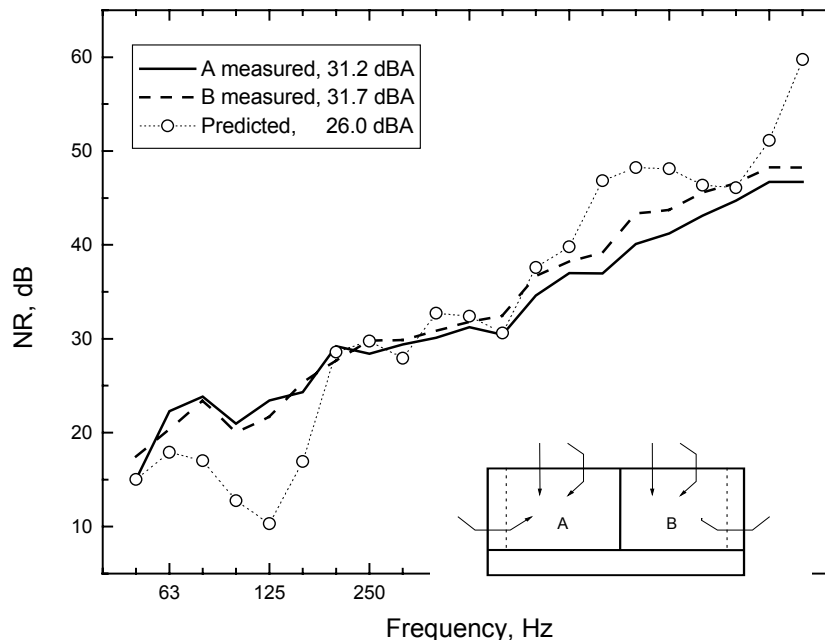


Figure 4. Comparison of measured noise reductions (NR) with simple calculations for the Case #2 results corresponding to only facing walls exposed to aircraft noise. The numbers in the legend give the overall A-weighted noise reductions. Symbolic plan at lower right illustrates configuration.

Comparison of measured and predicted noise reductions are given in Figure 4 for the Case #2 test configuration. As described in Table II of section 2.2 this corresponded to only the facing walls in each room being exposed and not masked. The exterior of the facing walls are exposed to the complete aircraft flyby making this the simplest case. The measured noise reductions for the two rooms are quite similar and the simple prediction results agree with the measurements at most frequencies. There is a small trend for NR values for room B to be larger at mid and higher frequencies. (Room B is the side of the building from which aircraft approach. See also Figure 1). The calculations predict a large reduction in the noise reduction around 125 Hz which is not observed in the measured field results. Conversely in the 1.25 kHz to 2 kHz region the predictions suggest higher noise reductions than were measured. The differences in the highest band (5 kHz) were usually related to inadequate indoor noise levels relative to the existing ambient noise levels, making accurate measurements impossible.

The overall A-weighted noise reductions are very similar for both rooms (31.2 and 31.7 dBA) and these are significantly greater than the predicted A-weighted level reduction of 26.0 dBA.

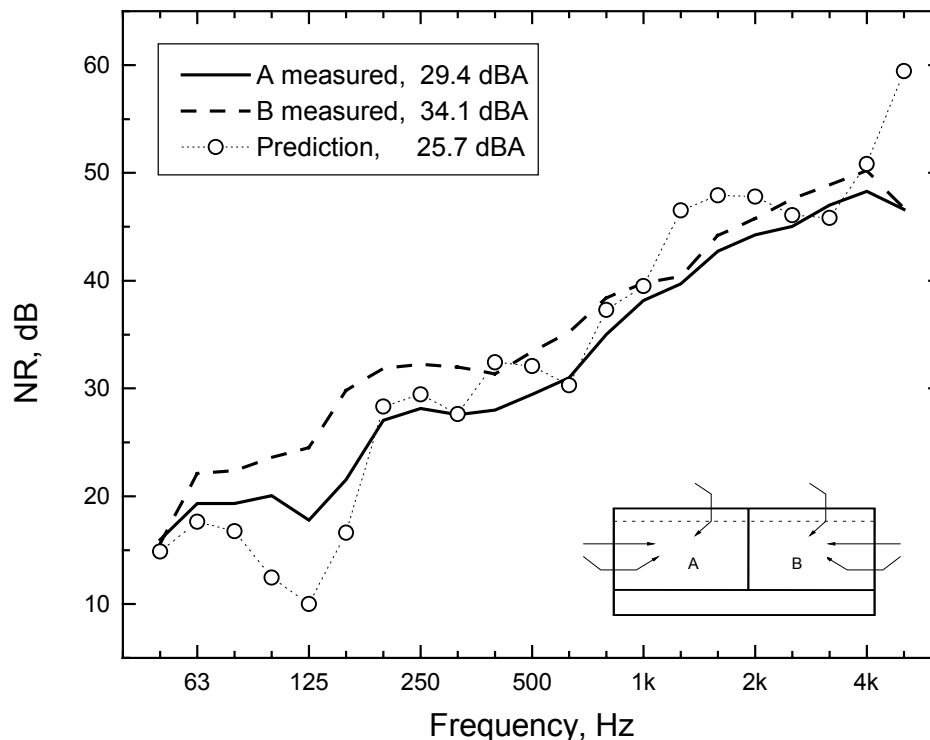


Figure 5. Comparison of measured noise reductions (NR) with simple calculations for the Case #1 results corresponding to only the end walls exposed to aircraft noise. The numbers in the legend give the overall A-weighted noise reductions. Symbolic plan at lower right illustrates configuration.

The comparison of measured noise reductions with the results of simple predictions for the Case #1 configuration are shown in Figure 5. This case corresponded to only the end walls being exposed and not masked. For these results the measured noise reductions for the two rooms are more different than the Case #2 results of Figure 4. The differences in

the peaks and dips in the 125 and 1.25 to 2k Hz regions are similar to the previous comparison illustrated in Figure 4.

In room B the end wall was exposed to the sounds of approaching aircraft and in room A, the end wall was exposed to the sounds from aircraft moving further away from the test house. Because aircraft are directional noise sources, the sound energy incident on the two ends of the building is expected to be different. For an average aircraft directivity (see Appendix II) the incident levels on the approach end of the building would be lower than on the depart end of the building. This leads to the observed differences in noise reductions for the two end walls because the same free-field outdoor levels were used to represent the incident sound energy in both cases. These free-field outdoor sound levels overestimate the sound energy incident on the approach end of the building (room B) and lead to the apparently larger noise reductions for room B.

The measured overall A-weighted level reductions for the two rooms are different (29.4 and 34.1 dBA) and both are greater than the predicted A-weighted noise reduction of 25.7 dBA.

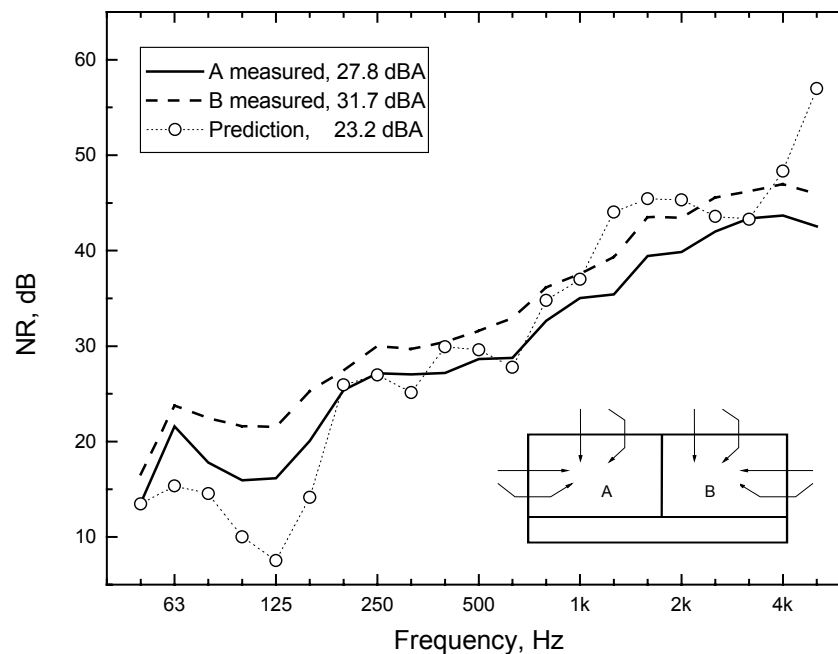


Figure 6. Comparison of measured noise reductions (NR) with simple calculations for the Case #3 results corresponding to both end and facing walls exposed to aircraft noise. The numbers in the legend give the overall A-weighted noise reductions. Symbolic plan at lower right illustrates configuration.

Figure 6 compares measured and predicted noise reductions for the Case #3 configuration for which both end and facing walls were exposed and not masked. As for the Case #1 results there are differences between the results measured in the two rooms and again the room B results indicate higher noise reductions at most frequencies. Similarly, differences are again seen around the peaks and dips of the prediction results around 125 Hz and the 1.25 to 2k Hz regions.

The overall A-weighted level reductions for the two rooms were different (27.8 and 31.7 dBA) and were greater than the predicted A-weighted noise reduction of 23.2 dBA.

The final comparison of the walls only cases is included in Figure 7 for the Case #5 results. This case was similar to the Case #3 results in that both end and facing walls were exposed and were not masked. However the construction of both the walls and the ceiling was changed relative to that of Case #3 to evaluate an improved wall construction and to create a more suitable base case for subsequent tests of the effects of windows and vents. For Case #5 the walls were changed from a single layer of directly attached 13 mm gypsum board to a double layer of gypsum board attached via resilient channels. At the same time the ceiling was changed from a double layer of 13 mm gypsum board attached with resilient channels to a directly attached single layer.

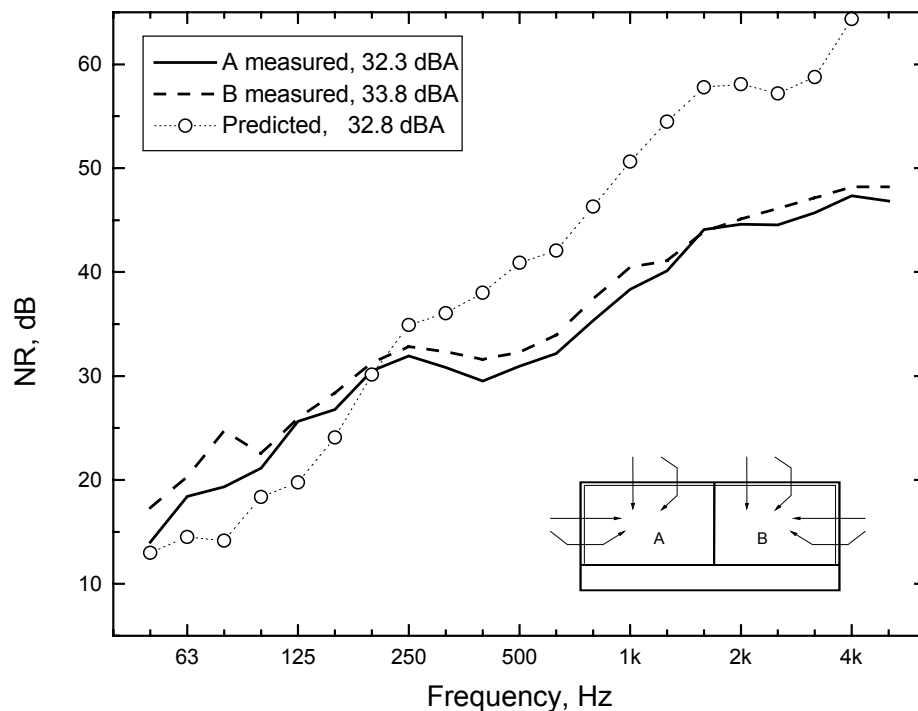


Figure 7. Comparison of measured noise reductions (NR) with simple calculations for the Case #5 results corresponding to both the end and facing walls exposed to aircraft noise. The numbers in the legend give the overall A-weighted noise reductions. Symbolic plan at lower right illustrates configuration.

The measured noise reductions in Figure 7 indicate quite similar results for both rooms but with slightly higher NR values for room B on the approach side of the building. The predictions deviate significantly from the measured noise reductions. Above 200 Hz measured noise reductions are much smaller than predicted by the simple predictions. Below 200 Hz measured noise reductions are significantly greater than predicted.

The overall A-weighted noise reductions are similar for both rooms (32.3 and 33.8 dBA) and are also very similar to the predicted result of 32.8 dBA. Thus while the simple A-weighted noise reductions suggest excellent agreement, the 1/3 octave band noise reductions indicate large differences that happen to average out when considered as only overall A-weighted levels.

The large differences between measured and predicted results in Figure 7 are quite helpful in explaining the differences in all of the plots for the walls only cases. The changes of the construction to the Case #5 configuration should have made the transmission loss characteristics of the walls and roof-ceiling similar. The laboratory measurements of the sound transmission loss of the various construction components are shown in Figure 8. These results show the similar transmission loss characteristics of the wall with a double layer of gypsum board on resilient channels and the raised heel wood truss (RHWT) roof with a single layer of directly attached gypsum board.

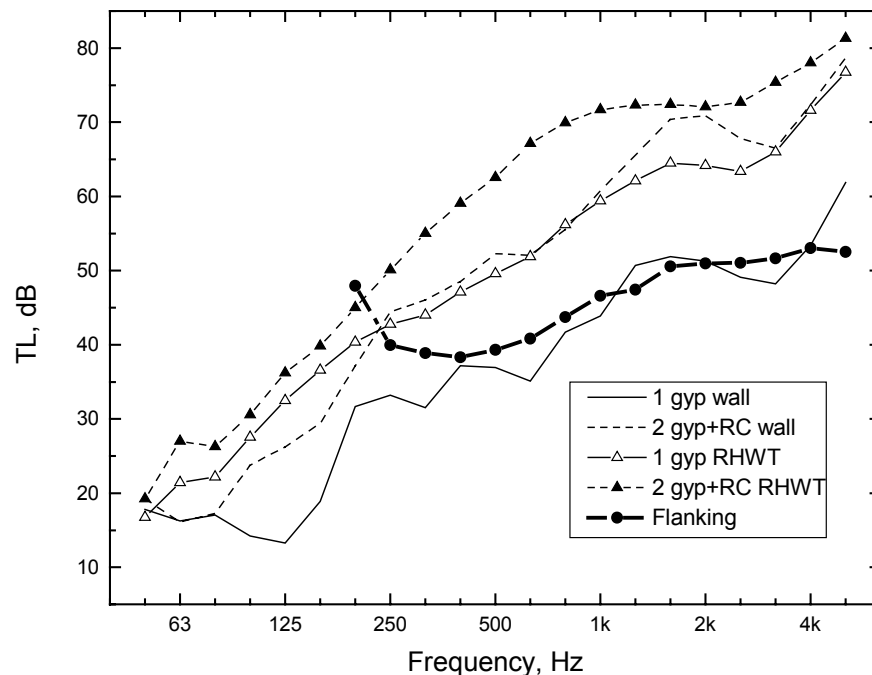


Figure 8. Comparison of the laboratory measurements of the sound transmission loss (TL) of the façade components and the effective total TL of the flanking paths.

The fact that the Case #5 results did not achieve the large increase in noise reductions that were predicted above 200 Hz is indicative of a flanking path that allowed sound energy to by-pass the direct path through the wall. Figure 9 illustrates the likely form of this flanking path. The aircraft noise incident on the external surfaces of the walls is transmitted as vibrational energy through the wall studs and floor joists to be radiated into the room from the floor surface. A similar path via the ceiling joists and radiated from the ceiling surface may also contribute to the measured indoor sound levels. The result is that changing the wall construction to a double layer of gypsum board on resilient channels for this particular construction is very ineffective and produces only very small improvements.

A similar result is seen from the laboratory measurements of staggered stud walls with and without resilient channels [8]. Without resilient channels there is a structural flanking path via the header and footer of the staggered stud wall. When resilient channels are added, this structural flanking path is eliminated. The resulting change in transmission loss is very similar to the apparent effects of flanking above 200 Hz in Figure 7.

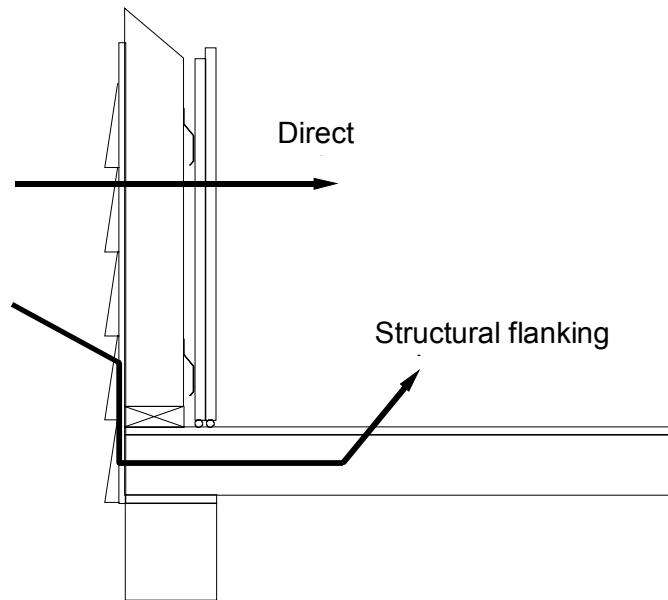


Figure 9. Cross section of the Case #5 wall and floor details illustrating direct and flanking transmission paths.

One can estimate the effective transmission loss of the flanking path (no matter what its physical cause) from the difference between the measured and predicted results in Figure 7. This was done assuming this flanking path was associated with total area of the two exterior walls for each room. The results for the two rooms were slightly different and the average of the two results is plotted in Figure 8 with the transmission loss values of the other elements. The predicted effective transmission loss of the flanking path is quite similar, at higher frequencies, to the values for the wall with a single layer of directly attached gypsum board. It was not possible to estimate the transmission loss values of the flanking path below 200 Hz because the results from Figure 7 were not reduced at lower frequencies. The effective transmission loss values of the flanking path are seen to be capable of significantly limiting the total sound insulation of the building. The flanking path also probably limits the noise reduction in the 1.25k to 2k Hz region for the Case #1, #2 and #3 results and inclusion of the flanking path in the predictions would lead to better predictions in this frequency region.

The differences between measurements and predictions in Figure 7 are reversed at lower frequencies (below 200 Hz). In this lower frequency region there are two different complex effects that combine to produce the observed differences between measurements and predictions from laboratory results. The laboratory measurements of transmission loss for the wall with a single layer of directly attached gypsum board have a pronounced dip at 125 Hz. This is due to the primary structural resonance of the ribbed panel system formed by the surface layers rigidly connected to the stud system [9]. Predictions from the laboratory measurements suggest that this would severely limit the overall noise reduction of the wall. However, the magnitude of this resonance may be sensitive to the angle of incidence of the sound. (Tests with a loudspeaker source, in section 4.1, showed that this is true for the mass-air-mass resonance of windows). Presumably the 125 Hz resonance in the walls is best excited when there is normally incident sound energy. Normal incidence is included in the laboratory tests but not in the field tests. The aircraft

noise is never normally incident and on average the aircraft passed the test house at a vertical angle of 55 degrees above horizontal. Thus the aircraft noise may not excite this resonance well and the noise reduction to aircraft noise is better than expected from the lab results. This would partly explain the large difference between measured and predicted noise reductions for the results in Figures 4, 5 and 6 for Case #1, #2 and 3 results. However, this resonance dip is not expected for the Case #5 results because when the gypsum board is mounted on resilient channels the ribbed panel system is broken up. Thus the differences between measurement and prediction for the Case #5 results are not due to the effects of angle of incidence on this primary structural resonance of the walls.

Another phenomenon is present and explains the differences at lower frequencies between measured and predicted noise reductions in the Case #5 results. The differences, after subtracting the contribution of the flanking path, are plotted in Figure 10 and are seen to peak at about 80 Hz. Calculations have demonstrated (see Appendix III) that this is consistent with the expected cancellation of the incident sound energy due to interference of direct and ground-reflected sound. Thus the measured noise reductions at low frequencies, centred around about 80 Hz, are all expected to be greater than predicted due to this modification of the total incident sound energy on the test house. The results for Cases #1, #2 and #3 include the combination of this effect and the differences in the primary structural resonance of the walls. Because the Case #5 construction does not have this resonance, the differences between measured and predicted noise reductions for this case can be totally attributed to the effect of ground reflections. (This could be confirmed by measurements at a higher floor level but unfortunately the test house only had a single floor level).

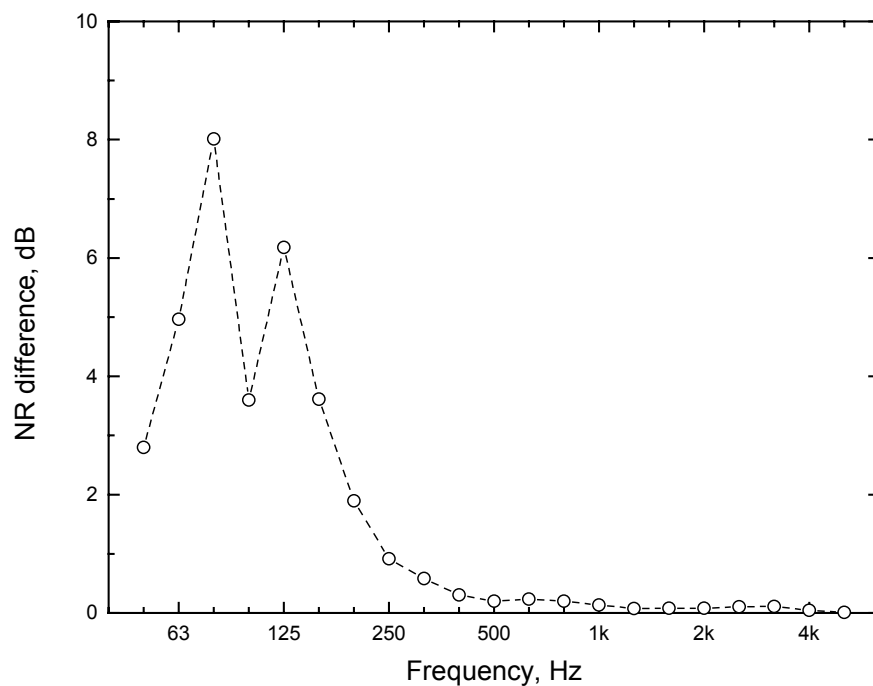


Figure 10. Differences between measured and calculated lower frequency noise reductions from the Case #5 results.

3.1.2 Ground reflection and flanking path effects.

The predictions of the expected noise reductions for Case, #1, #2, and #3 could be improved by including the additional effects of the flanking paths (above 200 Hz) and of ground reflections (below 200 Hz). This was done and the results are presented in this section. That is, the corrections were derived from the Case #5 results and are applied to the other 3 cases. The results are compared in terms of A-weighted indoor noise levels because this directly illustrates the most important components of the indoor aircraft noises. The total transmission loss (TL) including the flanking path (as described in Figure 9) was first calculated. Using the standard aircraft noise spectrum (see Chapter 6), indoor noise levels were then calculated. These were further modified by the expected decrease in incident low frequency sound levels due to the ground reflection effect illustrated in Figure 10. Finally the indoor sound levels were all A-weighted to better reflect which frequency components would seem loudest. Because the effective flanking path TL was a little different for rooms A and B, results are given separately for each room and for each configuration case.

The measured indoor levels were obtained by applying the measured noise reductions to the same standard outdoor noise spectrum levels. Thus both measured and predicted indoor levels are directly comparable levels relative to this assumed outdoor source spectrum.

Figures 11a and 11b compare the predicted and measured indoor A-weighted noise levels for the Case #2 results for rooms A and B respectively. The results in Figure 11 show that the simple predictions overestimate the indoor levels at the 125 Hz resonance peak and at lower frequencies. As also was seen in Figure 4, the simple predictions underestimate the measured indoor levels in the 1.25k to 2k Hz region. Adding the contribution of the flanking path improves the agreement between measured and predicted values above 200 Hz for these Case #2 results. The low frequency ground reflection correction (from Figure 10) improves the agreement between measured values and the improved predictions below 200 Hz. However the improved predictions do not correct for the differences at the 125 Hz resonance dip.

For both rooms, the Case #2 results are much better predicted by the improved predictions. The overall A-weighted level attenuations are improved from 26.0 for the simple predictions to 28.5 dBA for room A and to 28.9 dBA for room B. For both rooms these predictions still underestimate the measured results by just under 3 dBA. Figures 11a and 11b illustrate that this is due to the dominant differences at the 125 Hz resonance peak.

Figures 12a and 12b compared measured and predicted indoor A-weighted noise levels for the Case #1 results in which only the end walls were exposed and not masked. The overall trends are similar to the Case #2 results in the previous figures but there are also differences between the two rooms. Adding the contribution of the flanking path again improves the agreement above 200 Hz and adding the effect of the ground reflection again improves the agreement below 200 Hz. Because the differences at the 125 Hz resonance are not accounted for in the calculations, these differences are again seen in Figures 12a and 12b.

The overall A-weighted level reductions are in best agreement for room A on the side of the building where aircraft are departing from the test house where the improved prediction is only 1.1 dBA less than the measured result. However, for the room B results on the approach side of the building measured overall A-weighted levels are over-predicted by about 5 dBA. These differences in the success of the predictions for the two rooms are related to the directionality of the aircraft noise radiation. The directionality of typical aircraft (see Appendix II) indicates that they tend to radiate less sound in front than behind. The end wall of room A (depart side) is exposed to higher incident levels but for only about half of the aircraft flyby. The increased levels of the departing aircraft and the decreased angular view of the flyby, combined with the different ranges of angles of incidence, seem to somewhat average out and the resulting predictions are quite accurate. On the approach side of the building the decreased incident levels of the approaching aircraft and the decreased angular view combine to reduce the total incident energy for the room B end wall (approach side). This results in larger apparent measured noise reductions because the incident energy is taken from an integration over the complete aircraft flyby. Thus further corrections are required to account for the combined effects of the façade orientation and the directionality of the aircraft noise source.

The comparisons of measured and predicted indoor A-weighted noise levels are shown in Figures 13a and 13b for the Case #3 results. Case #3 is the same construction as Case #1 and #2 but both exterior walls of each room were exposed and not masked. The results are very similar to the Case #1 results. Adding the contribution of the flanking path and the effect of the ground reflection improves the prediction of the measured effects, but there are significant differences between the two rooms. The addition of the flanking path contribution again improved the predictions above 200 Hz and the addition of the ground reflection correction improved the agreement below 200 Hz.

The overall A-weighted reduction was predicted within 1.4 dBA for room A (depart side of the building). Due to the combined effects of the aircraft directionality and the façade orientation, the room B (approach side of the building) difference between measured and predicted overall A-weighted level reductions was about 5 dBA.

Figures 14a and 14b compare measured and predicted A-weighted noise reductions for the Case #5 configuration. These comparisons include only the measured and simple prediction results. Since the additional corrections included in the improved predictions were derived from this case they cannot be used to predict the results for this case. (They would, of course, appear to result in perfect agreement). As noted previously, the overall A-weighted level reductions were in close agreement with the measured values with differences of only 0.5 (room A) and 1 dBA (room B).

These results have explained the major differences between laboratory and field results for constructions involving walls without windows or vents. The assumed flanking path was confirmed by the improved agreement between prediction and measurements for the Case #1, #2 and #3 results when it was included in the improved predictions. Similarly, the correction for the effect of ground reflections was seen to improve predicted noise reductions for all of these measurement results. Further corrections to account for the effects of aircraft directionality and façade orientation will be considered in Chapter 6.

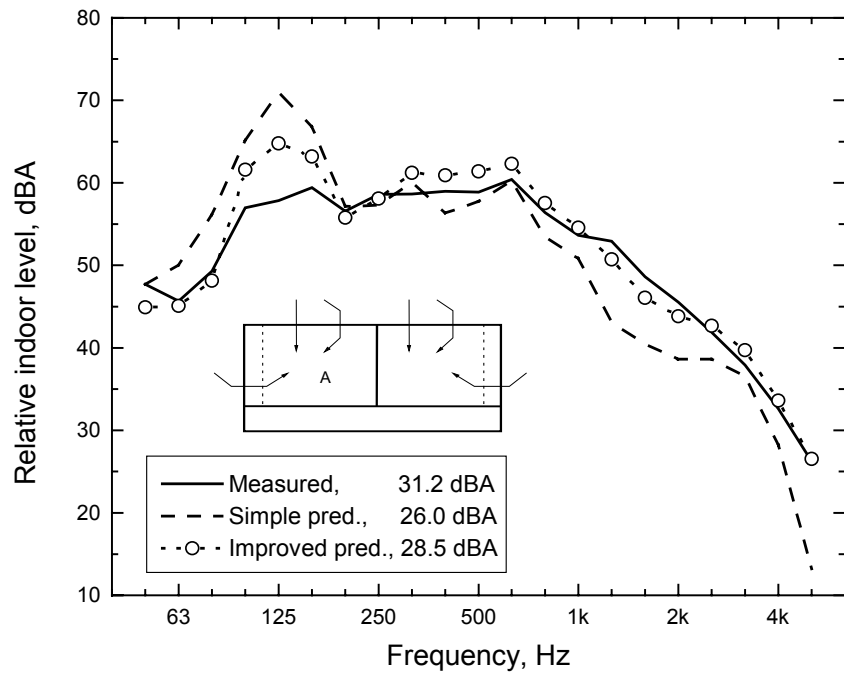


Figure 11a. Comparison of measured and predicted indoor A-weighted sound levels for Room A (depart side) Case #2 (facing walls exposed).

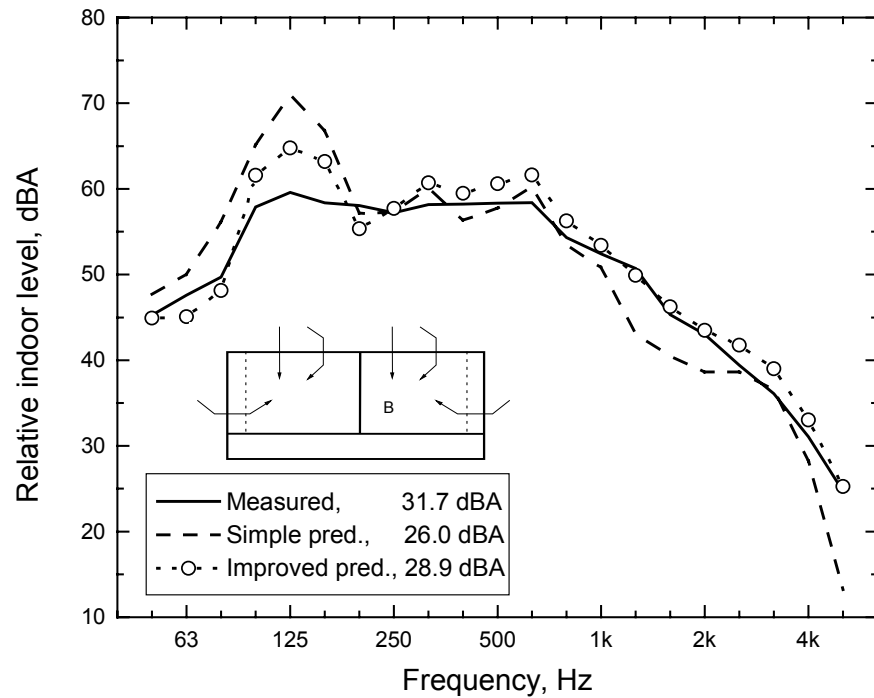


Figure 11b. Comparison of measured and predicted indoor A-weighted sound levels for Room B (approach side) Case #2 (facing walls exposed).

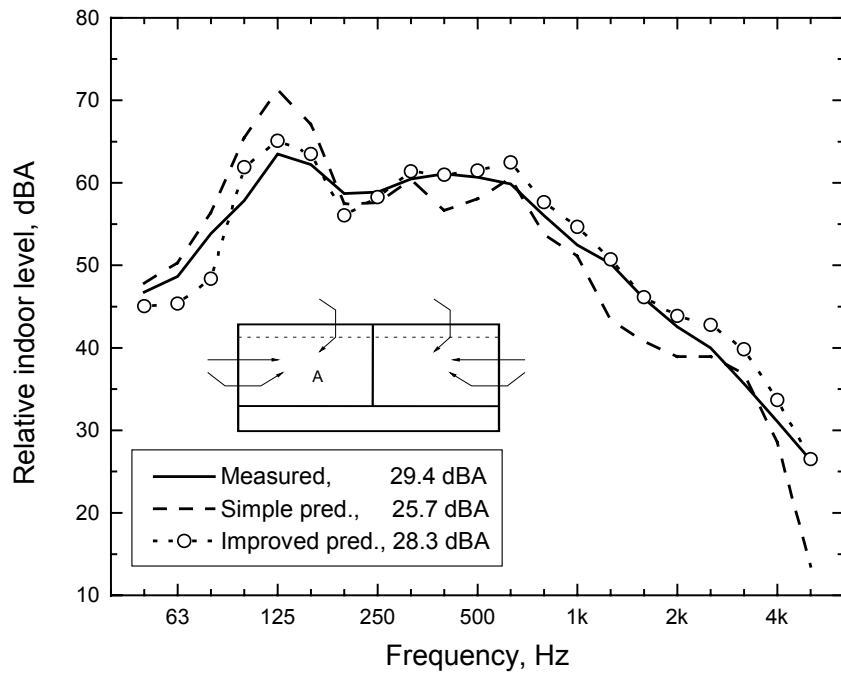


Figure 12a. Comparison of measured and predicted indoor A-weighted sound levels for Room A (depart side) Case #1 (end walls exposed).

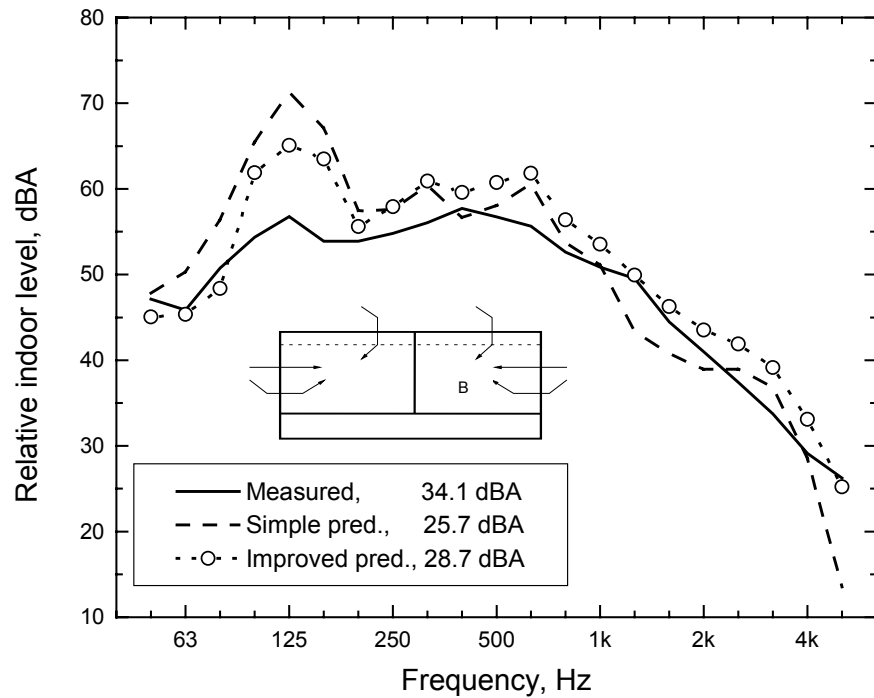


Figure 12b. Comparison of measured and predicted indoor A-weighted sound levels for Room B (approach side) Case #1 (end walls exposed).

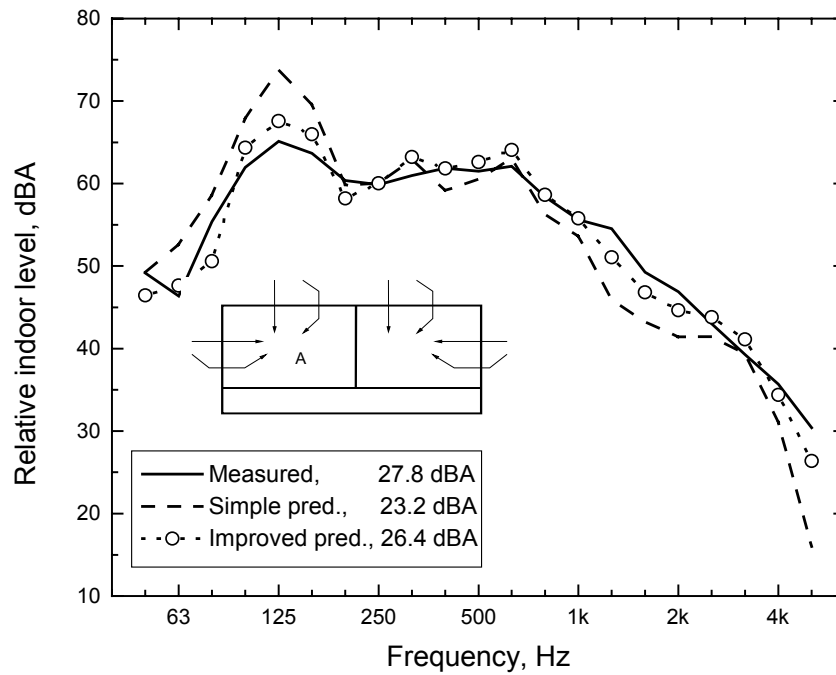


Figure 13a. Comparison of measured and predicted indoor A-weighted sound levels for Room A (depart side) Case #3 (both walls exposed).

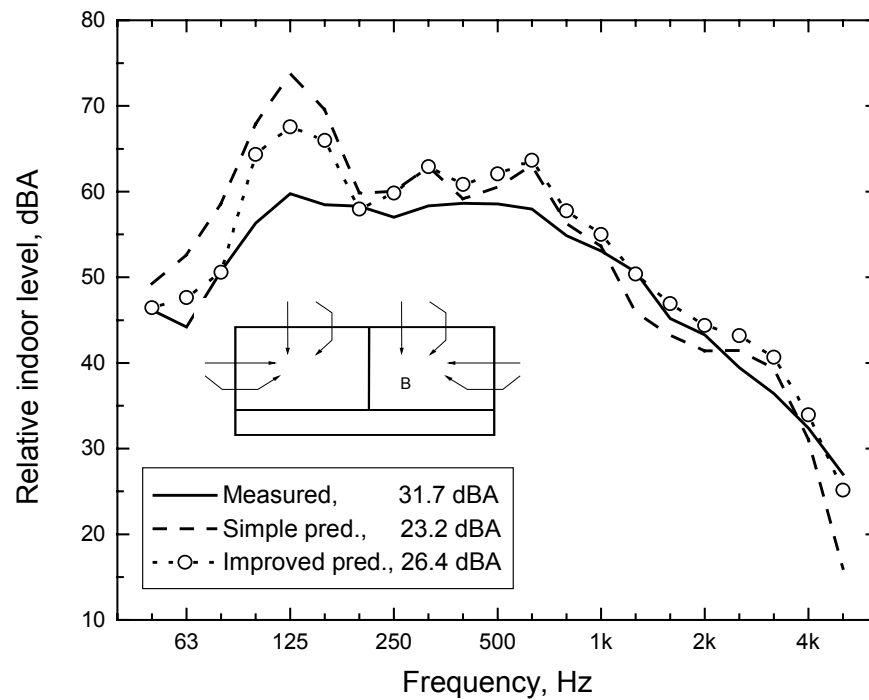


Figure 13b. Comparison of measured and predicted indoor A-weighted sound levels for Room B (approach side) Case #3 (both walls exposed).

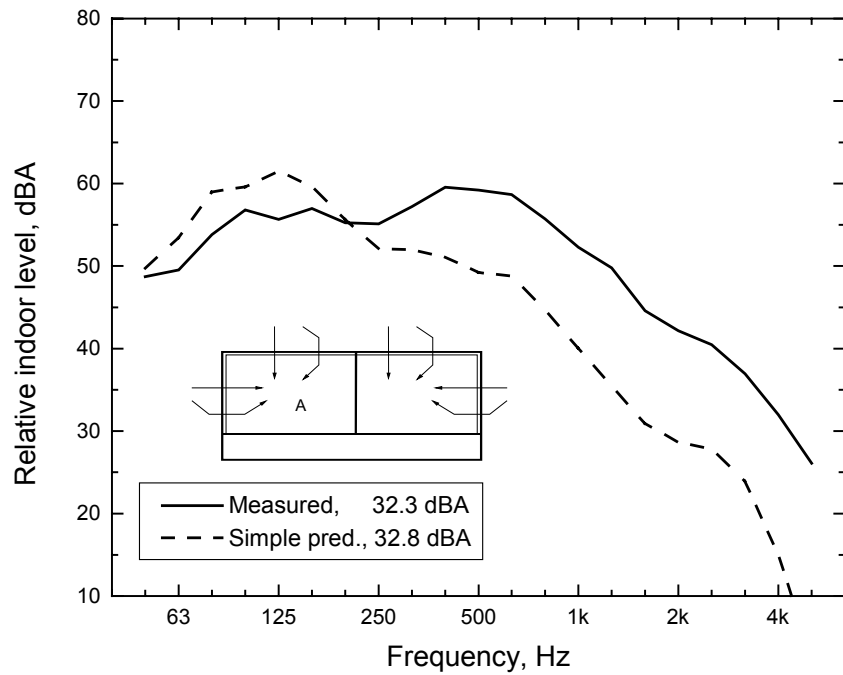


Figure 14a. Comparison of measured and predicted indoor A-weighted sound levels for Room A (depart) Case #5 (both walls exposed).

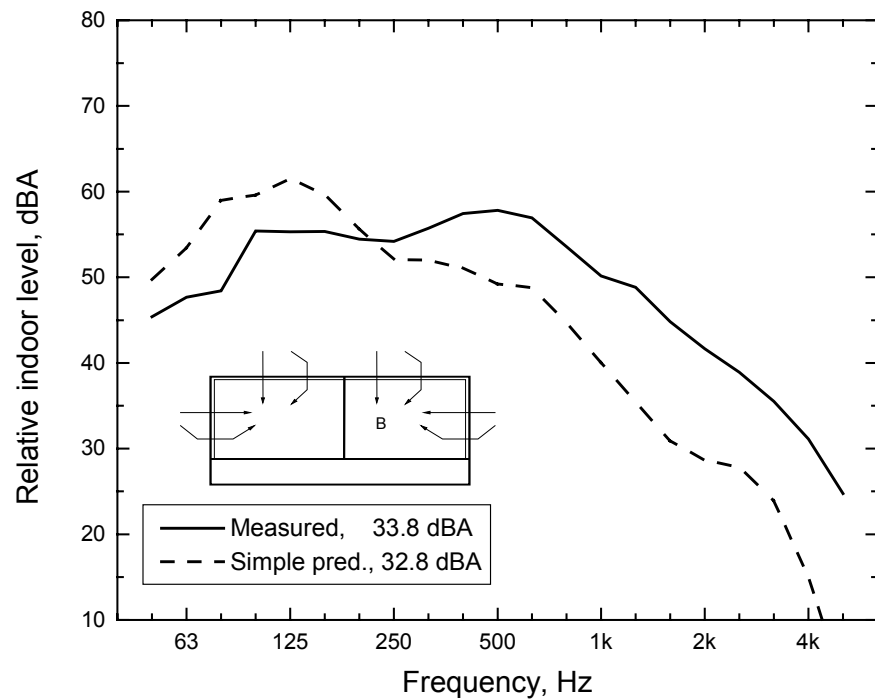


Figure 14b. Comparison of measured and predicted indoor A-weighted sound levels for Room B (approach) Case #5 (both walls exposed).

The overall A-weighted level reductions are summarised in the bar chart of Figure 15. This compares the measured values, with the results of the simple predictions and the improved predictions that included the corrections for flanking paths and ground reflections. The comparisons are given for rooms A and B and for all of the test cases for walls without vents or windows. The measured overall A-weighted level reductions vary from just below 28 dBA (Case 3, room A) to about 34 dBA (Case 1, room B). The improved predictions were always better predictors of measured values than the simple predictions. The simple predictions predicted measured values with a mean error of -6.4 dBA and varied from -8.7 to -4.3 dBA differences. The improved predictions predicted measured values with a mean error of -3.1 dBA and varied from -5.4 to -1.1 dBA. Measured reductions were almost always better than predicted and the improved predictions were about a 3 dBA improvement over the predictions of the simple predictions. The results in Figures 11 to 14 indicate that the over-prediction of the indoor levels around 125 Hz is a major cause of the remaining error.

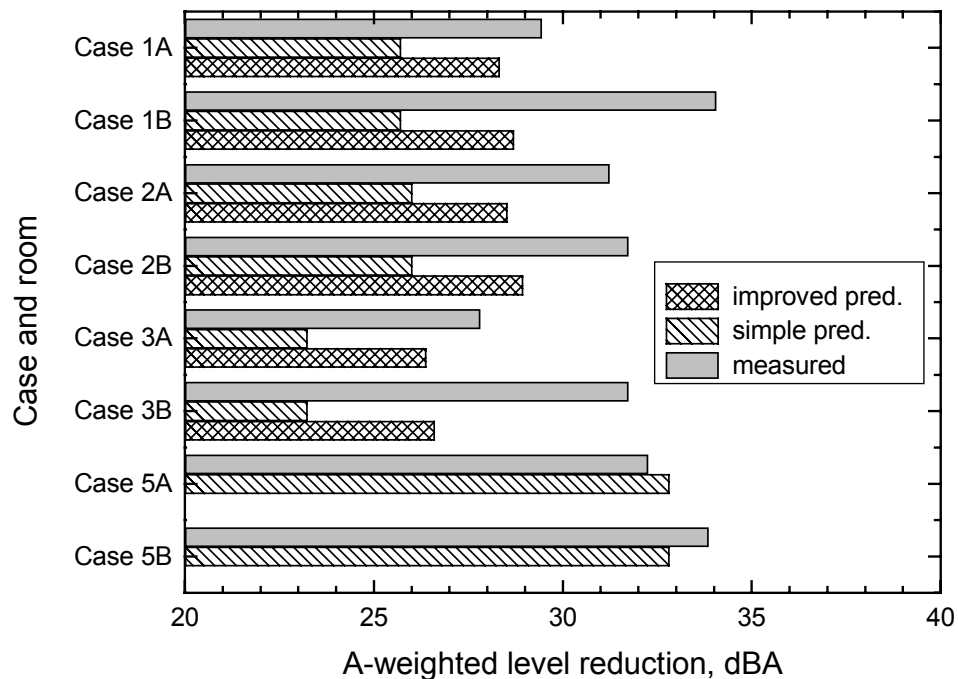


Figure 15. Comparison of overall A-weighted level reductions for cases of walls without windows or vents.

3.2 Walls with Windows

Measurement cases 10, 11 and 12 included windows in the walls of the test house. Case #10 included windows only in the end walls of each room and the other walls were masked (see also Figure 1). Case # 11 included windows in the facing walls of each room only. Case #12 included windows in both exterior walls of each room of the test house. As for the cases for walls without windows, the measured noise reductions were first compared with predicted noise reductions from the laboratory measurements of the same combination of façade elements. Using the same standard aircraft source spectrum,

A-weighted indoor sound levels were also predicted for each room and for each configuration.

The simple predictions used the surface areas and laboratory measurements of transmission loss of each façade component as described in section 2.5. As for the walls only cases, ‘improved’ predictions were performed that also included corrections for the effective flanking paths and the ground reflection effects. These improved predictions still underestimated high frequency sound levels. This was thought to be at least partially due to sound leakage through the ridge and soffit vents. The windows were tested after the installation of these vents that were found to lead to small increases in high frequency indoor sound levels. These results are discussed in section 3.3. The differences between the case #5 and case #8 results are due only to the addition of the ridge and soffit vents. Thus these measured differences can be used to determine an effective TL of the sound paths through the vents. This effective TL of the vents was added as a final correction to the previous ‘improved’ predicted results. The measurements and various predictions are compared in ‘a’ and ‘b’ parts of Figures 16 to 21.

Figures 16 and 17 compare measurements for the case #11 configuration for rooms A and B respectively. Case #11 corresponded to windows in the end walls only. These results show that the simple predictions were not very accurate because they under-predicted the measured noise reductions at low frequencies and over-predicted the measured noise reductions at high frequencies. The ‘improved’ predictions led to better agreement at lower frequencies mostly because of the inclusion of an estimate of the effect of ground reflections. Adding the effect of the flanking paths (in the ‘improved’ predictions) and adding the effects of vents both improved the agreement between measured and predicted values with a combined improvement of up to 5 dB at higher frequencies.

The overall A-weighted noise reductions shown in each plot indicate that these case #11 measurements were predicted within a fraction of a decibel for both rooms.

The case #10 results are given for rooms A and B in Figures 18 and 19 respectively. This measurement configuration included windows in the end walls only. For these results the simple predictions were more successful than in the previous case. The simple predictions agreed more closely with the measured results at higher frequencies for both rooms and also better predicted the low frequency results in room A on the depart side of the building. At higher frequencies the ‘improved’ predictions and the further correction for the effect of the vents both improved the agreement with measured values. Including the estimated effect of ground reflections also improved the agreement at low frequencies in room B on the approach side of the building. The agreement at lower frequencies was a little less successful for the room A results in Figure 18.

The overall A-weighted level reductions were predicted within 1.6 dBA.

Figures 20 and 21 compare measured and predicted noise reductions for the case #12 results in which both walls of each room included windows. However, one window was not the same as in the other window tests. The measurements of the configuration #12 were made before the configuration #10 and #11 results and masking walls were used to eliminate significant sound transmission through the other window. After the case #12 measurements, the (depart) end window in room A was replaced because its frame failed creating an obvious sound leak. Laboratory measurements of this window also indicated

unreliable seals and the laboratory sound transmission loss values used in these predictions were the average of two tests that were slightly different. For the room A case #10 results, this window was replaced with a different window with somewhat better sound insulation characteristics.

The results in Figure 20 show the inferior high frequency noise reduction due to this less satisfactory window. In spite of these practical problems, the predictions are again successful in predicting the measured noise reductions. Adding the correction for ground reflections in the 'improved' predictions improved the agreement between measured and predicted values at lower frequencies. The corrections for flanking paths and for vents again both improve the agreement at higher frequencies.

For room A, the measured overall A-weighted levels were predicted within 0.6 dBA and in room B within 2.5 dBA.

In general, the most significant differences between measured and predicted values tend to occur in room B and around 250 Hz. Room B is on the approach side of the building and incident sound energy is expected to be less than measured at the remote free field microphone location. This probably contributes to the larger differences between measured and predicted values for room B. The larger differences around 250 Hz are probably because the mass-air-mass resonance of the window is situated at about this frequency. The tests with a loudspeaker source (see section 4.1) showed that sound transmission at this resonance varied with the angle of incidence of the sound and was greatest for normally incident sound. Thus the laboratory measurements predict a small dip in the noise reduction at 250 Hz which is seen in the predicted results of Figures 17a, 19a and 21a but is not found in the measured noise reductions for these results. Thus there is frequently a tendency for the measured noise reduction to be less than predicted in this frequency region.

Although including the expected effect of roof vents improves the prediction of higher frequency noise reductions, it does not greatly improve the accuracy of the prediction of overall A-weighted level reductions.

The measured and predicted overall A-weighted level reductions are summarised in Figure 22 for the cases with windows. The overall A-weighted level reductions were 2 to 4 dBA inferior to the corresponding simple walls without windows, but 3 to 7 dBA less than the improved Case#5 wall construction to which the windows were added. The measured values were predicted with a mean error of 0.5 dBA varying from -2.4 to +1.6 dBA differences using the 'improved' predictions with further corrections for the effects of vents. This was similar to the accuracy of the simple predictions. Although the improved corrections including the effects of vents are seen to produce improved agreement at higher frequencies in Figures 16 to 21, they only have small effects on the overall A-weighted indoor sound levels. The overall A-weighted levels are most influenced by small changes in the 200 to 630 Hz region such as those related to the mass-air-mass resonance of the windows. Accordingly, the lower frequency effects of ground reflections are less important for these walls with windows.

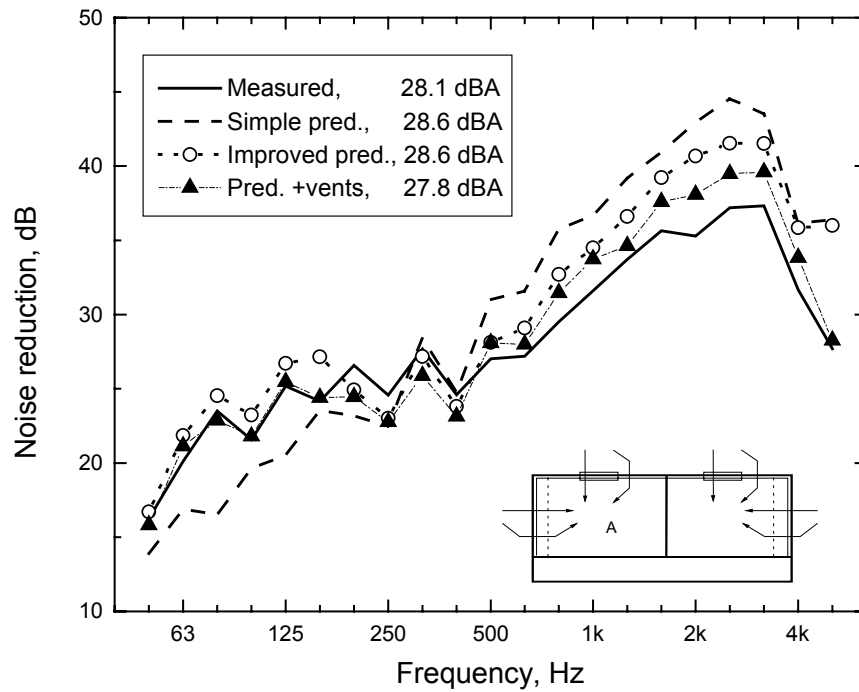


Figure 16a. Comparison of measured and predicted Noise reduction (NR) for Room A (depart side) Case #11 (facing windows exposed).

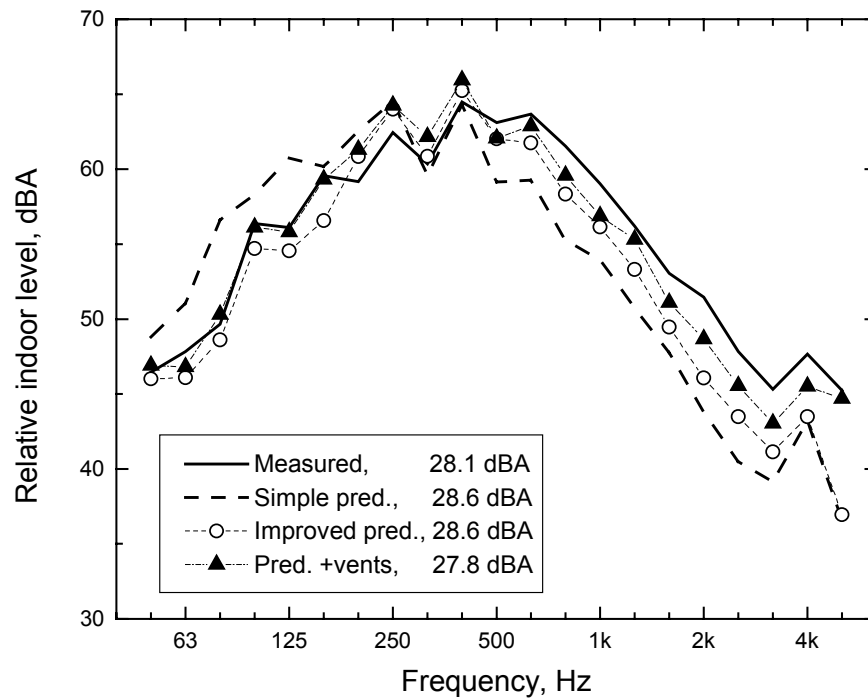


Figure 16b. Comparison of measured and predicted A-weighted indoor sound levels for Room A (depart side) Case #11 (facing windows exposed).

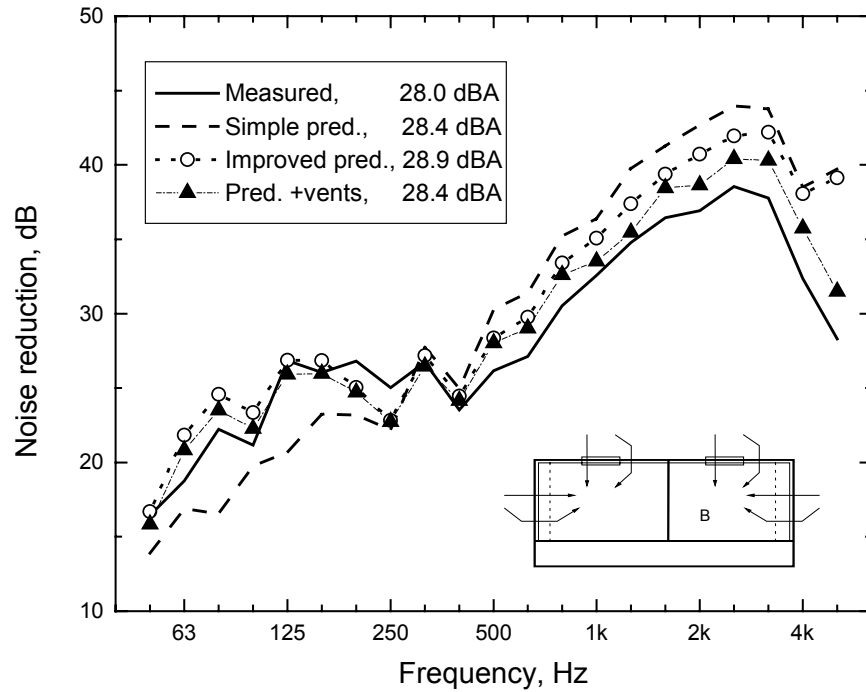


Figure 17a. Comparison of measured and predicted Noise reduction (NR) for Room B (approach side) Case #11 (face windows exposed).

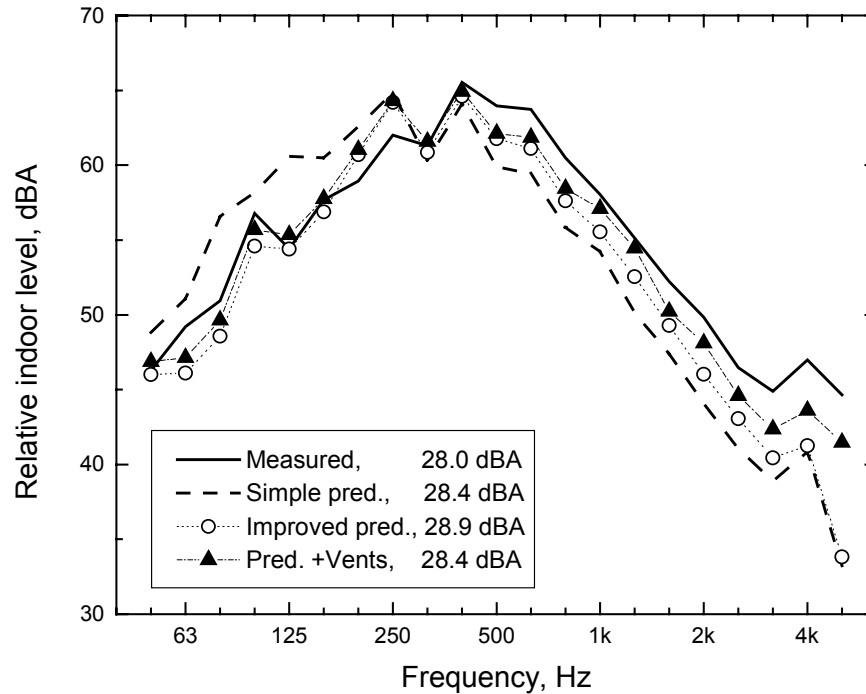


Figure 17b. Comparison of measured and predicted A-weighted indoor sound levels for Room B (approach side) Case #11 (face windows exposed).

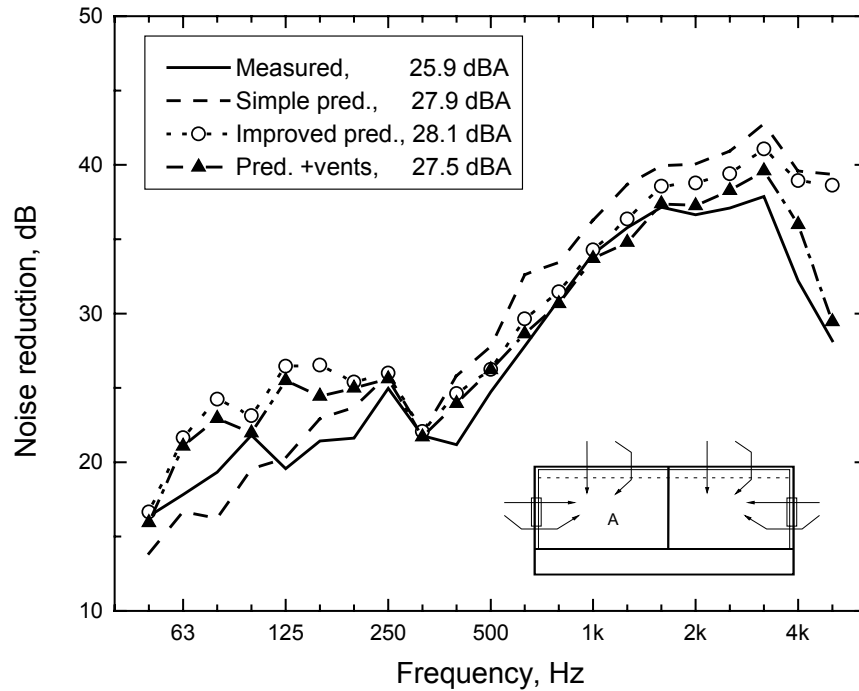


Figure 18a. Comparison of measured and predicted sound transmission loss (TL) for Room A (depart side) Case #10 (end windows exposed).

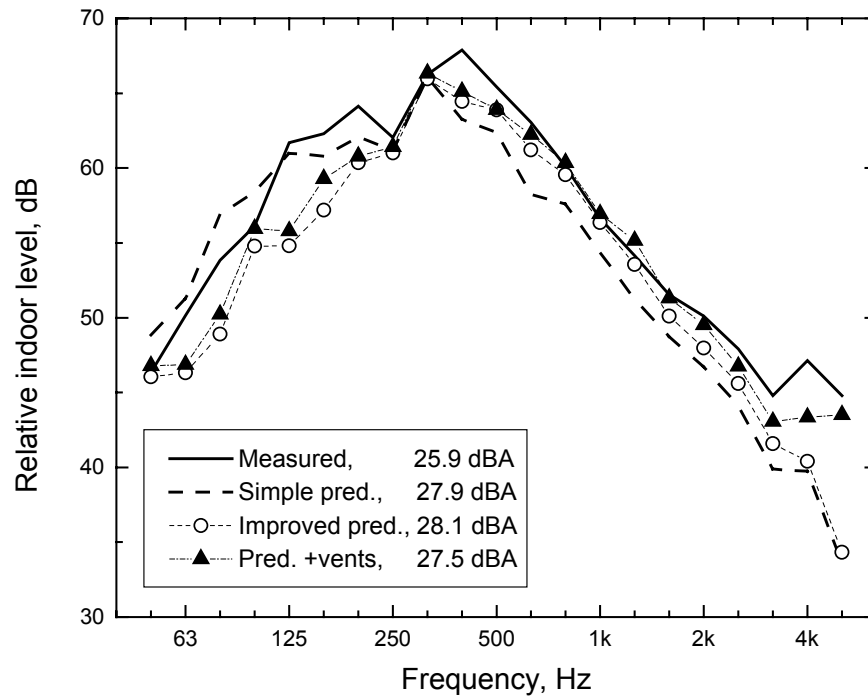


Figure 18b. Comparison of measured and predicted A-weighted indoor sound levels for Room A (depart side) Case #10 (end windows exposed).

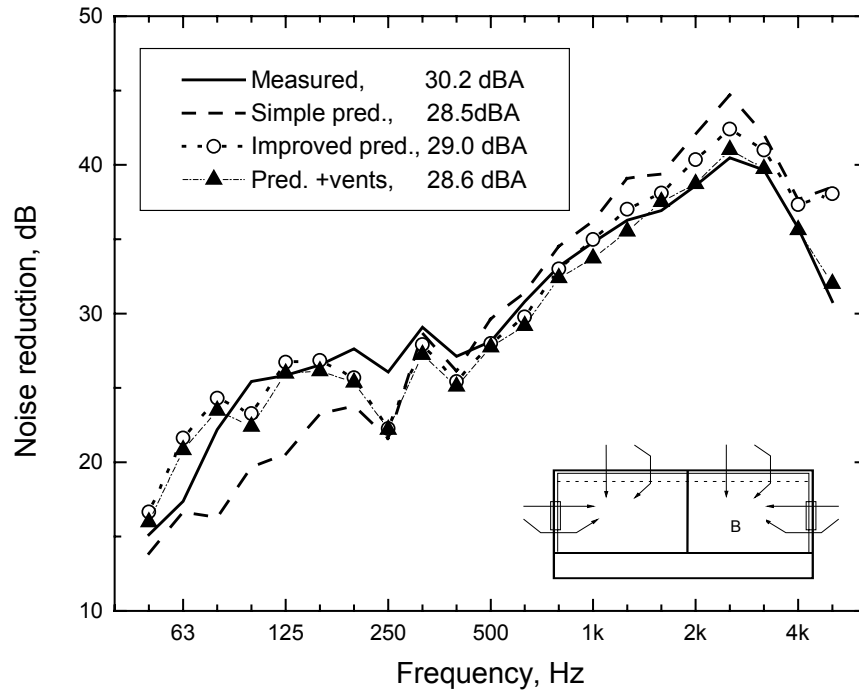


Figure 19a. Comparison of measured and predicted noise reduction (NR) for Room B (approach side) Case #10 (end windows exposed).

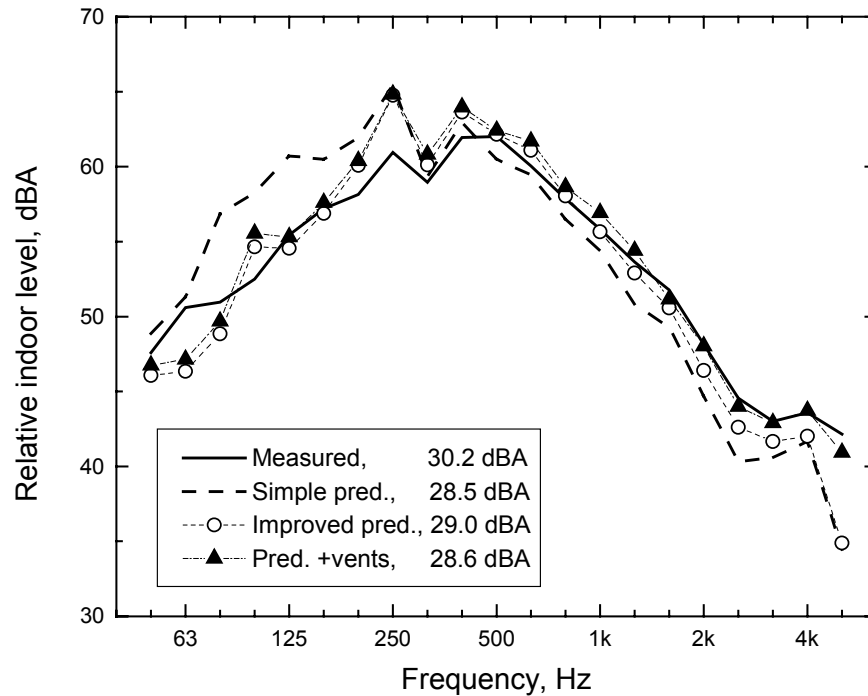


Figure 19b. Comparison of measured and predicted A-weighted indoor sound levels for Room B (approach side) Case #10 (end windows exposed).

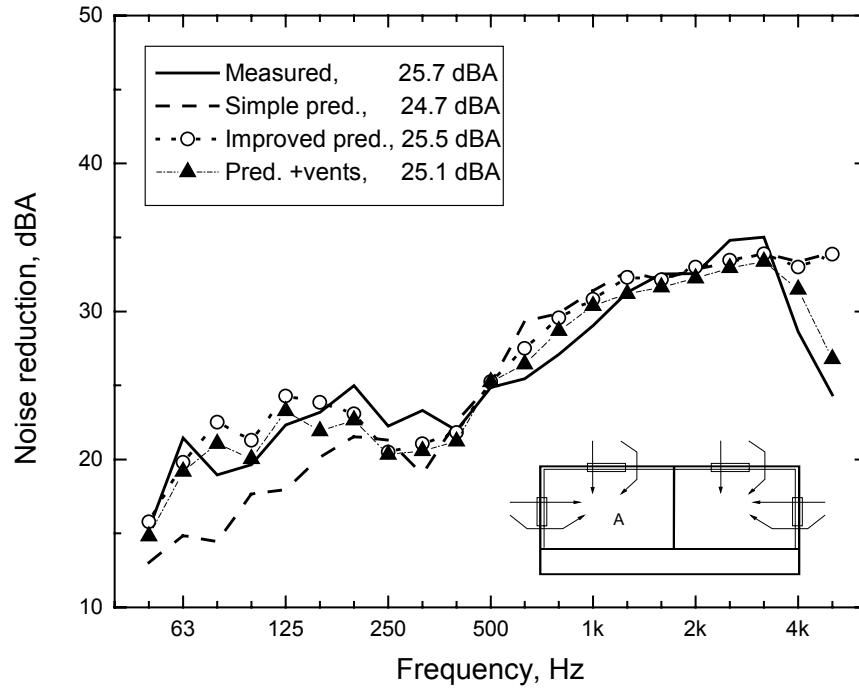


Figure 20a. Comparison of measured and predicted noise reduction (NR) for Room A (depart side) Case #12 (both windows exposed).

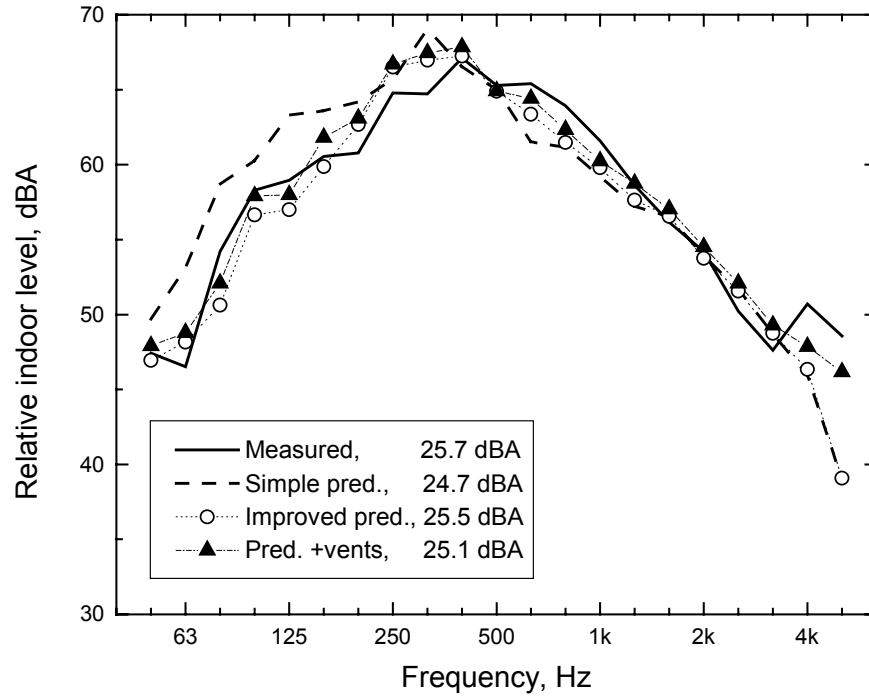


Figure 20b. Comparison of measured and predicted A-weighted indoor sound levels for Room A (depart side) Case #12 (both windows exposed).

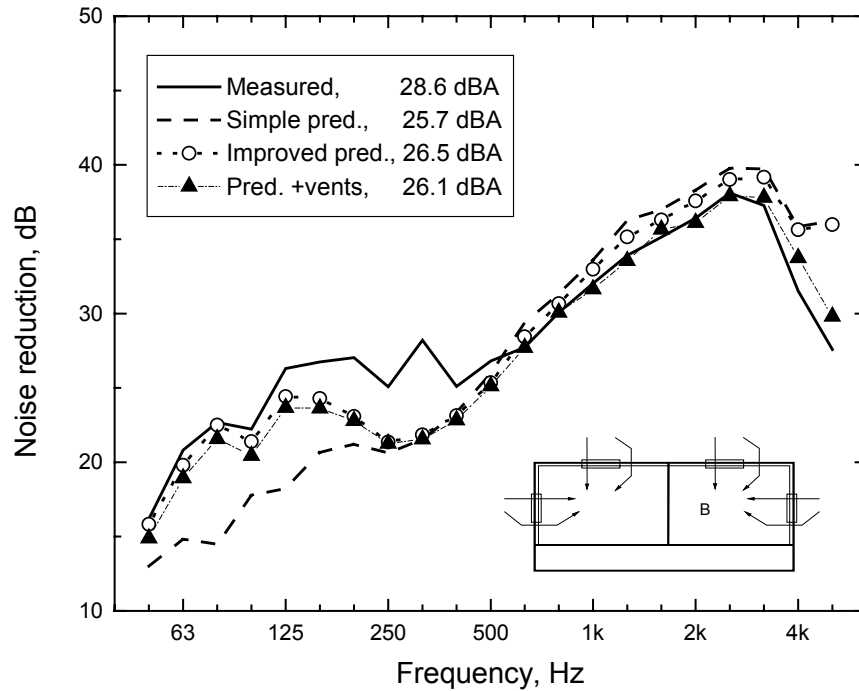


Figure 21a. Comparison of measured and predicted Noise reduction (NR) for Room B (approach side) Case #12 (both windows exposed).

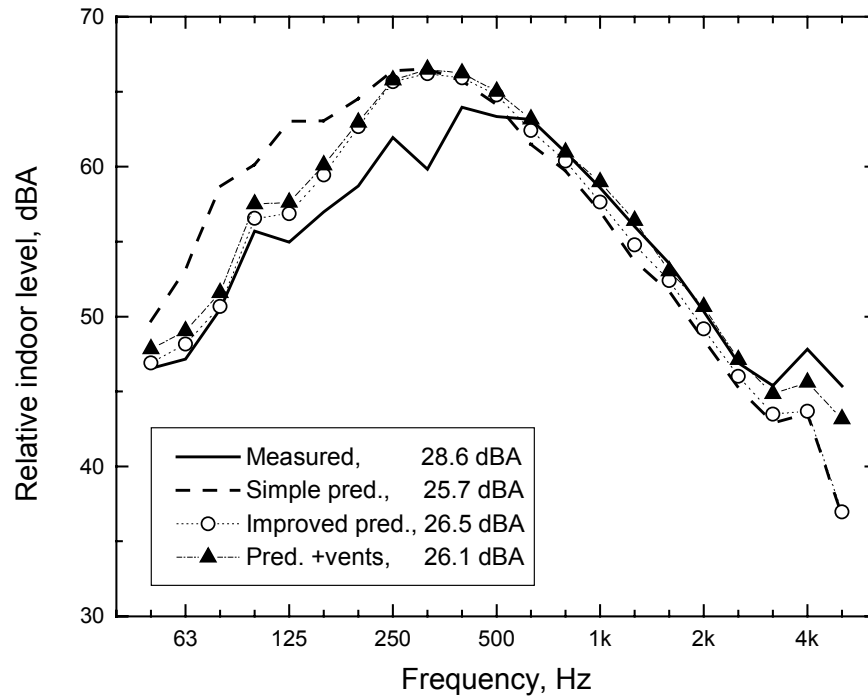


Figure 21b. Comparison of measured and predicted A-weighted indoor sound levels for Room B (approach side) Case #12 (both windows exposed).

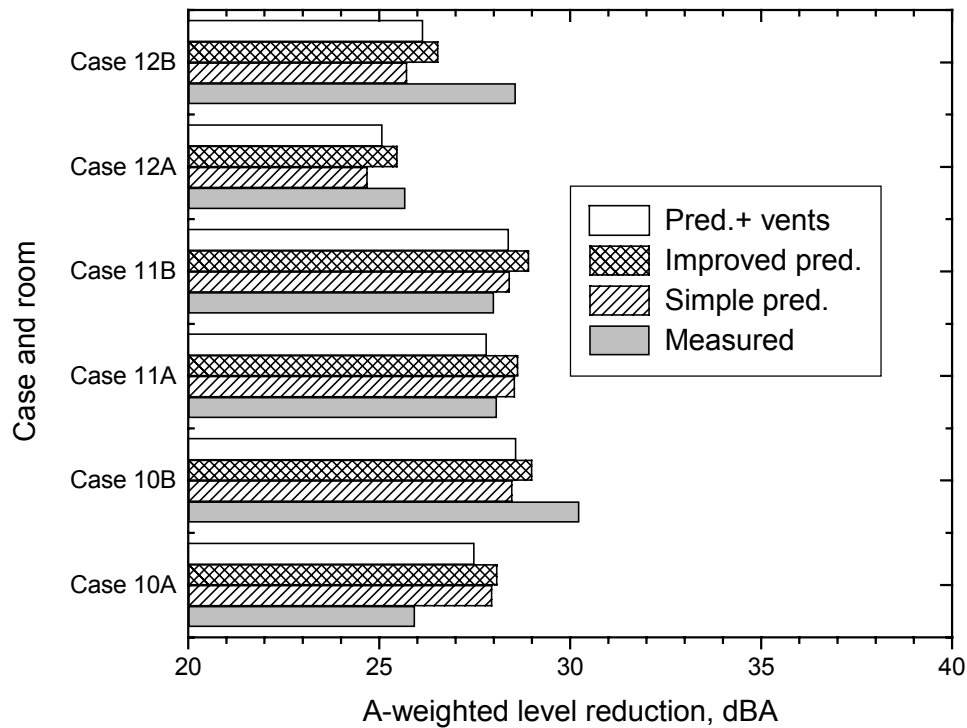


Figure 22. Comparison of overall A-weighted level reductions for cases of walls with windows.

3.3 Vents

3.3.1 Roof, Ridge and Soffit Vents

It is normally considered good building practice to vent unheated attic spaces to avoid moisture build-up. This commonly includes adding ridge vents along the peak of the roof or separate roof vents near to the peak, as well as vents in the soffit under the eaves of the roof. The combination of soffit vents with either roof or ridge vents is intended to encourage airflow through the attic space. However, they are also expected to influence the sound insulation of the roof. Various tests of the effects of adding vents were included in the laboratory tests of various roof structures as well as in the tests at the OATS.

Many more combinations of roof constructions with either ridge or roof vents were considered in the laboratory measurements than were possible at the OATS. Although the results of the laboratory tests were included in a previous report [1], a summary of the effects of roof vents from the laboratory tests is included here to aid comparisons with field results. The ridge vents extended along the complete length of the ridge or peak of the roof for both lab and field measurements. A sketch of the cross section of a ridge vent is included in Figure 23. Figure 24 includes a plan and section of one of the plastic roof vents that were used in both the laboratory tests and the tests at the OATS. The area of the opening is shown on this figure to be 0.053 m².

Table IIIa gives a summary of the results of adding ridge and roof vents to roofs in the laboratory tests. It was not possible to add soffit vents in the laboratory because the roofs were built in the opening between two reverberation chambers intended for testing floors. The overall A-weighted noise reductions for each sound transmission loss test were first calculated using the standard aircraft noise source spectrum (see Chapter 6). Table IIIa gives the differences in overall A-weighted level reduction when vents were added to each roof.

These laboratory results include various combinations of constructions for 3 types of roofs. These were: (1) flat roofs constructed on 2 by 10 joists, (2) flat roofs constructed on 14" deep wood trusses, and (3) raised heel wood truss sloping roofs. Although the first two are described as flat roofs they would also represent so called 'cathedral ceiling' type roofs where the interior and exterior layers are parallel and there is no attic space. The results include varied thermal insulation in the joist space, varied numbers of layers, and varied attachment of the gypsum board. They also include a few partial constructions to help to better understand the effects of each parameter.

For the 2 by 10 wood joist flat roofs, the overall A-weighted noise reduction was reduced by between -1 and -2.1 dBA when the 6 roof vents were installed. When the vent holes were left open and not covered by the plastic vents, the noise reduction was reduced -2.3 dBA. Similar results are seen for the 14" wood truss roofs.

The raised heel wood truss roof is essentially the same construction as the roof at the OATS. When this was tested without a ceiling, adding the 6 roof vents reduced the overall A-weighted level reduction -7.8 dBA. When a ceiling was included but with no thermal insulation in the attic space, the addition of the 6 roof vents decreased the overall A-weighted level reduction -5.1 dBA. When R20 (151 mm) glass fibre thermal insulation was included, the effects of vents reduced to -2.4 dBA and with R40 glass fibre insulation (256 mm thick) the effect of vents reduced to a -1.3 dBA change. These were both for a ceiling consisting of a single layer of directly attached gypsum board. Adding a second layer of directly attached gypsum board with the same R40 thermal insulation reduced the effects of adding six roof vents to a -0.8 dBA change.

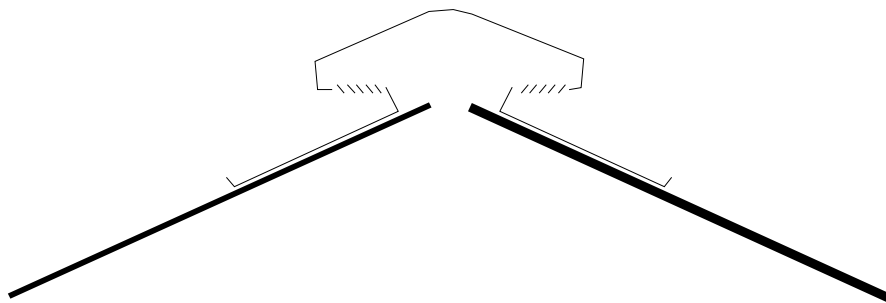


Figure 23. Sketch of section of the aluminum ridge vent used both in the laboratory tests and the tests at the OATS.

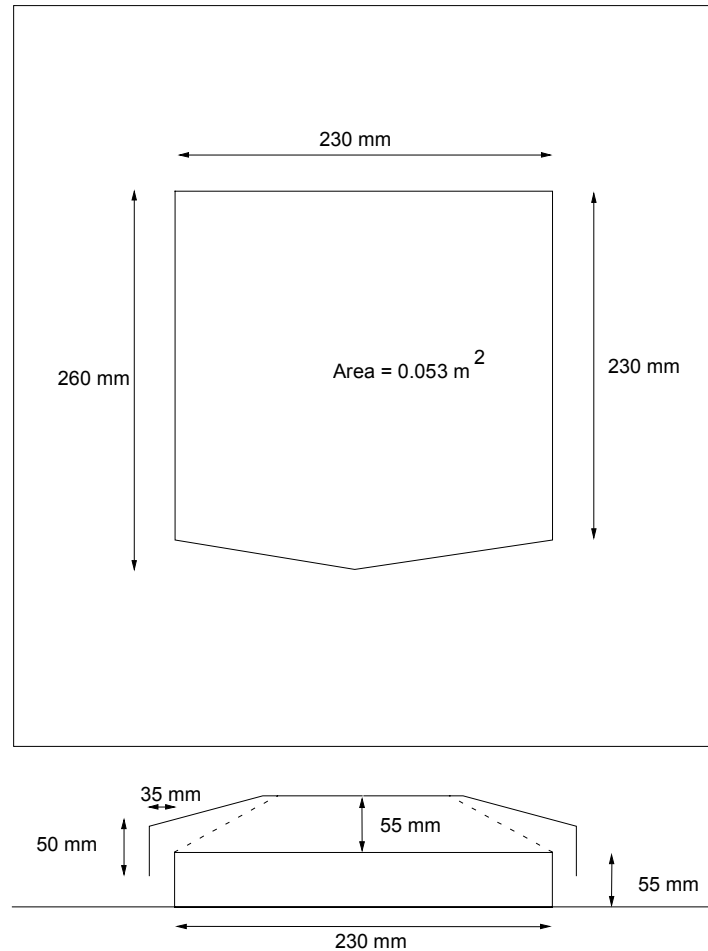


Figure 24. Plan and section of one of the plastic roof vents used both in laboratory tests and in the tests at the OATS.

For RHWT roofs with gypsum board attached via resilient channels, the changes when vents were added were slightly larger. Adding the 6 roof vents to a roof with one layer of gypsum board attached via resilient channels and with R40 thermal insulation caused a -2.5 dBA change. When a second layer of gypsum board (attached to the same resilient channels) was added, the change was reduced to -1.7 dBA.

Similar trends were found when ridge vents were added in the laboratory tests. Changes to the overall A-weighted noise reductions as large as -6.9 dBA for a roof without a ceiling and -4.7 dBA for a roof with a ceiling, but no thermal insulation, are shown in Table IIIa. These were reduced to changes of -2.4 and -1.3 dBA, when ridge vents were added to RHWT roofs with R20 or R40 thermal insulation respectively.

The six roof vents were about double the number that would normally be required but were included here to obtain more distinct effects. Table IIIa also shows the results of further tests for a RHWT roof where the number of vents was varied. While 1 vent only reduced overall A-weighted noise reductions by -0.3 dBA, 3 vents led to a -1.4 dBA change compared to the -2.4 dBA change when all 6 vents were added.

Change in dBA	Description
	2"x10" wood joists with perlin
	<i>six vents installed</i>
-1.0	SHN_BPAP0.7_OSB13_WS38(406)_WJ235(406)_GFB203_G13
-2.1	SHN_BPAP0.7_OSB13_WS38(406)_WJ235(406)_GFB203_RC13(610)_G13
-1.4	SHN_BPAP0.7_OSB13_WS38(406)_WJ235(406)_GFB203_RC13(610)_2G13
	<i>six vent holes but no vents installed</i>
-2.3	SHN_BPAP0.7_OSB13_WS38(406)_WJ235(406)_GFB203_RC13(610)_2G13
	14" deep wood trusses
	<i>six vents installed</i>
-0.4	SHN_BPAP0.7_OSB13_WT356(406)_GFB264_G13
-1.2	SHN_BPAP0.7_OSB13_WT356(406)_GFB264_RC13(610)_2G13
	Raised Heel Wood Trusses
	<i>six vents installed</i>
-7.8	SHN_BPAP0.7_OSB11_RHWT1626
-5.1	SHN_BPAP0.7_OSB11_RHWT1626_G13
-2.4	SHN_BPAP0.7_OSB11_RHWT1626_GFB152_G13
-1.3	SHN_BPAP0.7_OSB11_RHWT1626_GFB264_G13
-0.8	SHN_BPAP0.7_OSB11_RHWT1626_GFB264_2G13
-2.5	SHN_BPAP0.7_OSB11_RHWT1626_GFB264_RC13(610)_G13
-1.7	SHN_BPAP0.7_OSB11_RHWT1626_GFB264_RC13(610)_2G13
	<i>ridge vent installed</i>
-6.9	SHN_BPAP0.7_OSB11_RHWT1626
-4.7	SHN_BPAP0.7_OSB11_RHWT1626_G13
-2.4	SHN_BPAP0.7_OSB11_RHWT1626_GFB152_G13
-1.3	SHN_BPAP0.7_OSB11_RHWT1626_GFB264_RC13(610)_2G13
	<i>varied number of roof vents</i>
-0.3	SHN_BPAP0.7_OSB11_RHWT1626_GFB152_G13 - 1 vent
-1.4	SHN_BPAP0.7_OSB11_RHWT1626_GFB152_G13 - 3vents
-2.4	SHN_BPAP0.7_OSB11_RHWT1626_GFB152_G13 - 6 vents
	<i>steel roof, ridge vent installed</i>
-0.5	STE0.3_WFUR19(406)_RHWT1626_GFB152_G13
-0.4	STE0.3_WFUR19(406)_RHWT1626_GFB264_G13
-0.4	STE0.3_WFUR19(406)_RHWT1626_GFB264_RC13(610)_2G13

Table IIIa. Changes to the overall A-weighted level reductions when vents were added using the standard aircraft noise source spectrum for the laboratory measurement results. The various symbols describing the constructions are explained in Table IIIb.

BPAP	Building paper
G13	13mm (1/2") regular gypsum board
GFB	Glass fibre batt insulation
OSB	Oriented strand board
RC	Resilient channels
RHWT	Raised heel wood-truss
SHN	Roofing shingles
STE	Corrugated steel roof
WFUR(xxx)	Wood furring strips xxx mm on centre
WJ	Wood-joists
WS(xxx)	Wood studs spaced xxx mm on centre
WT	Wood-trusses

Table IIIb. Explanation of symbols describing components of constructions in Table IIIa.

Finally Table IIIa shows the results for adding a ridge vent to RHWT roofs that were covered with steel sheeting rather than asphalt shingles. Varying the thermal insulation or adding a second layer of gypsum board using resilient channels led to similar small changes, when the ridge vent was added, of -0.4 to -0.5 dBA.

In general, the laboratory results suggest that adding a ridge vent or roof vents will lead to small changes to the overall A-weighted noise reduction when there is at least R20 (152 mm) glass fibre in the attic space. With a more realistic number of roof vents and thermal insulation in the attic space, adding vents is likely to reduce the overall A-weighted level reduction by up to a maximum of 2 dBA.

The effects of roof vents were examined at the OATS in terms of the difference in noise reductions between the base case #5 without vents and the cases #6, #7 and #8 with vents.

For case #6, six roof vents were added. For case #7 soffit vents were added in addition to the six roof vents. For case #8 the roof vents were replaced by a ridge vent and the soffit vents remained in place. The effects of adding these vents were determined separately for measurements in both rooms of the test house.

Figure 25 shows the measured changes due to the addition of the 6 roof vents to the OATS. The results for rooms A and B are quite similar and so the average of the 2 rooms can be used. This average is also compared with laboratory measurements of the effects of roof vents to a similar RHWT roof. The average OATS results are somewhat intermediate to the laboratory results with R20 and those with R40 thermal insulation in the attic. Thus although there was R40 glass fibre thermal insulation in the attic at OATS, the field measurements indicated a slightly larger decrease in NR at mid frequencies when roof vents were added than the corresponding laboratory results with R40 thermal insulation. However, the total effect is still very small. The average overall A-weighted level reduction change was -1.0 dBA at OATS and -2.4 and -1.3 dBA for similar roofs with R20 and R40 thermal insulation respectively in laboratory tests (see Table IIIa).

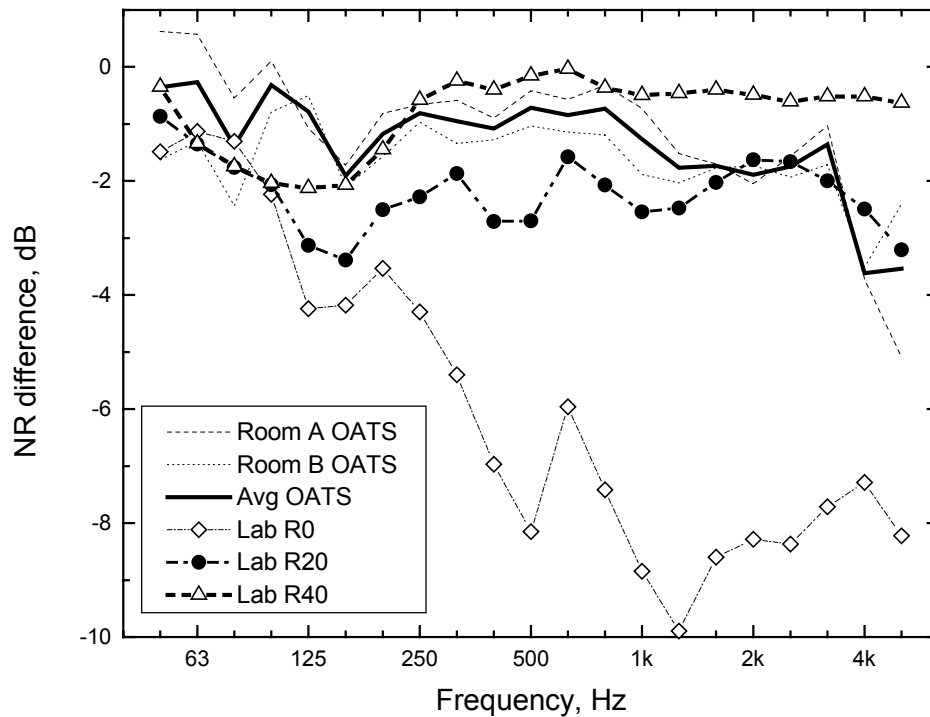


Figure 25. Changes to measured noise reductions (NR) with the addition of 6 roof vents for laboratory results and tests at the OATS .

The measured changes in noise reductions when soffit vents were added to the roof vents are shown in Figure 26 along with the results for the previous case of roof vents only. Again the results for the two rooms are generally quite similar but surprisingly, adding soffit vents appears to increase rather than decrease the noise reductions. This will be discussed further below but appears to be due to different average angles of incidence of the aircraft noise for the two cases.

Figure 27 gives the measured results for the case of adding both a ridge vent and soffit vents to the OATS. There are some slightly larger differences between the results for the two rooms at lower frequencies but generally similar results were obtained in both rooms. The combination of a ridge vent and soffit vents seems to reduce the noise reduction more than the other vent tests above about 500 Hz. The overall A-weighted changes for the 3 cases tested at the OATS are included in Table IV and show changes between -0.7 and -1.9 dBA.

When the measurement data is examined in more detail the unexpected effects of adding the soffit vents to the roof vent case can be explained. When the measured noise reductions for individual aircraft events are plotted versus the vertical angle of the aircraft, there is a trend at higher frequencies for measured noise reductions to decrease with increasing vertical angle of the aircraft. Figure 28 plots the 2 kHz measurements. Over the range from about 30 to 60 degree vertical angle, measured noise reductions for the three different cases with vents and the case #5 reference case reduction varied by approximately 3 dB. Thus to accurately compare constructions, the incident aircraft noise should have the same average vertical angle of incidence. The average angle of incidence

Change, dBA	Description
-0.7	Roof vents, room A
-1.3	Roof vents, room B
-1.0	Roof and soffit vents, room A
-0.8	Roof and soffit vents, room B
-1.9	Ridge and soffit vents, room A
-1.2	Ridge and soffit vents, room B

Table IV. Measured reductions in overall A-weighted sound levels for each room and each addition of ridge, roof and soffit vents to OATS.

for the case #6 results (roof vents only) is about 50 degrees but for the case #7 results (roof and soffit vents) is about 35 to 40 degrees. This could easily explain the apparent negative effect of adding the soffit vents that was seen in Figure 26. Thus, it seems that the actual effect of adding soffit vents to the roof vents was probably very small and the observed difference was due to differences in angle of incidence of the aircraft noise.

It would clearly be desirable to test each configuration of OATS using a much larger sample of aircraft events. This was unfortunately not possible because financial constraints limited the field measurements to one season. In general the effects of adding vents were too small to be accurately measured in the field. Because there is no convincing evidence that adding soffit vents significantly changes measured noise reductions, it is probably more accurate to estimate the expected effects of adding vents

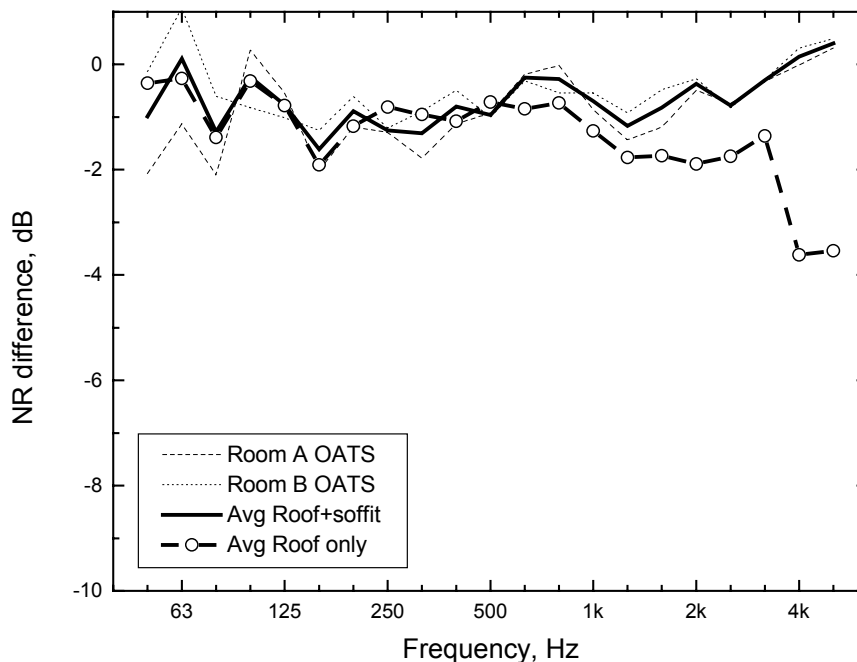


Figure 26. Changes to measured noise reductions (NR) with the installation of soffit vents in addition to 6 roof vents for laboratory results and tests at the OATS.

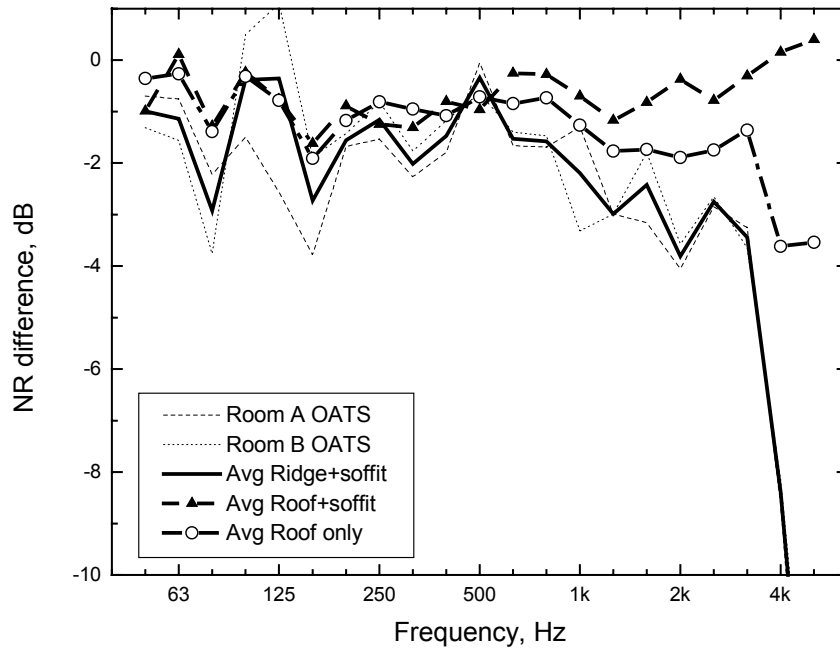


Figure 27. Changes to measured noise reductions (NR) with the addition of ridge and soffit vents for laboratory results and tests at the OATS.

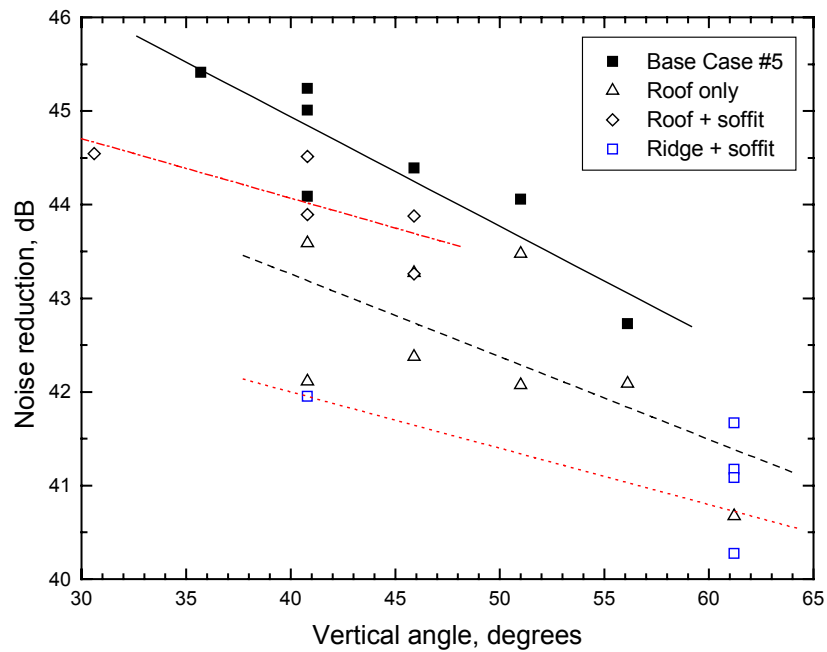


Figure 28. Variation of measured noise reductions at 2 k Hz with aircraft vertical angle.

from the laboratory test results. The differences between the case #5 results (with no vents) and the case #8 results were used to determine an effective transmission loss for the ridge vents. These effective TL values were calculated using measured noise reductions and the area of the roof-ceiling as the associated area. These results, shown in Figure 29, were used to correct the calculated noise reductions for the effects of ridge vents for the configurations for walls with windows in the previous section.

Table IV summarises the changes to the overall A-weighted level reductions when ridge, roof and soffit vents were added to the OATS. Adding roof vents decreased overall noise reductions by about 1 dBA (-0.7 and -1.3 dBA). Adding a ridge vent reduced the overall noise reduction by 1 to 2 dBA (-1.9 and -1.2 dBA). In the laboratory results in Table IIIa, adding roof vents caused a change of -1.3 dBA which is very similar to the -0.7 and -1.3 dBA reductions at the OATS from Table IV. The laboratory tests did not include the same construction with a ridge vent but when a ridge vent was added to RHWT roof with the same amount of glass fibre insulation but where the ceiling was a double layer of gypsum board on resilient channels, the change was -1.3 dBA (from Table IIIa). Thus the overall trends in the OATS results are very similar to those obtained in the laboratory tests.

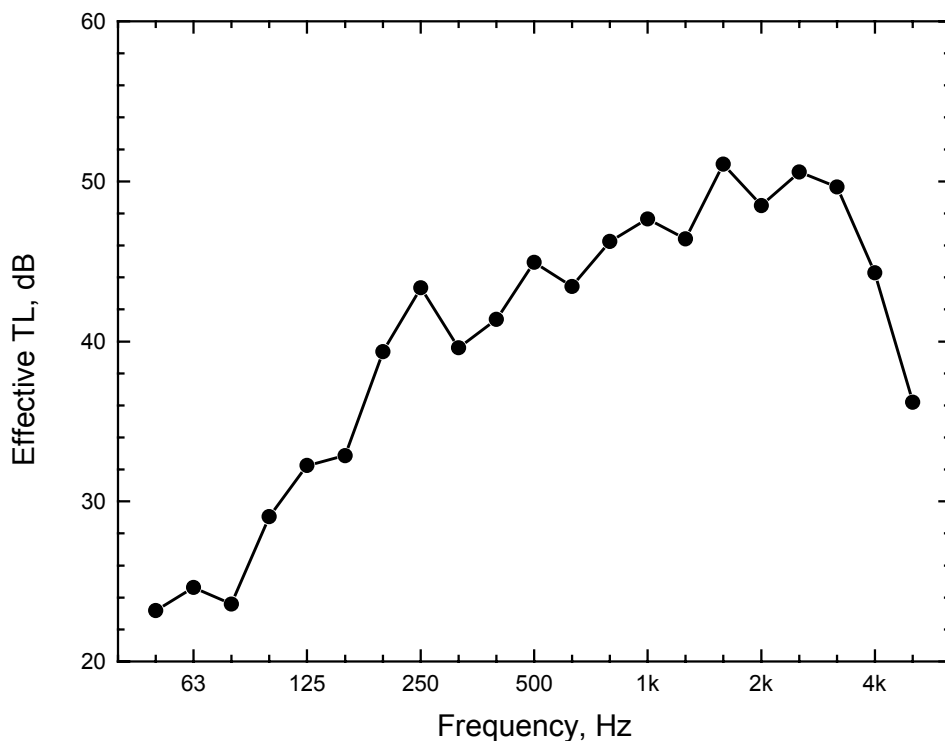


Figure 29. Effective transmission loss (TL) of the ridge vents calculated using the measured noise reductions with the total area of the ceiling and averaged over both rooms.

3.3.2 Wall Vents

The previous section discussed the effects of vents into the attic space of the roof. These do not create direct sound leaks into the interior of the building and so typically have quite small effects. In this section the effect of a limited number of tests of wall vents are considered. These were vents that directly connected the outside to the interior of the test rooms and hence had much larger acoustical effects. Two types of wall vents were tested at the OATS and one of these was also tested in a laboratory test. Figure 30 illustrates the principal dimensions of the vents as installed in the OATS test rooms. A conventional kitchen range hood that would normally be located over a stove for exhausting cooking fumes was located in room A. It was connected directly to the outside through a short duct through the exterior wall of the building. It include two light-weight metal flaps at either side of the exterior wall to reduce unwanted air flow from outdoors to indoors. The same range hood exhaust was tested in a high transmission loss wall in the laboratory. The other vent consisted of a round pipe with a total length of 0.91 m in room B and was a simple approximation to a bathroom vent. Like the other vent it had an outdoor rain shield over the exterior opening and include one light-weight metal flap to control unwanted airflow.

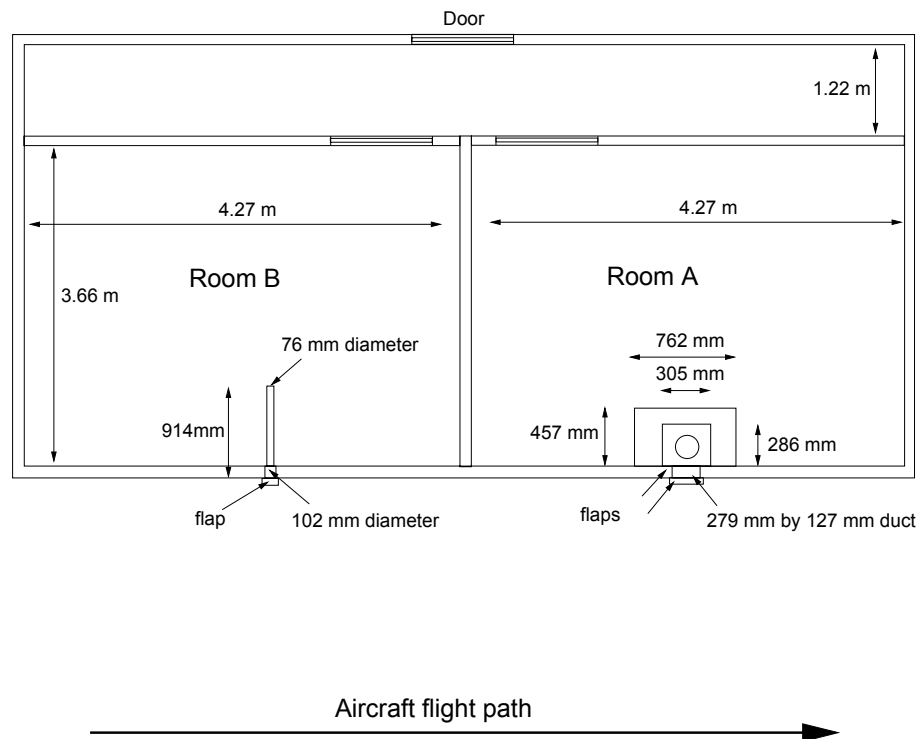


Figure 30. Plan of OATS showing the details of the two wall vents.

Figure 31 plots the measured TL values in the lab for the high TL test wall and for the same wall with the range hood exhaust added. Above 125 Hz there are large differences in the measured TL values when the exhaust vent is added. Figures 32 and 33 show similar plots for the addition of the two different vents at the OATS. The TL values for the OATS without the vents are not as high as the laboratory test wall but the effects of

adding the wall vents are again quite large. Above about 160 to 200 Hz, adding the vents significantly reduces the noise reduction of the building. Below this frequency adding the vents has little effect.

One simple estimate of the effect of vents that connect directly to the outside is to assume that they have a transmission loss of 0 dB. Thus one could calculate the expected effect of adding the vents from the areas of the openings and assuming a TL of 0 dB. For the current results we can calculate the effective TL values for each of the wall vents tested and compare them with the simple expectation of a hole with a TL of 0 dB.

The areas associated with each wall vent were the areas of the duct sections passing through the wall and were 0.0355 m² for the range hood exhaust and 0.0081 m² for the pipe vent. Figure 34 plots the calculated TL values for the range hood exhaust tests. The results from OATS and from the laboratory are quite similar. They suggest that the effective TL of this vent approaches 0 dB over a band of frequencies from 315 to 800 Hz. The TL was expected to increase at lower frequencies because adding the vents had no effect on the measurement results. At higher frequencies the higher TL seems to level off at about 10 to 15 dB.

Figure 35 shows similar results for the pipe vent which was only tested in room B at the OATS. Again the results are seen to approach a TL of 0 dB over a band of frequencies which in this case extend from 315 Hz to 1250 Hz. For this vent the higher frequency TL values level off at a lower level of about 7 or 8 dB.

Both vents seem to behave like a band pass filter in that they allow a band of frequencies to pass but attenuate other frequencies. The low frequency effects of these vents are

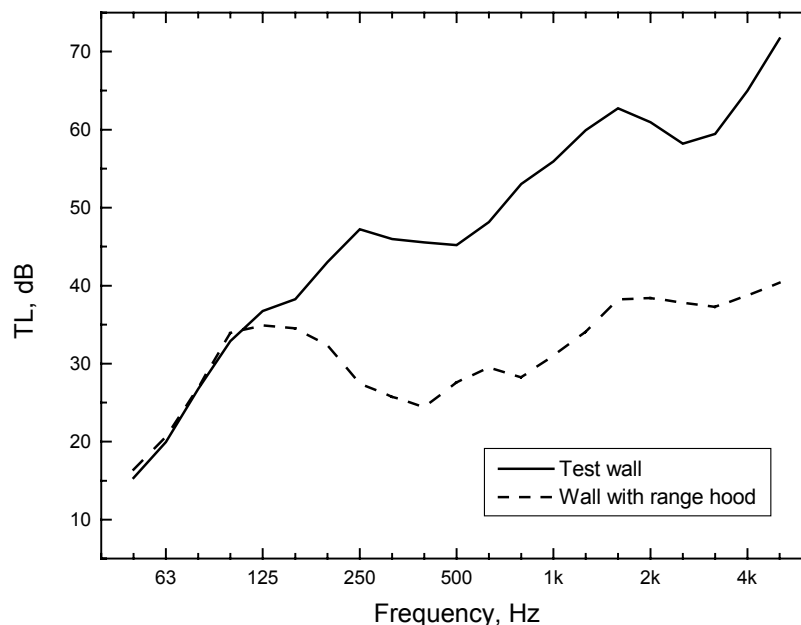


Figure 31. Laboratory measurements of the sound transmission loss (TL) of a high TL test wall both with and without the addition of the range hood wall exhaust vent.

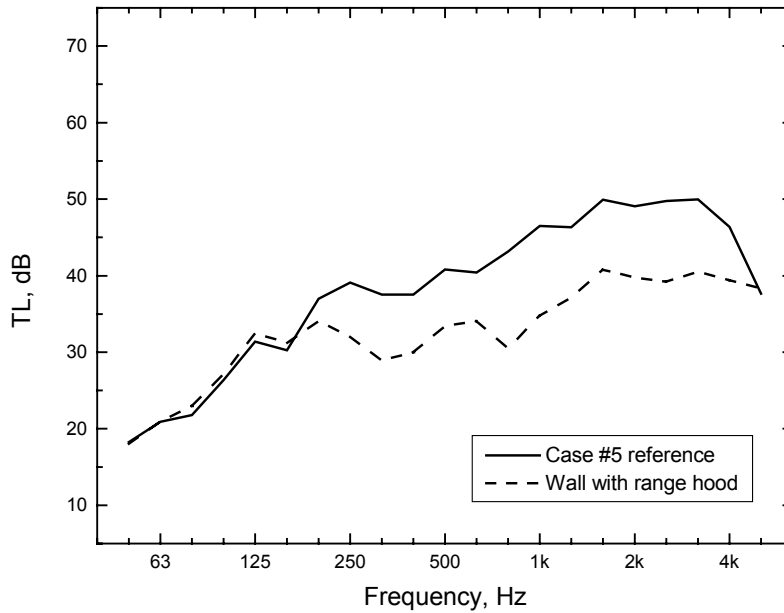


Figure 32. Measurements at the OATS of the sound transmission loss (TL) with and without the addition of the range hood wall exhaust vent in room A.

consistent with previous studies of the effects of cracks and holes on sound transmission through panels [8]. The high frequency effects may relate to the properties of the light-weight metal flaps in these vents. Presumably the high frequency TL values are larger for the range hood exhaust fan because it included a double flap system.

Adding the wall vents had large effects on the measured overall noise reductions.

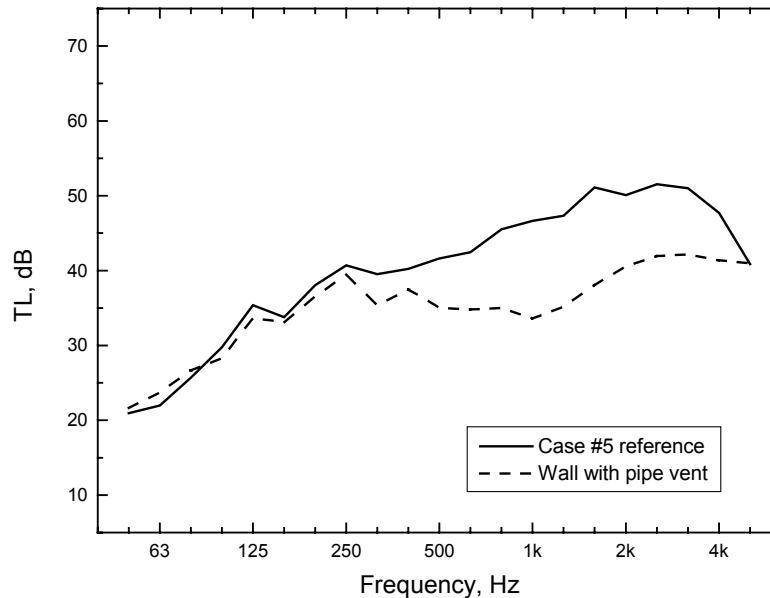


Figure 33. Measurements at the OATS of the sound transmission loss (TL) with and without the addition of the pipe wall exhaust vent in room B.

Adding the range hood exhaust vent in room A, changed the overall noise reduction by -8.7 dBA. Adding the pipe vent in room B, changed the overall noise reduction by -7.7 dBA. Clearly, it is not acceptable to include untreated vents that directly connect the outdoors to the indoor spaces. Where such ducts are necessary, they should include acoustical treatment such as sound absorbing duct liners, and should be located on the quiet side of the building away from aircraft noise sources.

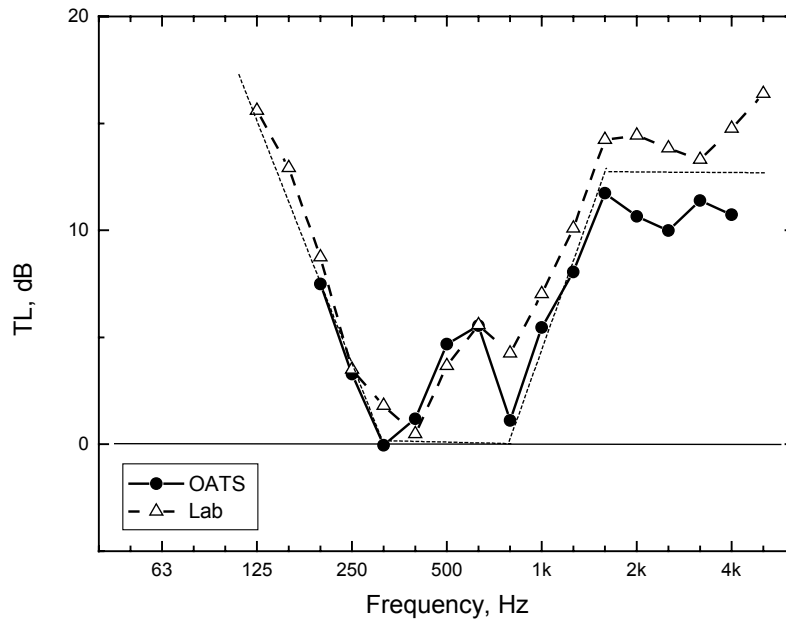


Figure 34. Calculated effective sound transmission loss (TL) of the range hood wall exhaust vent in room A and in the laboratory.

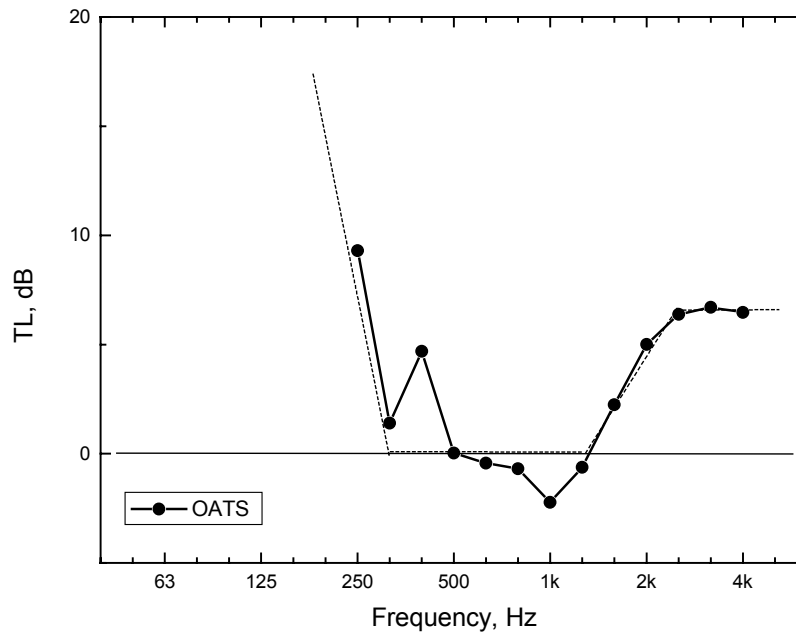


Figure 35. Calculated effective sound transmission loss (TL) of the pipe wall exhaust vent in room B.

4. Angle of Incidence Effects

This section presents various tests and analyses that consider the effects of the angle of incidence of the sound on the resulting noise reductions. These include tests using a loudspeaker sound source moved to various positions to vary the angle of incidence of the sound and analyses of a range of aircraft events in terms of the vertical angle of the aircraft as they flew by the test house.

4.1 Loudspeaker Source Tests

A loudspeaker sound source was located at a range of positions illustrated in Figure 36 so as to systematically vary the horizontal and vertical angles of incidence. Noise reductions were then measured from the façade microphone position to the average of the measurements at the three microphones in each room. The sound source was a Tracoustics sound source mounted on a pneumatic tower, which was located on the frozen surface of the adjacent swamp. Figure 36 indicates that there were 5 horizontal angles and 3 vertical angles for the source. However, all 15 combinations were not used. The three vertical angles were only used at the horizontal positions 1, 3 and 5. At the

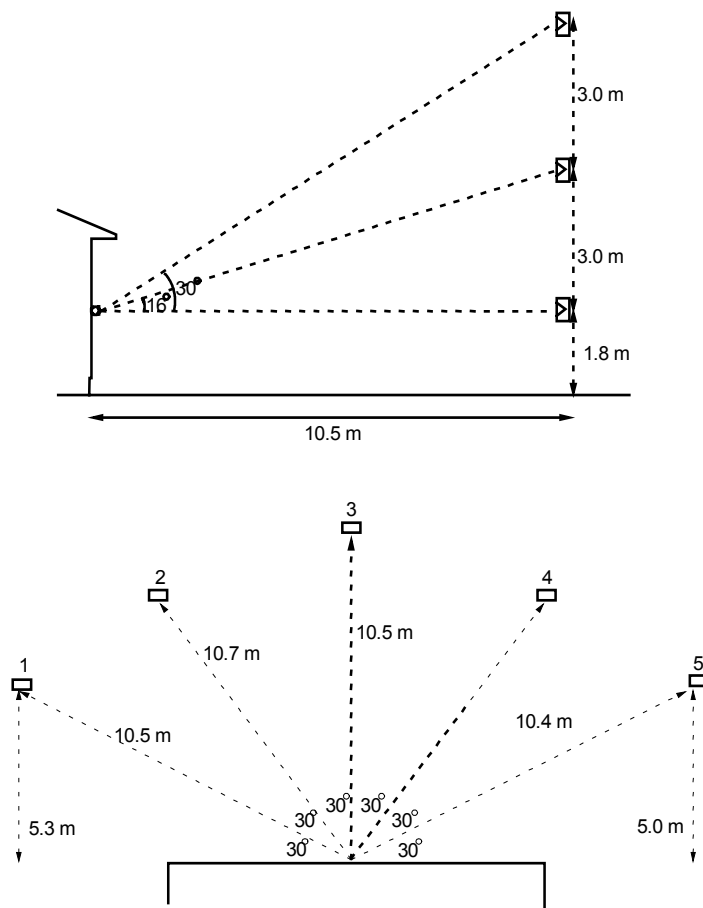


Figure 36. Source locations for the Tracoustics sound source relative to the OATS.

other two horizontal positions only the low source height was used.

The OATS was in the same configuration as the case #11 results illustrated in Table II. This included exposed windows in the facing walls and masking walls in front of the end walls in each room of the test house.

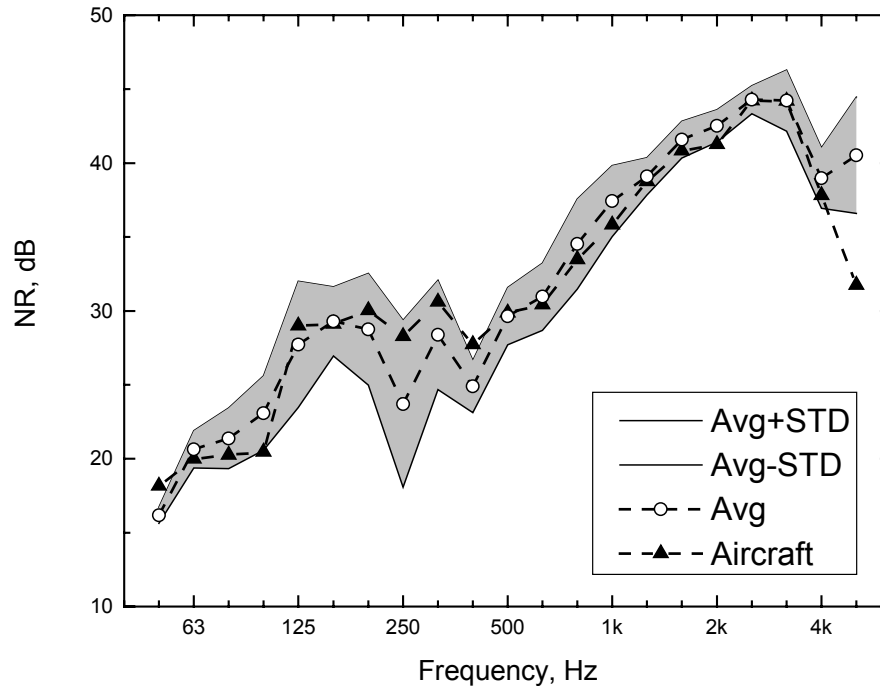


Figure 37. Comparison of noise reduction measurements relative to the façade microphone for loudspeaker and aircraft sources. The average (Avg) and ± 1 standard deviation (STD) are shown for the loudspeaker source measurements by the shaded area.

The measured noise reductions relative to the façade microphone measurement show many detailed changes with angle of incidence. It was only possible to achieve adequate indoor noise levels with the loudspeaker source no more than about 10.5 m from the façade of the OATS. A much larger distance would have been preferred to better approximate the more distant aircraft sources. Because of this relatively small distance to the source, the sound would not approximate plane waves and different parts of the façade would receive different incident sound intensities. The results are still useful to explore some angle of incidence effects.

Figure 37 compares the average measured noise reductions for all of the loudspeaker source measurements with the average aircraft source results. The shaded area shows ± 1 standard deviation about the mean for the loudspeaker source results. The average aircraft results agree quite well with the average loudspeaker source results and so the aircraft results can be said to represent a reasonable average over a wide range of angles of incidence. The differences at 5 kHz are due to inadequate indoor noise levels relative to the existing ambient noise levels.

The largest differences occur in the 250 Hz region and the shaded area of Figure 37 indicates that measured noise reductions vary most with angle of incidence in this frequency region. The mass-air-mass resonance frequency of the double glazing of the windows occurs in this frequency band. The variation of the measured noise reduction at the mass-air-mass resonance frequency is further explored in Figure 38. This figure compares the average noise reductions from aircraft to two groups of the loudspeaker source measurements. These are the averages of the low loudspeaker source positions and the high positions. The two average results for the loudspeaker source again agree reasonably well with the aircraft noise source results at most frequencies. However, there are large differences in the 250 Hz region. When the loudspeaker source was low, and the sound closer to normal incidence, the 250 Hz dip is larger. When the source is high, measured noise reductions are more similar to the aircraft results. The mass-air-mass resonance seems to be best excited, and the dip at 250 Hz greatest, when the incident sound is closer to normal incidence. Because the aircraft were at an average vertical angle of 55 degrees, the measured noise reductions were larger for the aircraft noise at 250 Hz. Thus in general, noise reductions in buildings exposed to actual aircraft noise will be better than laboratory results would suggest near to mass-air-mass resonance frequencies.

This same dependence of sound transmission loss on angle of incidence is also likely to occur at the primary structural resonance that occurs for the wood stud walls without resilient channels. This resonance led to a pronounced dip at about 125 Hz in the laboratory measurements that was much less evident in the field tests illustrated in Figures 4, 5 and 6. This would then explain the difference between laboratory and field

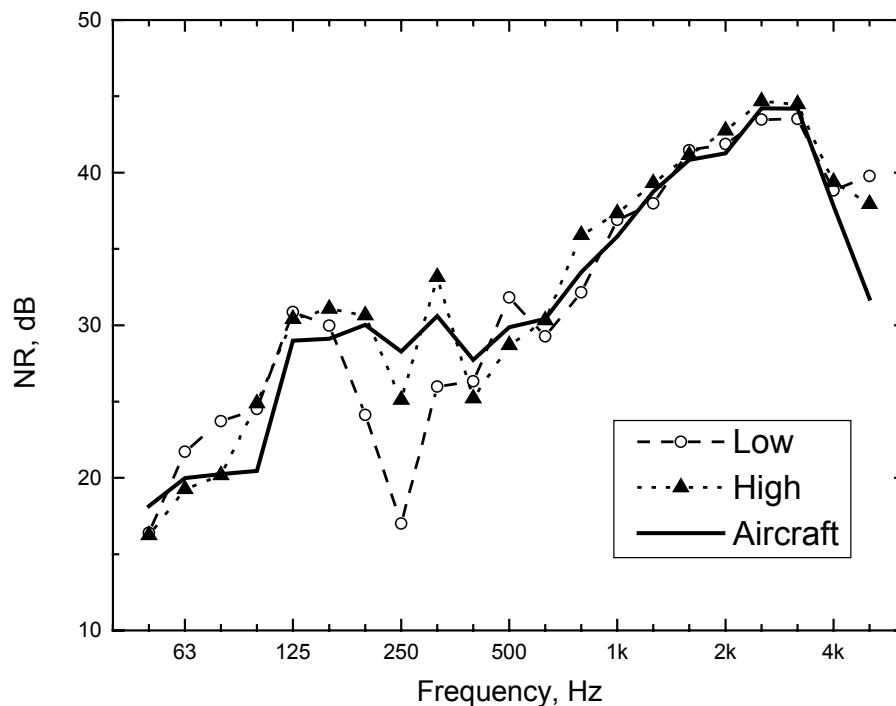


Figure 38. Comparison of measured noise reductions to aircraft noise with the average of the low and high positions of the loudspeaker source.

measurements in this frequency region and again suggests that higher noise reductions are to be expected in buildings exposed to actual aircraft noise at this resonance frequency. This is important because the laboratory measurements of sound transmission loss would predict that this dip would limit the overall noise reduction of the wall. Unfortunately loudspeaker source tests could not be made of the other test configurations to confirm this.

4.2 Variation of Façade Effects

At least two measurement standards [10, 11] suggest that it is acceptable to use a façade mounted microphone to assess the noise reduction of a building façade with respect to outdoor noises such as aircraft noise. It is usually much more convenient to mount a microphone on the façade of the building than to mount it on a tall mast. The use of a tall mast avoids the influence of reflected sound and hence assesses the free field incident energy. For a microphone on the façade, it is commonly assumed that because the direct and reflected sound are exactly in phase at the reflecting surface of the façade, pressure doubling will lead to a 6 dB increase in outdoor sound levels relative to a free field measurement. This simple 6 dB increase is assumed to occur at all frequencies. Most recordings of aircraft events at the OATS included both a free field outdoor microphone and a façade mounted microphone. Thus there is a large amount of data that can be used to verify whether this 6 dB increase does occur.

A third option for measuring the incident outdoor sound levels is to place the outdoor microphone 2 m from the façade. While at the façade a 6 dB pressure doubling effect is assumed, at the 2 m position a 3 dB energy doubling effect is expected. Some measurements were also made with a microphone 2 m from the façade.

Figure 39 compares the average façade effects for a number of aircraft events. The average differences between the free field microphone and the façade microphone results at the OATS are shown along with similar results for measurements at houses near Pearson Airport (YYZ). (Sound insulation measurements were made in several new homes in the Meadowvale Village area west of the Toronto airport). The third curve in Figure 39 shows the differences between average measurements at a microphone 2 m from the centre of the façade and the free field microphone. As described in section 2.3, the free field microphone was located on a mast 8.5 m above ground level. The façade microphone and the microphone 2 m from the façade were located at the centre of the building façade 1.65 m above ground level. For the measurements at the houses near Pearson Airport, the façade microphone was 2.1 m above the ground and located on the face of a brick building exterior.

Neither of the façade microphone results indicates a 6 dB increase independent of frequency. The average façade effect (façade microphone – outdoor microphone) at OATS is approximately 6 dB at higher frequencies but is less at other frequencies. At very low frequencies the façade microphone levels were on average more than 8 dB less than the expected +6 dB difference. Similar results occurred for the façade effect at the houses near Toronto airport. Mid-frequency differences between the façade and free field microphone results are similar to those from the OATS results. However at higher frequencies the differences are lower and do not reach the expected +6 dB. At very low frequencies there are again larger differences from the expected +6 dB difference and the

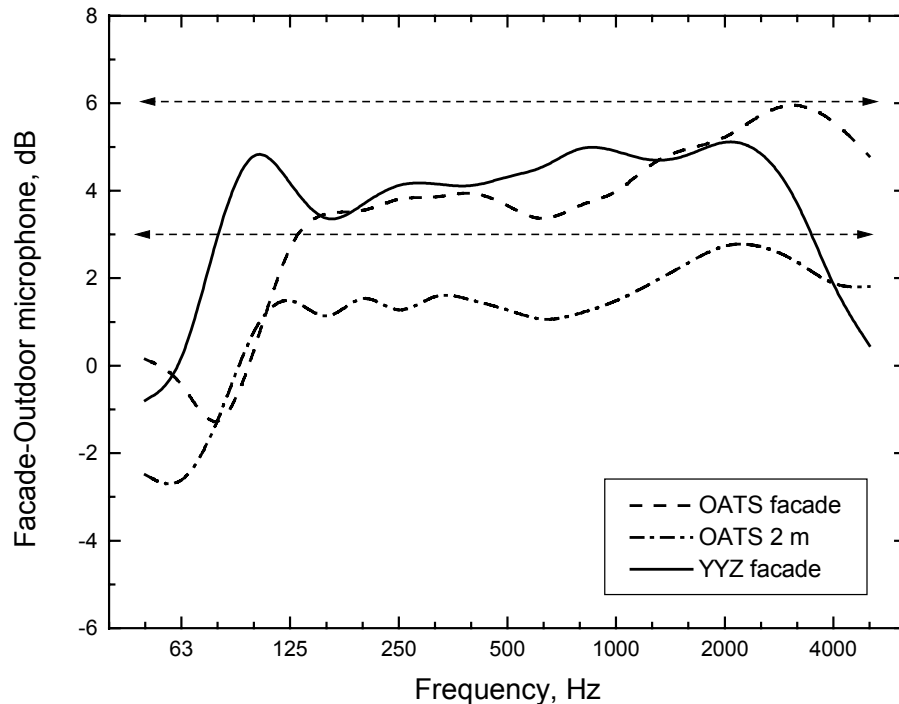


Figure 39. Average measured differences between façade microphones or a microphone 2 m from the façade and the free field outdoor microphone measurements.

dip in the curve is shifted lower in frequency than for the OATS results. The measured differences for the microphone 2 m from the façade are also less than the expected +3 dB difference. There are large deviations from expectations at very low frequencies and the measured differences do approach the expected +3 dB values at higher frequencies.

There are two different phenomena affecting the results in Figure 39. At low frequencies the combination of the direct and ground reflected sound leads to decreased sound levels at positions close to the ground and including the façade microphone positions. This is due to destructive interference of the direct and the ground reflected sound that is out of phase because it has travelled a slightly longer path. Because the low frequency sound levels at the façade microphone are decreased, the differences relative to the free field microphone shown in Figure 39 indicate a pronounced dip in the low frequency region. The dip is a little lower in frequency for the results from the houses near Toronto airport because the façade microphone was a little higher above the ground.

The second phenomenon that influences the façade microphone results is the effect of diffracted sound energy from the edges of the finite sized façades. This is also known to vary with the angle of incidence of the sound. Figure 40 shows that the measured façade effects at the OATS do indeed vary with angle of incidence. This graph was created by considering the measured façade effects for only one aircraft type to eliminate differences due to aircraft type. The measured façade effects for 23 different F28 aircraft fly bys were averaged in groups according to the vertical angle of the aircraft as they flew by the test house. There are large and complex variations of the façade effect that clearly vary with the vertical angle of the passing aircraft. These results suggest that for lower vertical

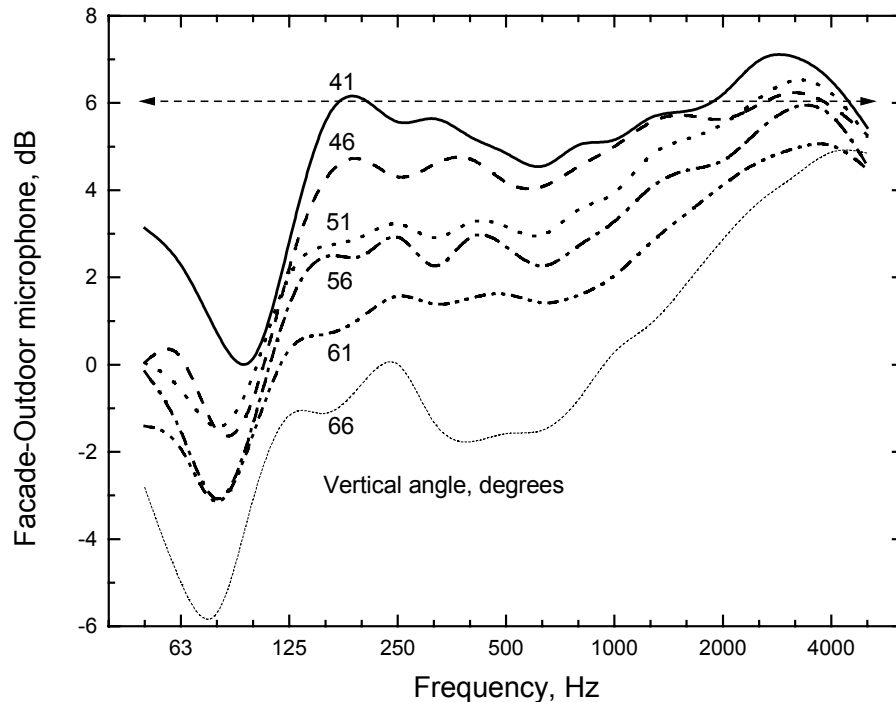


Figure 40. Measured façade effect at the OATS for F28 aircraft averaged over vertical angle groups.

angles of incidence the measured façade effects approach the expected +6 dB increases at frequencies above the low frequency dip due to ground reflections. Thus one might expect that for sources on the ground, the façade effect may well be close to the simple +6 dB expectation. However, for typical vertical angles of passing aircraft the façade effect is not +6 dB and varies considerably with frequency.

There were some indications that the measured façade effects varied a little with aircraft type. This might be due to differences in the directionality of the sound radiated by each aircraft type. However, although there is data on the horizontal directionality of aircraft noise (see Appendix II), there is no known information on the directionality of aircraft noise in the vertical plane perpendicular to the length of the aircraft.

To determine if similar variations with vertical angle of these façade effects occur for other aircraft types, an analysis similar to that shown in Figure 40 was performed for all aircraft types. The resulting average façade effects by vertical angle of the aircraft are plotted in Figure 41. The pattern of results is generally the same as for the F28 aircraft. There are again large effects of the vertical angle and not a simple +6 dB increase in sound levels at the façade. There are also detailed differences between the results for the F28 aircraft in Figure 40 and the averages over all aircraft types in Figure 41. The details of the directionality of the different aircraft types seem to further complicate the measured effects.

Measurements of sound insulation in the field, that use a façade microphone to assess the incident sound energy and that assume a +6 dB increase at the façade will underestimate the incident sound energy and the calculated noise reductions. Errors of 6

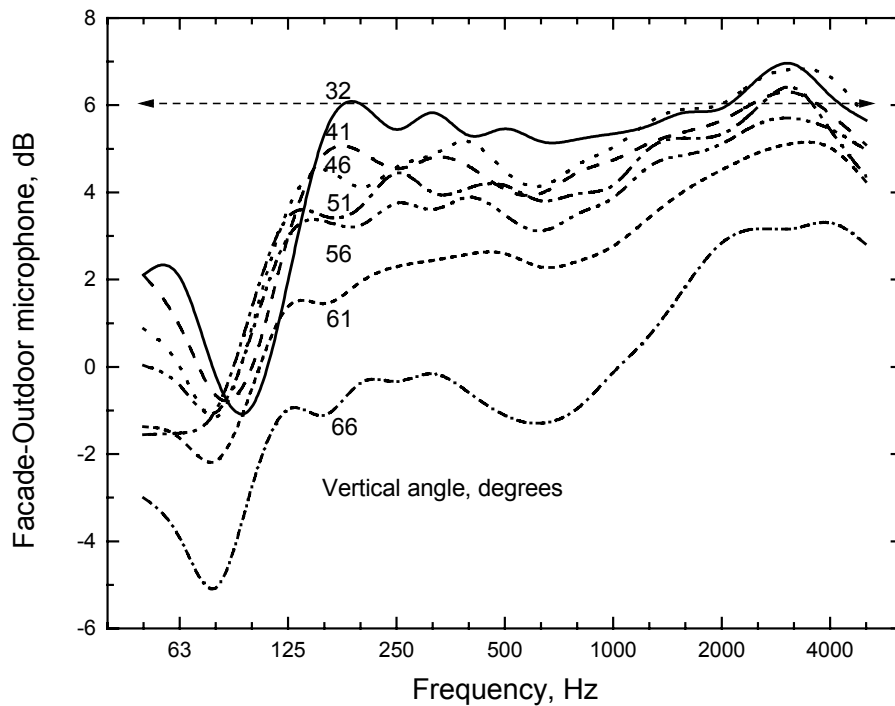


Figure 41. Measured façade effect at the OATS for all aircraft types averaged over vertical angle groups.

dB or more are possible at mid frequencies and larger errors will occur at lower frequencies.

To confirm the influence of diffraction effects and the variation of these effects with angle of incidence, measurements were made on a model façade in an anechoic room. The model façade was $\frac{1}{4}$ scale of the actual façade of the test house at Ottawa airport. Measurements were made using an omni-directional sound source and with a microphone located at the centre of the model façade and flush with its surface. The omni-directional sound source was moved by the measurement microphone in steps simulating a passing aircraft. This was repeated for several vertical angles of incidence. Façade effects were obtained by subtracting these façade measurements from measurements at the same position without the façade present.

The measured façade effects for the model are shown in Figure 42. Because it was a $\frac{1}{4}$ scale model, measurements were made at 4 times the full-scale frequencies. However, in Figure 42 results are plotted in terms of the equivalent full-scale frequencies and hence can be compared directly to the previous two figures. It was not possible to include results at higher frequencies because the measurement microphone was not capable of correctly recording the higher frequencies used in the model measurements.

The results in Figure 42 for the model façade again show complex variations with vertical angle of the sound source and tend to approach the simple +6 dB expectation for normal incidence of the passing sound source. The model is a simpler situation than the real building façade. The model did not include a ground surface and therefore the low frequency interference dip in the Figure 40 and 41 results is not present. The diffraction

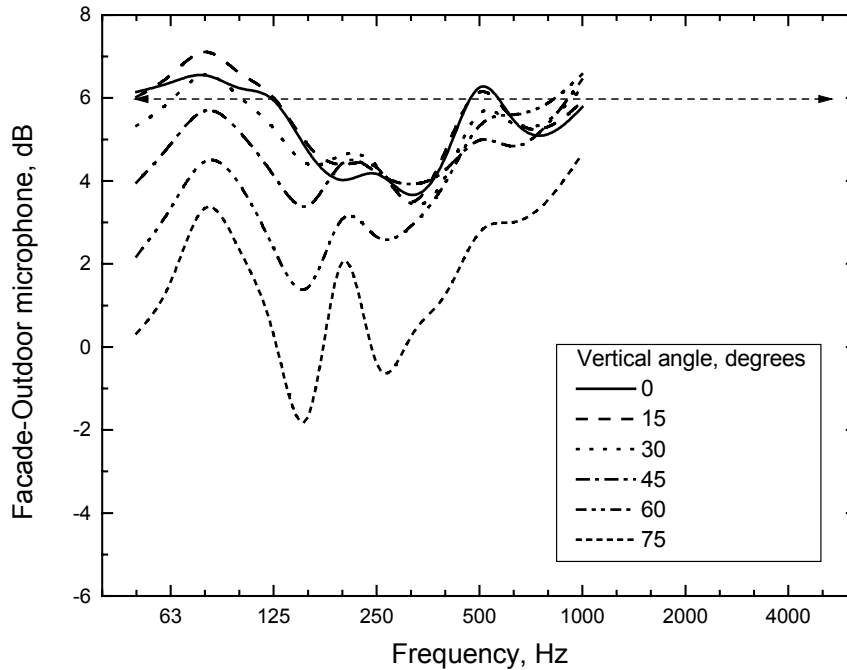


Figure 42. Measured façade effect for a 1/4 scale model façade for varied vertical angle. (plotted versus full scale frequencies).

effects will also be different because the model was a simple rectangular panel in a free field with no adjacent surfaces. The façade of the OATS was connected to the ground at the bottom and partly shielded by an overhanging roof at the top. Thus one would not expect the details of Figure 42 to match those of Figure 40 but again variations of 6 dB or more from the +6 dB expectation are evident.

The variation of the façade effect as a function of the vertical angle is examined in Figures 43 to 48. These plots compare the measurements for groups of F28 aircraft at each vertical angle with measurements from the model façade. They also show the expectation for a façade effect varying with a simple cosine relationship with the vertical angle. That is, the façade effect is calculated as,

$$10 \log (\cos(\text{vertical angle})) + 6 \text{ dB} \quad (4.1)$$

This predicts a 6 dB increase at normal incidence and decreasing façade effects as the vertical angle is increased.

The results in Figures 43 to 48 for frequencies from 63 Hz to 2000 Hz in octave intervals indicate a rough agreement with a simple cosine relationship that includes an offset at lower frequencies. The low frequency offset is due to the cancellation of low frequency sound energy due to interference with the ground reflected sound. If one determines the magnitude of this offset in each 1/3 octave band, one obtains an estimate of the spectrum of the effect of ground reflections similar to that in Figure 10. The measured results also suggest that the variation with angle decrease with increasing frequency.

The differences between free field incident aircraft noise levels and incident levels measured at the façade vary: with frequency, with aircraft type, and with the vertical

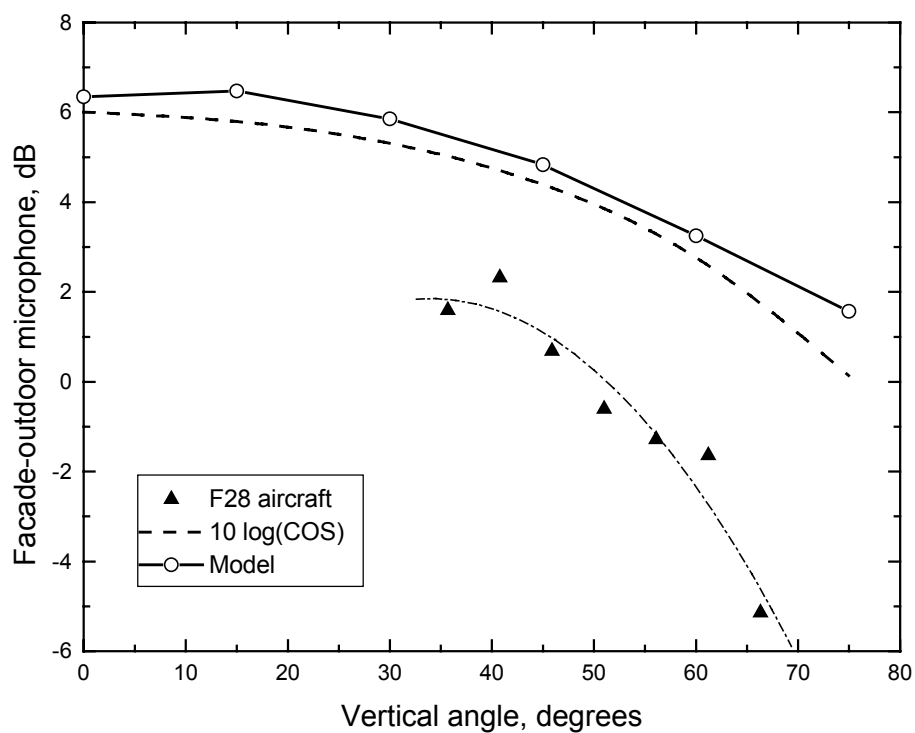


Figure 43. Façade effect versus vertical angle at 63 Hz.

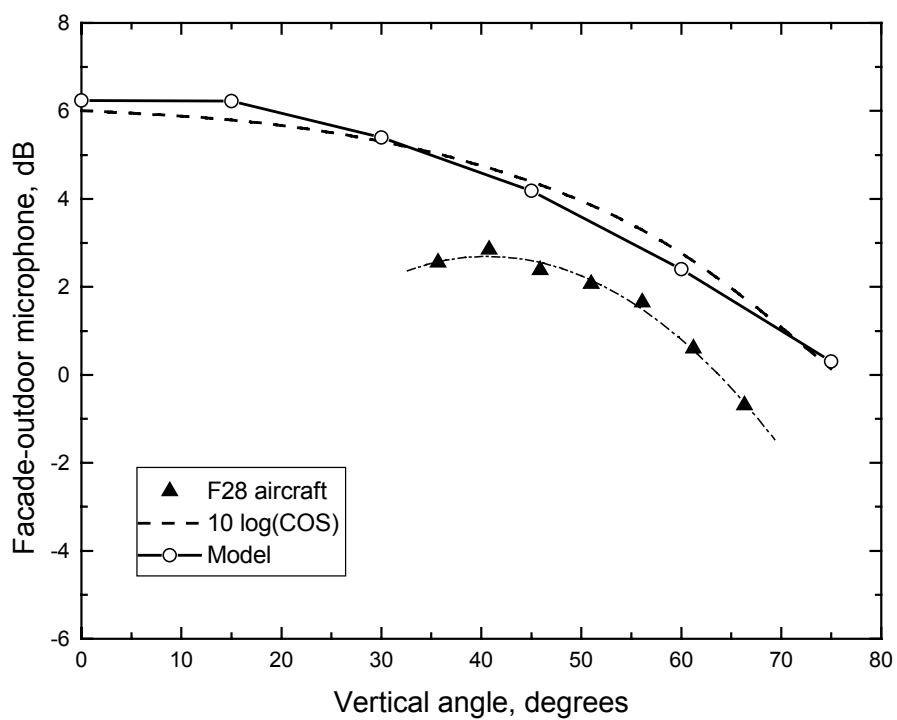


Figure 44. Façade effect versus vertical angle at 125 Hz.

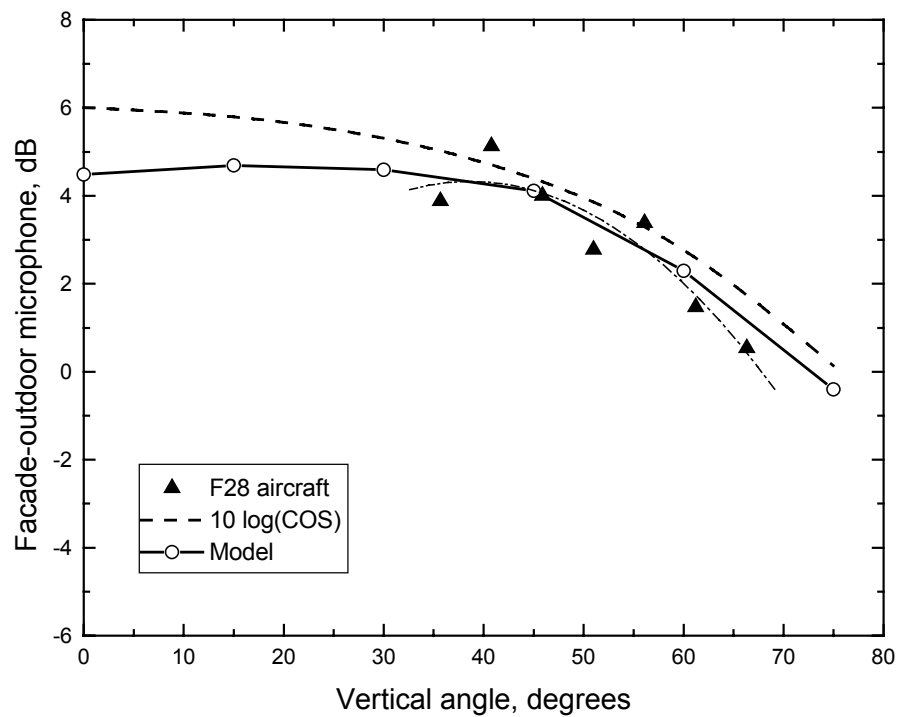


Figure 45. Façade effect versus vertical angle at 250 Hz.

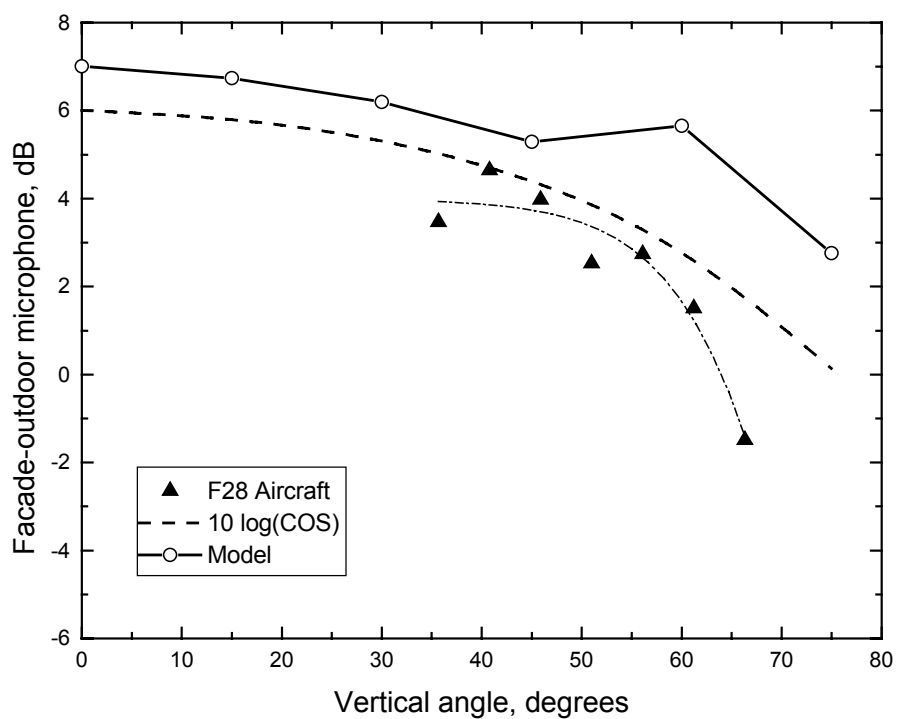


Figure 46. Façade effect versus vertical angle at 500 Hz.

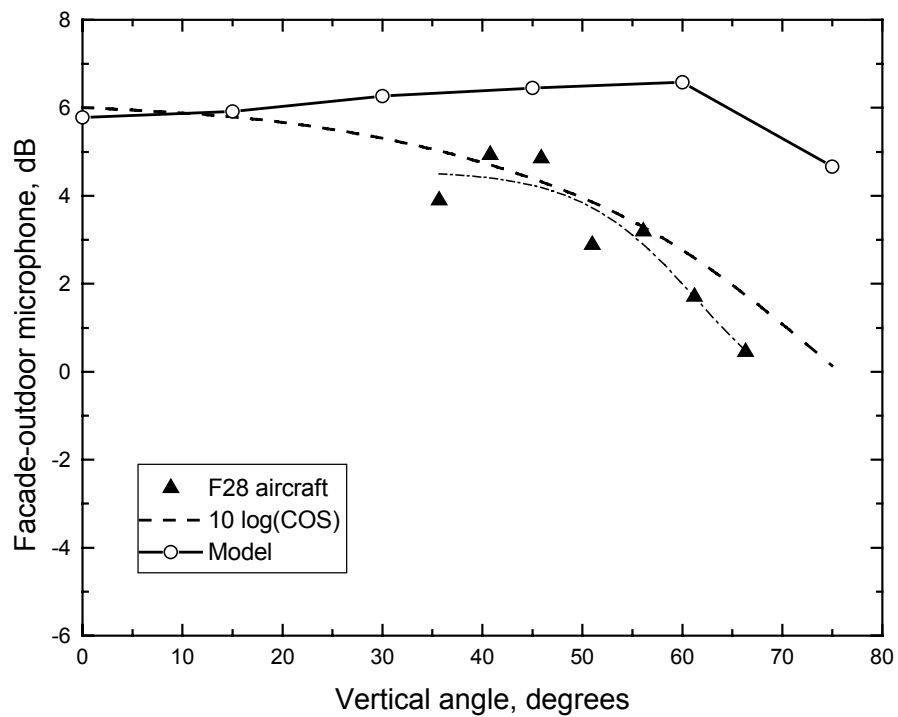


Figure 47. Façade effect versus vertical angle at 1000 Hz.

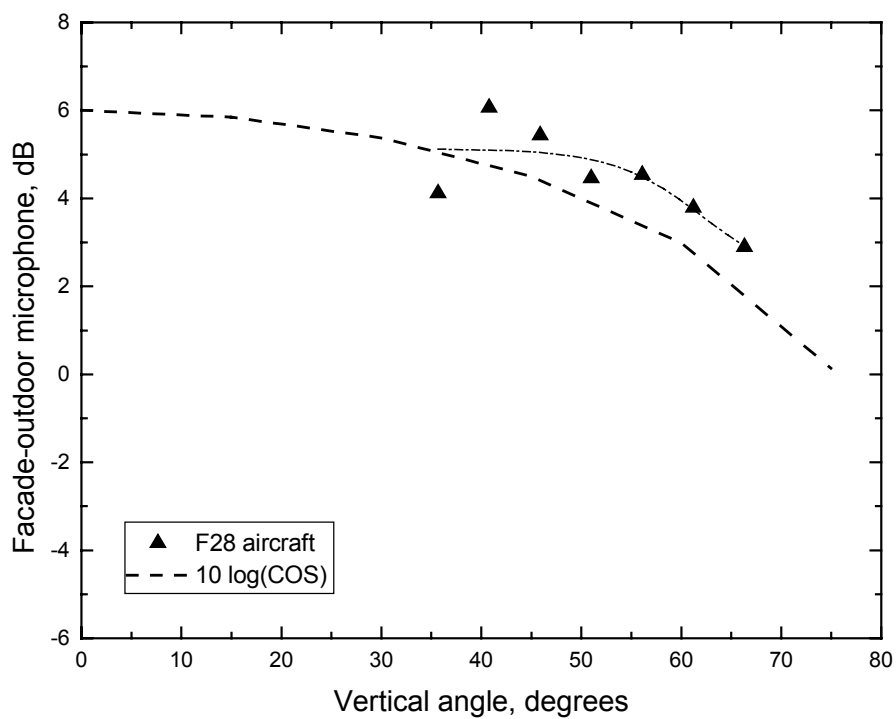


Figure 48. Façade effect versus vertical angle at 2000 Hz.

angle of the aircraft. Only for angles close to normal incidence and at higher frequencies do these differences approach the simple +6 dB expectation. Similarly measurements of incident sound levels at a point 2 m from the façade are probably influenced by the same factors and do not correspond to a simple +3 dB energy doubling relative to the free field case. Free field measurements of incident sound levels are to be preferred because they avoid these complex effects and it is unlikely that practical procedures could accurately correct for them.

4.3 Variation of Noise Reductions

The previous section discussed measurements of the variation of sound levels measured at the façade of the building. When compared with free field measurements of the incident aircraft noise, sound levels at the façade varied because of the effects of both ground reflected sound and diffracted sound from the edges of the façade. However these two different phenomena will not both affect the amount of sound transmitted into the building. Thus it is important to consider directly how measured noise reductions vary with the vertical angle of the passing aircraft. This section examines how the measured noise reductions vary with the vertical angle of the passing aircraft.

As equation (2.3) in section 2.5 indicates, we expect the measured noise reductions to vary as $10 \log\{\cos(\theta)\}$, where θ is the angle of incidence of the sound. For passing aircraft, the horizontal angle of incidence varies over a wide range of angles. However, the vertical angle varies over a smaller range of angles due to height changes as the aircraft climbs from takeoff. Because the measured aircraft noise levels are an integration over a wide range of angles (in the horizontal plane), the effects of angle of incidence may be somewhat averaged out. Also the variation of the vertical angle between aircraft events at a particular location generally vary over a relatively small range. Therefore observed effects due to varied angle of incidence are expected to be small if evident.

The data for four construction cases at the OATS were considered to investigate possible angle of incidence effects on measured noise reductions. These were cases #1, #2, #10 and #11 corresponding to only end walls exposed, only facing walls exposed, only end windows exposed, and only facing windows exposed respectively. (See also Table II for details of cases). For each of these configurations of the test house, measured noise reductions from individual aircraft events were plotted versus the recorded vertical angle of the aircraft as it passed the test house. Data from each receiving room at the OATS were plotted separately and this was done for each 1/3 octave band frequency. These measurement results were compared with a calculated variation with angle that added the following adjustment to the previously calculated noise reductions that were based on the levels integrated over complete passbys.

$$NR_c = NR + 10 \log\{\cos(\theta) / \cos(60)\}, \text{ dB} \quad (4.2)$$

That is the corrected noise reductions (NR_c) were corrected by assuming a cosine variation with vertical angle. The correction was normalised to 60 degrees because at this angle of incidence results are expected to approximate diffuse incidence results from laboratory tests [8]. For these measurements the maximum correction was only 1.5 dB.

Figure 49 plots the measured noise reductions for the case #2 configuration where the facing walls were exposed to the aircraft noise. Although there are some indications that the measured noise reductions may increase with increasing angle of incidence, the scatter in the data is probably as large as the expected effects. To test whether the measured values reliably indicate a variation with vertical angle, the measured noise reductions were correlated with the measured vertical angles. These linear correlations showed that only 17 of the 42 sets of measurement results (21 frequencies by 2 rooms) in Figure 48 were significantly related to vertical angle even at the significance level of $p < 0.1$. Thus there is only weak evidence to support the expected variation with vertical angle of incidence.

The results in Figure 50 for the case #1 configuration, corresponding to only the end walls being exposed, show fewer significant relationships between measured noise reductions and vertical angle. This is at least partly due to the smaller number of aircraft events. Only 12 of the 42 sets of measurement results indicated significant relationships at the $p < 0.1$ level and 11 of these were significant at the $p < 0.05$ level.

Figure 51 plots the measured noise reductions versus vertical angle of the aircraft for the case #11 configuration where only the facing windows were exposed. Of the four cases considered these results show the clearest variations with vertical angle. Of the 42 sets of measured noise reductions 30 were significantly related to vertical angle at the $p < 0.1$ level and 23 of these were significant at the $p < 0.05$ level.

The measured noise reductions are plotted versus vertical angle for the case #10 configuration in Figure 52. This configuration corresponded to end windows exposed to the aircraft noise and the facing walls masked. Only two of the 43 sets of measured data in this figure were significantly related to vertical angle at the $p < 0.1$ level of significance. This is again partly due to the limited number of aircraft events included in these comparisons.

The case #2 and case #11 results where the facing wall or the facing windows were exposed to the aircraft noise are perhaps the simplest cases where the exposed façade is exposed to the complete aircraft flyby. For these cases there is some evidence that measured noise reductions do vary with vertical angle of incidence for passing aircraft. For the end walls and end windows exposed cases, there is little evidence to confirm the expected effects. Because the expected effects are very small and generally no more than 1 dBA in magnitude, it would be very difficult to precisely confirm the effects with field measurements. There would have to be an order of magnitude increase in the number of aircraft events recorded for each configuration of the test house to reliably confirm such small effects. This could not be justified in view of the expected very small magnitude of these effects.

While the expected effects were not strongly confirmed, they are based on sound physical arguments. Therefore, the current results will be interpreted as not disproving the expected variation of noise reduction with the cosine of the vertical angle of incidence.

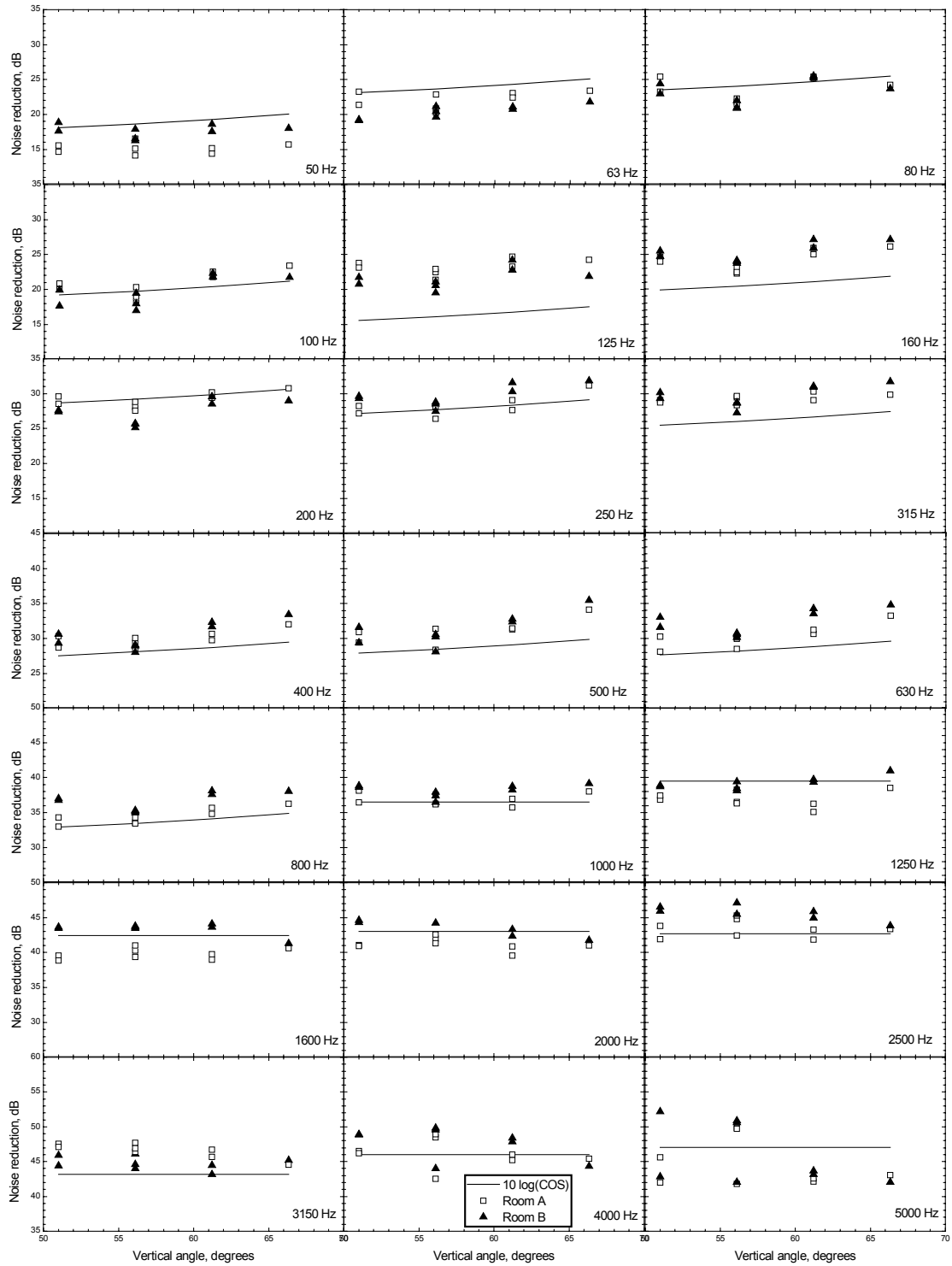


Figure 49. Measured noise reductions versus vertical angle for each room and each 1/3 octave band for Case #2 results (facing walls exposed).

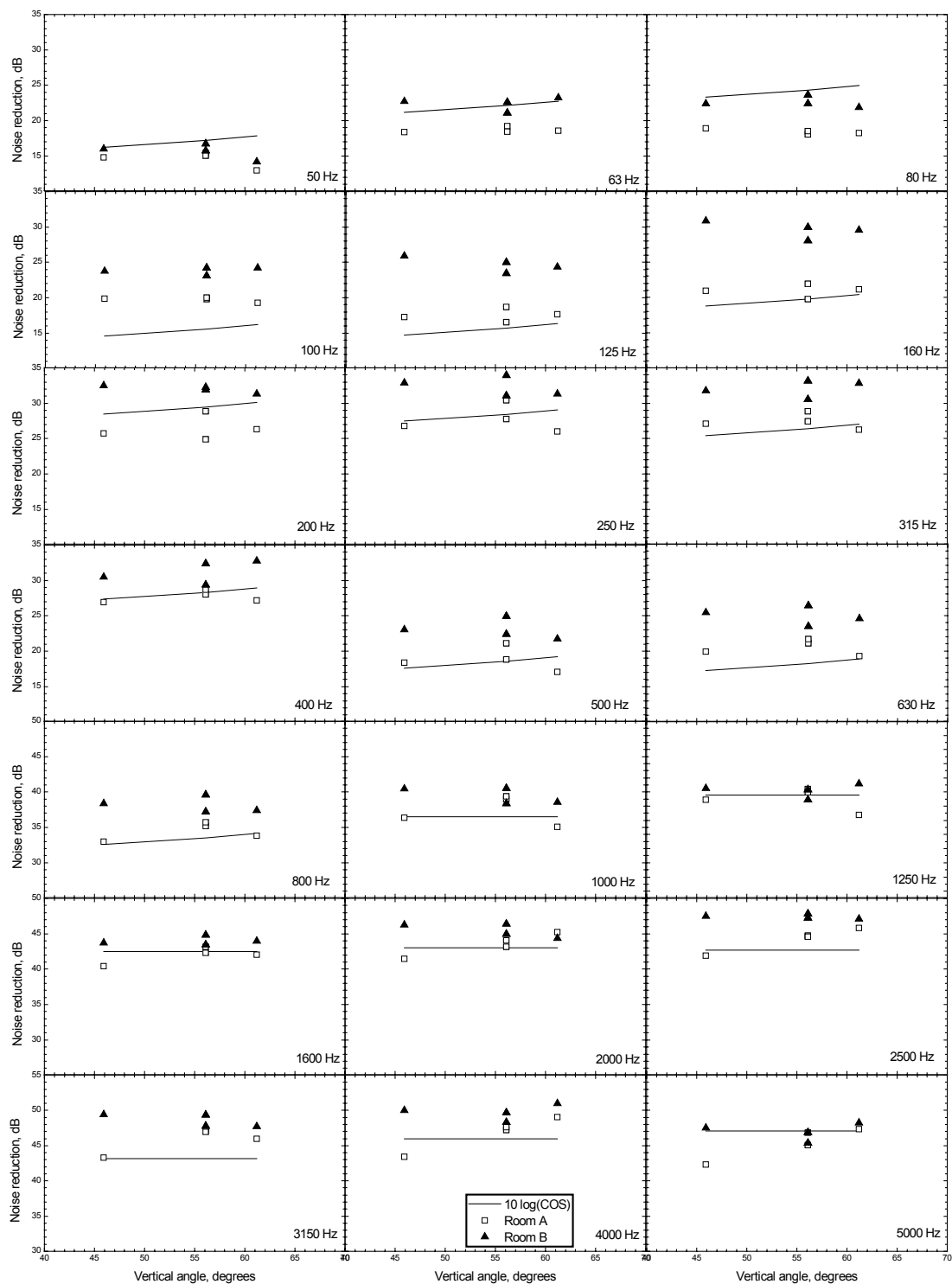


Figure 50. Measured noise reductions versus vertical angle for each room and each 1/3 octave band for Case #1 results (end walls exposed).

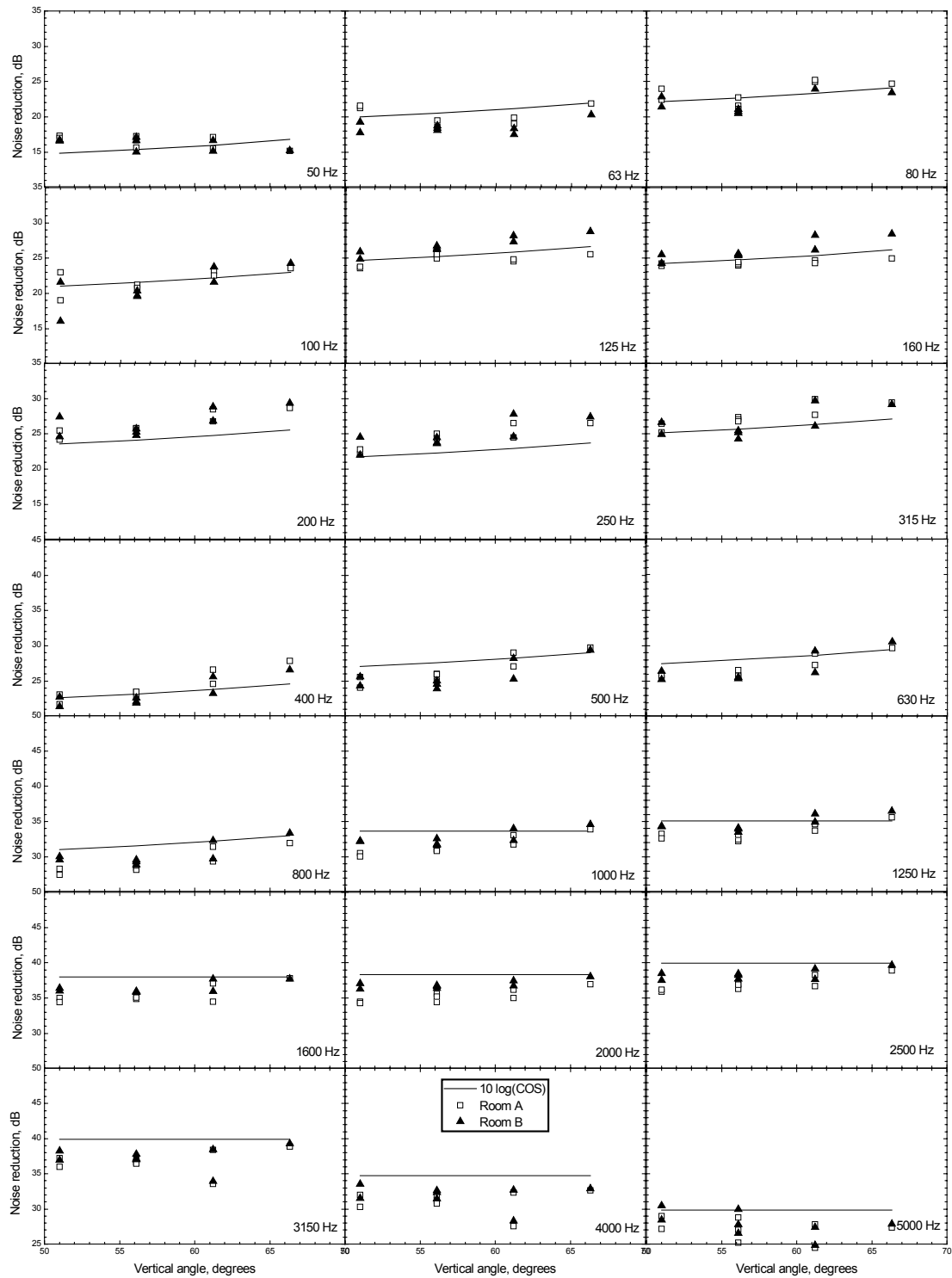


Figure 51. Measured noise reductions versus vertical angle for each room and each 1/3 octave band for Case #11 results (facing windows exposed).

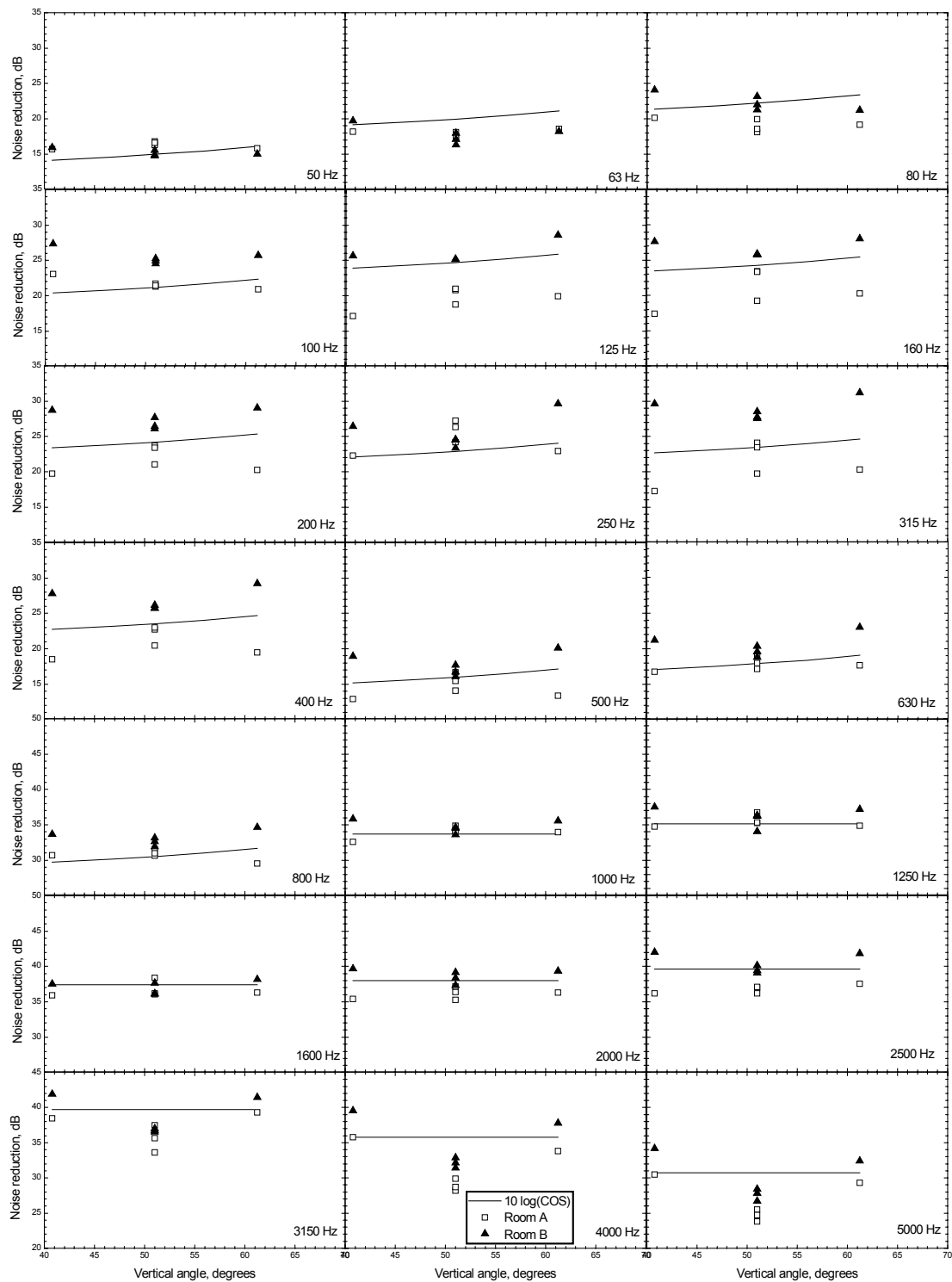


Figure 52. Measured noise reductions versus vertical angle for each room and each 1/3 octave band for Case #10 results (end windows exposed).

5. Façade Orientation Effects

5.1 The problem

The angular orientation of a façade relative to the aircraft flight path determines the fraction of the total aircraft sound energy from a complete aircraft flyby that is incident on that façade. The sound energy transmitted via each façade to indoors is expected to vary with the variation in façade orientation. The two rooms at the OATS were oriented so that their facing walls were parallel to the aircraft flight track and so were exposed to the complete aircraft flyby as illustrated in Figure 53. However, the two end walls were perpendicular to the aircraft flight track and so were exposed to only half of the complete aircraft flyby. It is usually assumed that the sound energy incident on a particular façade is proportional to the angular view of the complete flyby. The facing wall of each room is exposed to the complete flyby and Figure 53 illustrates that it has a 180 degree angular view of an ideal aircraft flyby. The end walls have a 90 degree angular view of the aircraft flyby. Thus the incident sound energy on the end walls would be expected to be half that incident on the facing walls or 3 dB less.

This simple angular view concept assumes an infinitely long and level aircraft flyby. That is, for the facing façade one is assuming that the aircraft is visible over the complete 180 degree angular view. This is not always true and was not true at the OATS. All aircraft were taking off and were not visible at the test house until an angle of incidence of about 70 to 80 degrees in the horizontal plane. Also the aircraft were climbing and so the propagating sound might be more attenuated initially when the aircraft was at lower heights. Therefore, there would be less incident sound energy on the approach and facing

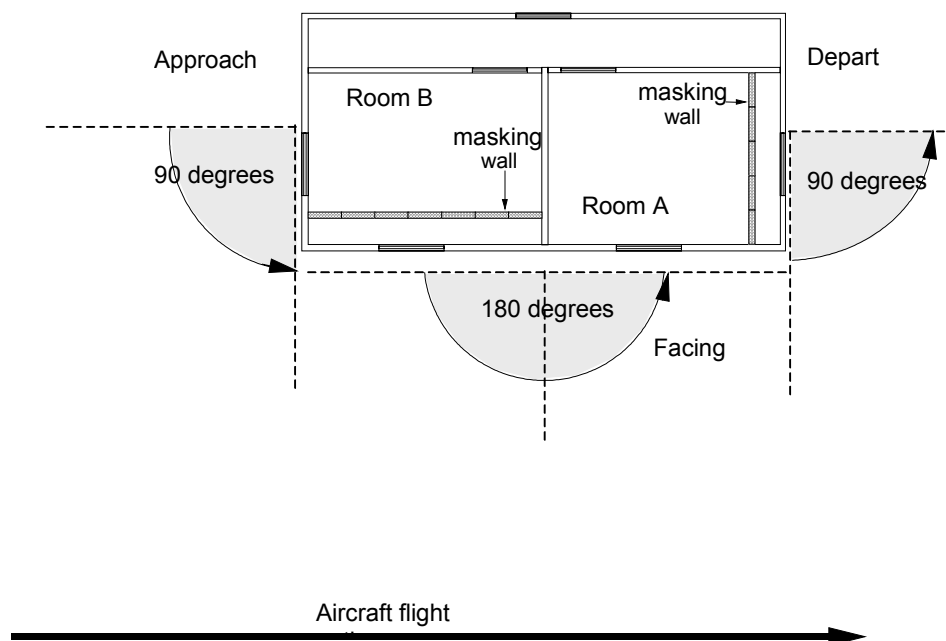


Figure 53. Angular view of aircraft flyby at approach, facing and depart façades.

walls than expected.

There are several other factors that make the situation more complicated. First, aircraft are not omni-directional sound sources. They radiate sound more strongly in some directions relative to others and this directionality varies with frequency. The Swiss lab EMPA has put a large effort into measuring the directionality of aircraft in the horizontal plane [18]. Some analyses of their data are included in Appendix II. In simple terms there is a tendency for modern commercial jet aircraft to radiate more sound energy to the rear than from in front which would tend to create higher sound levels at the depart façade than at the approach façade of the test house. However, there are significant differences between aircraft types.

As discussed in the previous section, the noise reduction of a façade is expected to vary with the angle of incidence of the sound. The orientation of the façade changes the angles of incidence and limits the range of possible angles for some façade orientations. Although the measured variations with vertical angle presented in the previous section were small, these may not fully represent the variations that could occur for the more extreme cases of the end walls where the higher sound levels are incident at near grazing incidence.

A further complication is that the effective angular view will be larger than the simple geometrical angular view because of diffraction effects. That is, for the end walls, sound will diffract or bend around the corner of the building and increase the total incident sound energy. This effect varies considerably with frequency.

5.2 The proposed approach and complications

Because of the complexity of the combination of factors influencing the sound energy incident on each façade, an experimental approach was taken to estimate façade orientation effects. It was first intended that the differences between the various measurement configurations would help to explain façade orientation effects. In addition, a special set of measurements was made at the OATS with microphones on the surfaces of all relevant façades of the building to directly measure the differences in incident sound energy. Finally, the EMPA data on aircraft directionality were used to calculate expected differences in incident sound energy due to the directionality of an average aircraft.

The various configurations of the test house (see Table II) were intended to make it possible to separately measure the indoor sound levels due to transmission through each façade. For example, the case #2 configuration used masking walls and an improved ceiling construction to block sound transmission thorough all paths except via the facing walls. The case #1 configuration was intended to only allow sound transmission via the end walls. The differences in the indoor sound levels for these two cases were expected to relate to the differences in façade orientation. Similarly the differences between the indoor sound levels for the case #11 (facing windows exposed) and case #10 (end windows exposed) would give another estimate of the effect of façade orientation.

This experimental approach was compromised by the unexpected importance of flanking paths in the test house. Although the average effects of these flanking paths have been estimated, it seems unlikely that they can be determined with sufficient accuracy for two

separate measurement cases to make it possible to estimate façade orientation effects of a few decibels in magnitude from differences between the two cases.

To get a second set of results that would estimate the effects of façade orientation on indoor sound levels, measurements were made with microphones on the exterior surfaces of all key façades of the test house. It was intended that these would directly estimate the differences in incident sound energy on the facing and end walls. This experiment was also compromised. The unexpected importance of ground reflections and façade effects creates larger errors than the expected façade orientation effects. As discussed in section 3.1.2, ground reflections decrease the incident sound energy at lower frequencies. The magnitude of these effects has been estimated but it is not possible to determine precisely how these effects would vary with façade orientation. The new results in this report also establish that incident sound levels measured at the façade surface are not a reliable indicator of the incident aircraft noise because they vary in a complex manner with frequency and angle of incidence.

The third possible approach would be to use the EMPA aircraft directionality data to calculate estimates of the differences in incident sound energy at the different façades of the test house. The EMPA data can be used to estimate differences in sound energy radiated from the aircraft but do not include the effects of ground reflections and flanking paths in the building and so such calculations would not accurately relate to the measured indoor sound levels.

Because the expected façade orientation effects are only a few decibels in magnitude, it is difficult to get reliable estimates from either of the measurement approaches. Both experimental approaches would derive estimates of façade orientation effects from differences of measurements either for different measurement cases or at different façades of the building. Attempts to estimate the corrections for either flanking paths or façade effects from these differences would almost certainly introduce large errors. The following section presents the results of these experiments and proposes a practical solution to estimating the effects of façade orientation.

5.3 Measurement results

Three types of data will be presented to illustrate the effects of façade orientation. Two were mentioned above. The third set of data was obtained from measurements of sound insulation in several rooms of a building at Vancouver International Airport (YVR) [12]. One face of the building was parallel to the runway and approximately beside the point of lift off for the aircraft taking off. The other façade of the building was perpendicular to the runway. Because the construction for rooms on both façades was the same, the differences between noise reduction measurements for rooms on both façades were used to estimate façade orientation effects. Because the measurements were made only in second floor rooms of this building, the effects of ground reflections should be minimal. These average differences are shown in Figure 54.

A simple angular view argument would suggest that all of these differences should approximate 3 dB independent of frequency. The best fit linear regression line suggests that the mean difference increases from about 1 dB at low frequencies to 3 dB at high frequencies. This is physically reasonable because diffraction effects would be expected to decrease the difference at lower frequencies. However, there is a large amount of

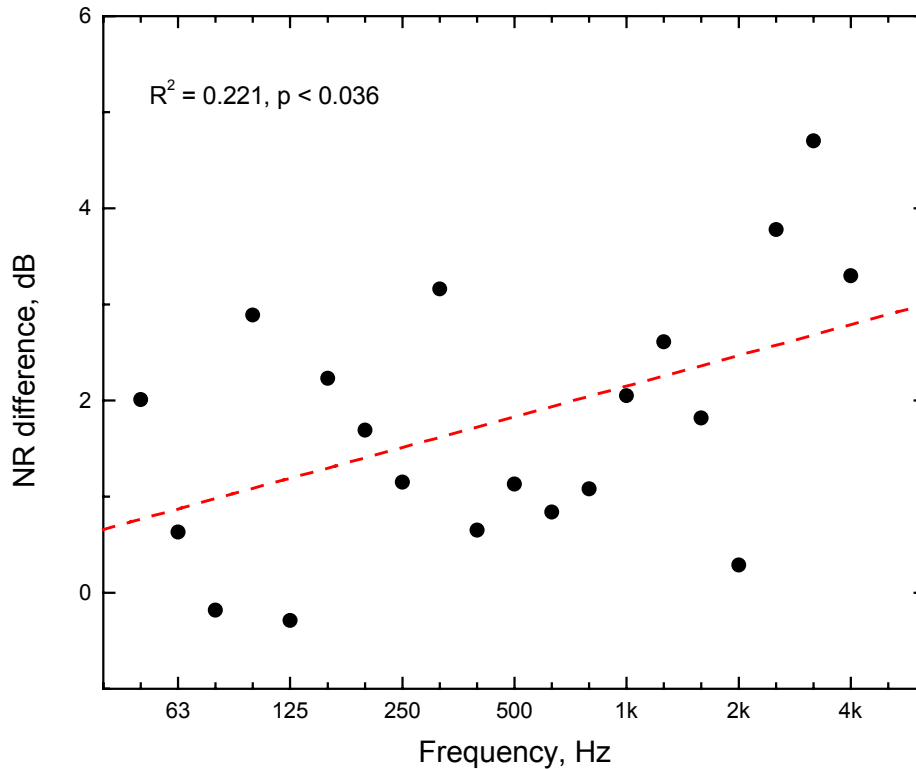


Figure 54. Noise reduction differences for depart façade – facing façade at Vancouver airport building.

scatter and one might also argue that using a simple average value would be adequate. The average difference over all frequencies for the data in Figure 54 is 1.8 dB. The actual angular view of the aircraft at the facing façade was estimated to be 160 degrees and not 180 because of the point at which the take off started. The expected effect of angular view would then be $10 \log\{90/160\}$ or 2.5 dB rather than 3 dB.

The second type of data intended to explore façade orientation effects was obtained from recorded aircraft events with microphones on the relevant façade surfaces of the OATS. Examples of these data are plotted both versus time and versus frequency. Figure 55 plots the overall A-weighted sound levels at each façade as a function of time while a DC9 aircraft was passing the test house. The levels at the facing façade microphone, at the roof, and at the outdoor microphone follow a similar pattern and peak at about the mid-point of the recording. The levels recorded at the approach façade reach a maximum sooner than this and are reduced for the depart half of the recording on the right hand side of the graph. Conversely the levels at the depart façade are reduced during the approach half of the recording but are higher than the other microphone positions during the departure half of the recording. If one examines the time histories in individual frequency bands the results are much more complicated than indicated in Figure 55. Clearly the spectrum of the incident sound is varying with time as well as the overall sound levels.

Figure 56 compares the average measured spectra at the same measuring points as in Figure 55. These are the averages of results that were integrated over several complete

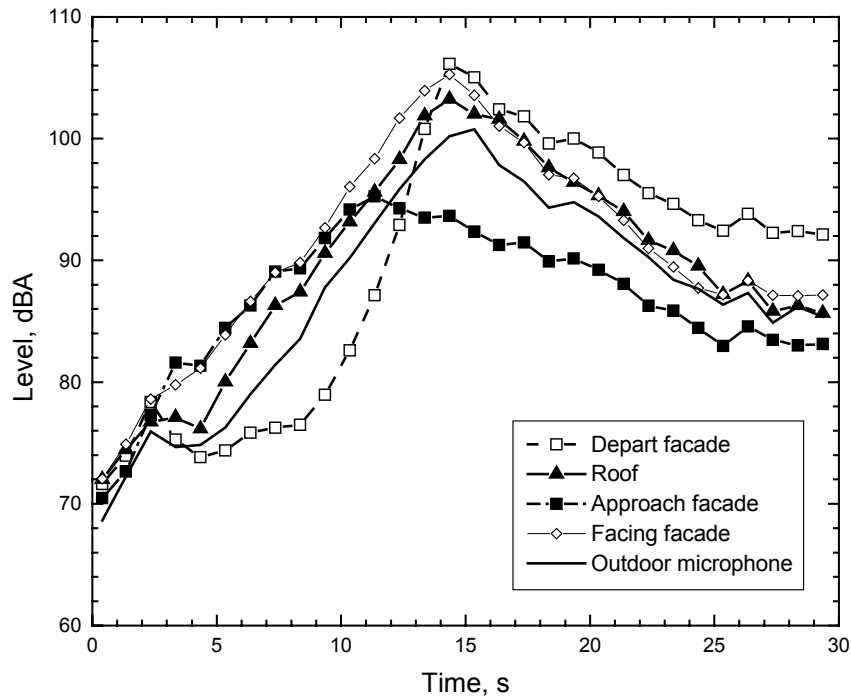


Figure 55. A-weighted sound levels recorded at each façade and at the outdoor microphone position versus time during a flyby of a DC9 aircraft.

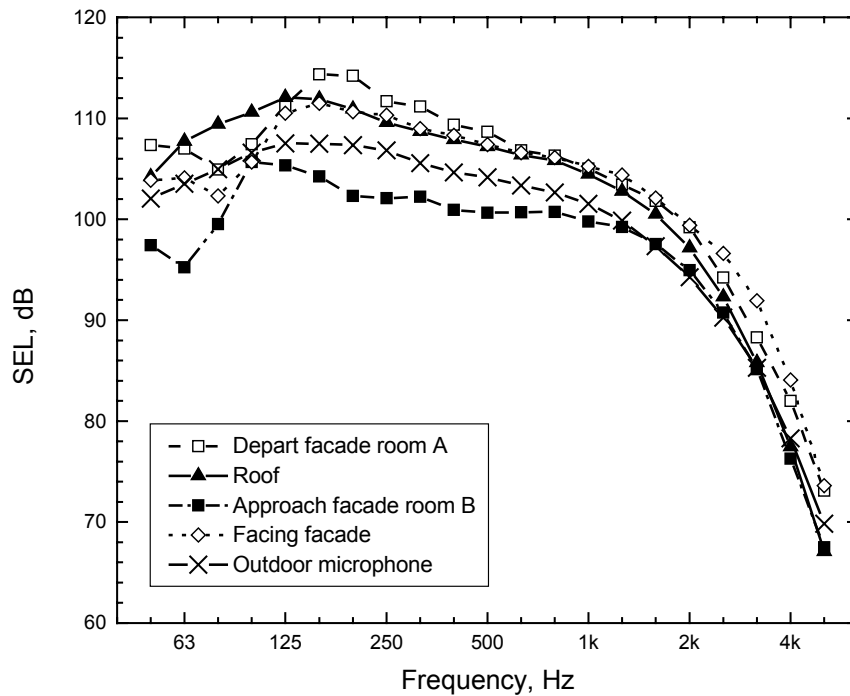


Figure 56. Comparison of aircraft noise spectra at each façade and at the outdoor microphone position averaged over several aircraft flybys.

aircraft flybys. There are large differences between the various measurement points and they tend to be larger at mid and lower frequencies. The approach and depart façade results are most different with differences of up to 12 dB. Although these differences are partially due to façade orientation, other effects further complicate the differences. The diffraction effects, illustrated in Figures 40 to 42, would be different for each façade because of different angles of incidence and different façade dimensions.

The measured spectra at the roof and at the facing wall are very similar at mid frequencies. This may indicate that there are similar ranges of angles of incidence for these two surfaces and hence integrated over a complete passby incident levels are similar. There are differences at the lower frequencies and again the sound levels at the facing façade are about 8 dB less than at the roof at 80 Hz. This is further proof the ground reflected sound leading to reduced low frequency levels at the facing façade. This effect is not expected to occur at much higher receivers such as on the roof. The average results at the approach and depart facades in Figure 56 are most different. Levels at the depart façade are greater than at the facing façade even though the depart façade is only exposed to one half of the complete passby. Because the approach and depart facades are symmetrically positioned relative to the flight track, the differences between the measurements at these two facades must be largely due to aircraft directionality. (That is, noise levels tend to be higher to the rear of the aircraft relative to the front).

The third type of measurement results were derived from the differences of the indoor sound levels for the various configurations of the test house. Indoor sound levels were calculated using the standard aircraft noise source spectrum and by adding the measured noise reductions. In this way the indoor sound levels between the different configurations of the OATS can be compared. Differences in indoor levels between the case #2 (facing walls exposed) and the case #1 (end walls exposed) can be used to examine the effects of these two different façade orientations. This, of course assumes, that other differences between the two cases are minimal. By examining the differences for each room of the OATS separately, one can separately consider differences for both approach and depart façades. In addition the same comparisons can be made for differences between the case #11 (facing windows exposed) and the case #10 (end windows exposed) configurations of the test house.

Figure 57 compares these estimated differences in normalised indoor sound levels for the depart wall side of the test house (room A) with several other results. These include the 3 dB difference expected from simple angular view arguments and the best fit line to the Vancouver data (YVR) from Figure 54. Also shown is the expected difference in incident energy from the EMPA aircraft directionality data. The average directionality of aircraft types measured at the OATS is calculated in Appendix II. By combining these average directionality values with expected variations with distance, the expected incident energy in the approach and depart halves of the passby were compared to the total passby. (See also Figure AII-2 Appendix II). This difference curve from the EMPA data does not include additional effects of ground reflections and façade diffraction.

There is not good agreement among these various difference curves. The differences from the wall and window measurement cases are in closest agreement and tend to roughly increase to close to +3 dB at higher frequencies. The Vancouver results [12] approximately agree with these measurement differences at the OATS except for

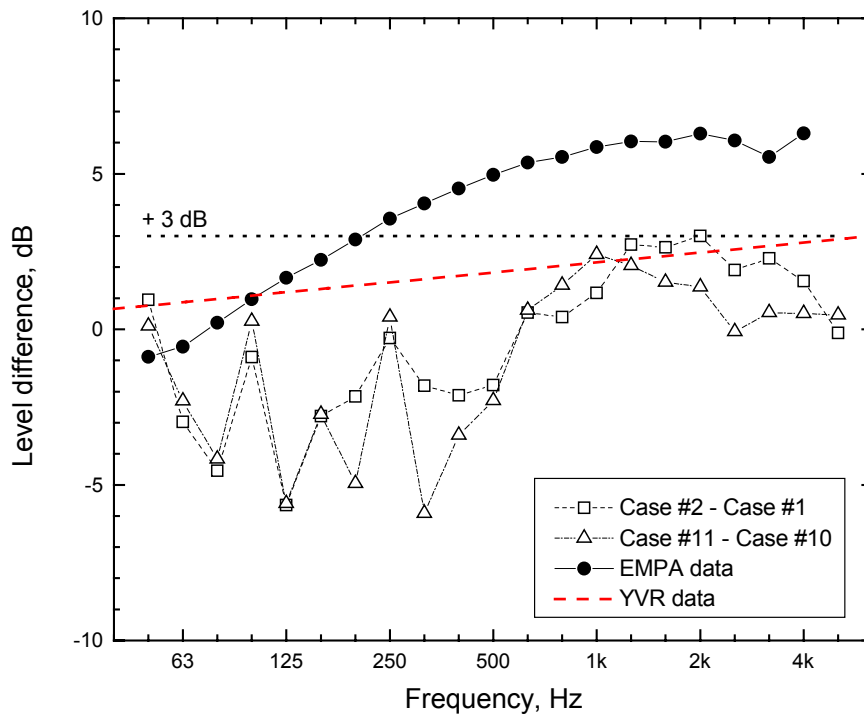


Figure 57. Calculated differences in normalised indoor sound levels to show differences between facing and depart façade cases.

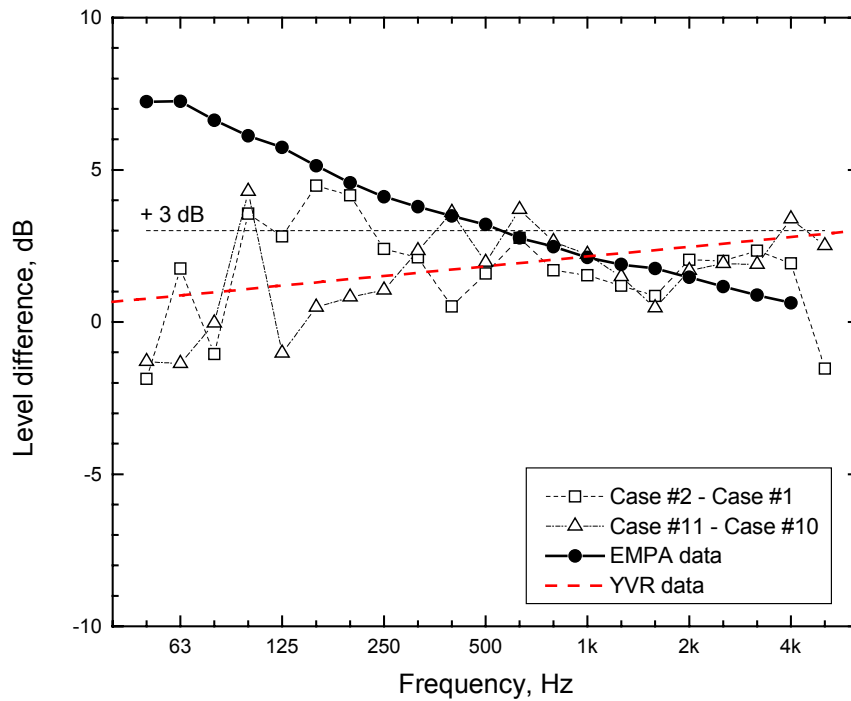


Figure 58. Calculated differences in normalised indoor sound levels to show differences between facing and approach façade cases.

differences at lower frequencies that were only present at the OATS and that were presumably mostly due to ground reflection effects. (Ground reflection effects did not occur at the Vancouver airport building site because only second floor rooms were measured). The differences from the EMPA data suggest larger differences at higher frequencies. This may indicate that the average aircraft directionality calculated in Appendix II is not representative of the aircraft recorded at the OATS. For example, the recordings at the OATS included many A319 and A320 aircraft which are more omnidirectional than most older aircraft types according to the EMPA data.

Figure 58 shows similar comparisons for the approach façade relative to the facing façade. This plot again includes the +3 dB expected from the simple angular view arguments as well as the best fit line to the Vancouver data (YVR). For these comparisons, the differences between the facing wall and the approach wall exposed cases (Case #2 – Case #1) are roughly 0 to 3 dB at most frequencies and roughly agree with the Vancouver best fit line. However, the differences between the facing window and approach window cases (Case #11- Case #10) do not agree well with the wall difference data or with expectations. Again the predictions from the average aircraft directionality do not agree well with the various measurement differences.

As suggested earlier, various other factors have larger influences on the various measurements, intended to estimate façade orientation effects, than the façade orientation itself. None of the experimental results provide completely convincing evidence that can precisely define the effects of façade orientation on the resulting noise reductions. The best fit regression line to the Vancouver results provides a rough but reasonable estimate of the expected effect of façade orientation and is based on reliable measurements that were not complicated by ground reflection effects or by structural flanking in the building. (The building had concrete exterior panels and sound transmission through the windows was clearly the dominant path). The YVR best fit regression line is also in rough agreement with 3 of the 4 sets of measurement differences from OATS shown on Figures 57 and 58 except where lower frequency interference effects complicate the results. Thus although the details are fuzzy, using the Vancouver relationship is judged to be a reasonable and conservative basis for estimating façade orientation effects.

6. Aircraft Source Spectra

In order to estimate indoor sound levels in buildings exposed to aircraft noise, it is necessary to determine representative spectrum shapes for various types of aircraft noise. These should be representative of the incident sound energy averaged over complete aircraft flybys and for free field conditions (i.e. excluding the influence of reflecting surfaces). Free field measurements of aircraft noise were made at the OATS as well as near Toronto and Vancouver airports with a microphone mounted on a mast 8.5 m above ground level and away from other reflecting surfaces. These data are used to derive suitable aircraft noise spectrum shapes representative of modern aircraft types. As no measurements of helicopters were made, a helicopter noise spectrum shape is derived from data reported by the US FAA [13].

6.1 Average measured spectra

The outdoor microphone recordings of all aircraft events at the OATS were averaged by aircraft type. These average outdoor SEL spectra for nine different jet aircraft models are plotted in Figure 59. Most are smaller twin-engine commercial jet aircraft. The older F28, DC9 and B737 aircraft spectra in Figure 59 group closely together and will be used to create an average spectrum for these older types which will be referred to as corresponding to ICAO type Chapter 2 aircraft. The quieter F100, A319, A320 and BA146 aircraft are mostly newer aircraft and these form a second group of similar spectra. This second group will be used to create a second average spectrum referred to as Chapter 3 type. The larger B767 aircraft, although they are newer Chapter 3 types, are noisier than the group of smaller Chapter 3 aircraft. Finally the CRJ regional jet aircraft

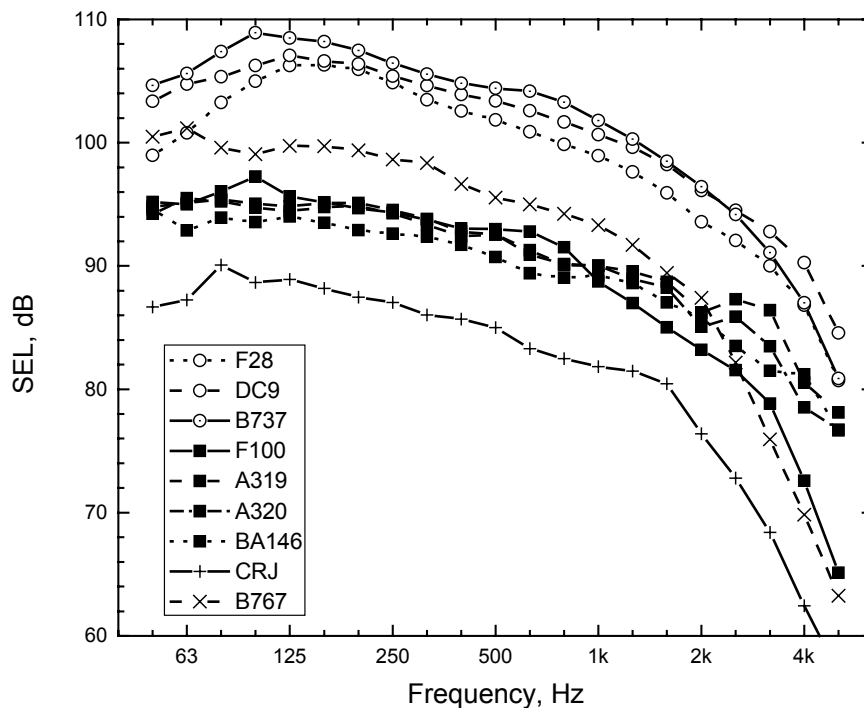


Figure 59. Average outdoor aircraft spectra by aircraft model for departing aircraft measured at the OATS.

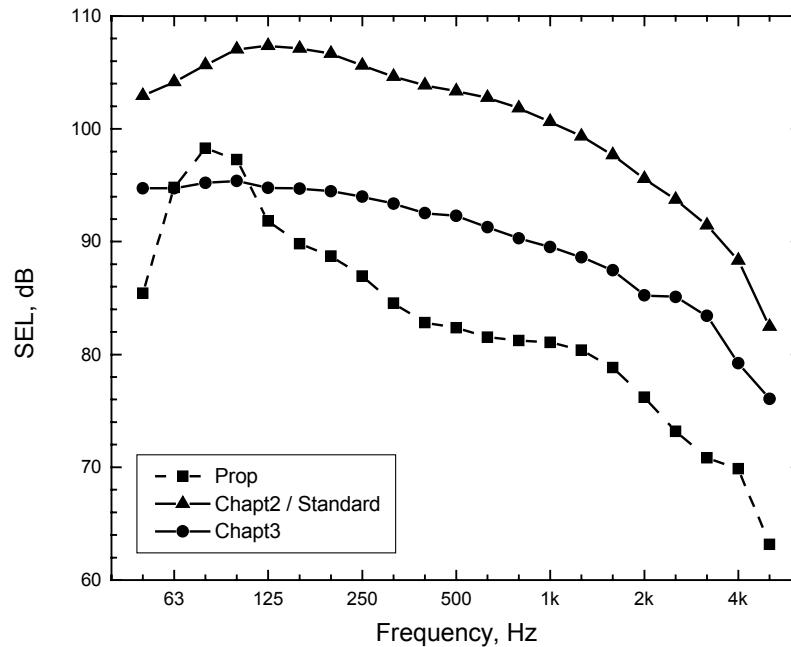


Figure 60. Average outdoor aircraft spectra for three groups of aircraft types from measurements at the OATS.

are quieter than all of the other aircraft models shown in this plot.

Figure 60 shows the calculated average source spectra for various groups of aircraft. These included the averages of the smaller Chapter 2 and the smaller Chapter 3 aircraft from Figure 59. They also show an average for propeller aircraft which were mostly Dash 8 aircraft. The Chapter 3 average spectrum indicates that these aircraft are much quieter than the Chapter 2 aircraft and also that the spectrum shape is flatter. That is, compared to the mid-frequencies the very low and very high frequency levels are relatively higher for the Chapter 3 aircraft. Although indoor levels from the Chapter 3 aircraft will be lower because they are generally much quieter, their spectrum shape suggests that it is even more important to obtain adequate low frequency sound insulation. The propeller aircraft are quieter than the jet aircraft at most frequencies but have higher levels in the low frequency bands from 63 to 100 Hz. Again, adequate low frequency sound insulation is required to minimise the intrusion of this predominantly low frequency noise from the propeller aircraft.

6.2 Air absorption and distance corrections

The average outdoor aircraft noise spectra measured at the OATS are for smaller commercial jet aircraft types. Larger aircraft would produce higher sound levels. Recordings that included larger aircraft were obtained near Toronto and Vancouver airports. Unfortunately the aircraft types were not identified because many of the measurements were made in the evening after dark. The measurements near Vancouver and Toronto airports were also at different distances from the aircraft flight track. This would affect the overall noise levels and would also lead to greater air absorption at the higher frequencies depending on temperature, relative humidity and distance [14,15]. The average of the outdoor aircraft noise levels obtained near Vancouver and Toronto airports are shown in Figure 61 along with the average Chapter 2 spectrum from Figure 60.

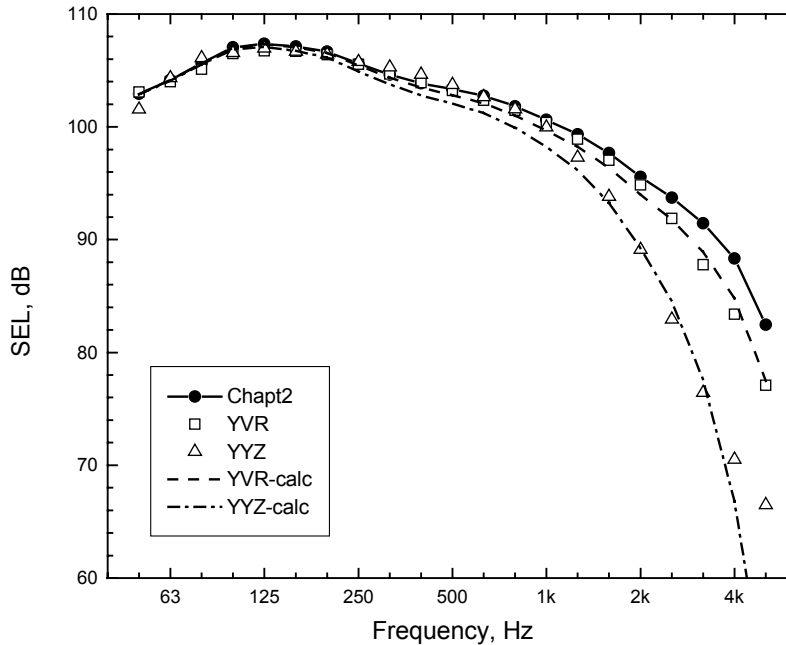


Figure 61. Comparison of average Chapter 2 spectrum from measurements at the OATS with normalised average spectra from Vancouver (YVR) and Toronto (YYZ).

In Figure 61, the Vancouver and Toronto data have been normalised to align with the OATS Chapter 2 average spectrum at lower frequencies. They are seen to be different at higher frequencies. It is proposed that the Chapter 2 average spectrum for smaller aircraft is a reasonable average of all aircraft types when larger aircraft are included and that the differences in Figure 61 are simply due to differences in air absorption. This was tested by adding the expected additional air absorption to the Chapter 2 spectrum to calculate the expected spectrum shapes for the Vancouver and Toronto data. These calculated results are also shown in Figure 61 and are in good agreement with the measurements made at Vancouver and Toronto. The distances, temperature and relative humidity associated with each set of measurements is given in Table IV.

Airport	Distance	Temperature	Relative Humidity
YOW (OATS)	240 m	20	50%
YVR	480 m	15	90%
YYZ	1000 m	10	80%

Table IV. Measurement distance, temperature and relative humidity associated with the measurements at Ottawa (YOW), Toronto (YYZ) and Vancouver (YVR).

The average aircraft spectra from OATS for smaller Chapter 2 and Chapter 3 aircraft can be used where the aircraft are known to match these precise categories. Similarly the propeller aircraft source spectrum can be used for commercial aircraft similar to Dash 8 aircraft. In general the Chapter 2 aircraft source spectrum can be used for all medium to large airports to represent a mix of various sizes of commercial jet aircraft. This will be used as the ‘standard’ aircraft noise spectrum shape and its shape should be adjusted to account for variations in air absorption with distance, temperature and humidity.

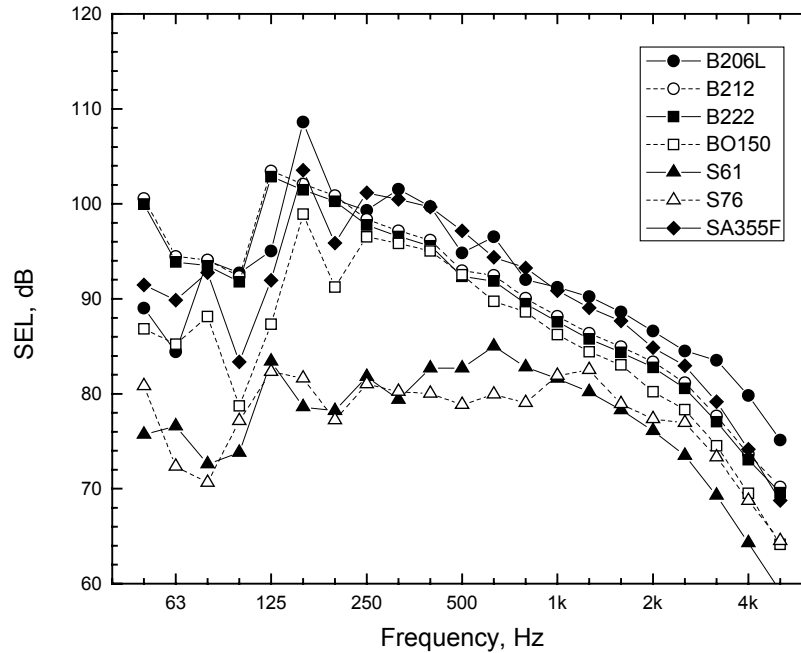


Figure 62. Comparison of 7 helicopter flyover spectra representative of Canadian helicopter operations.

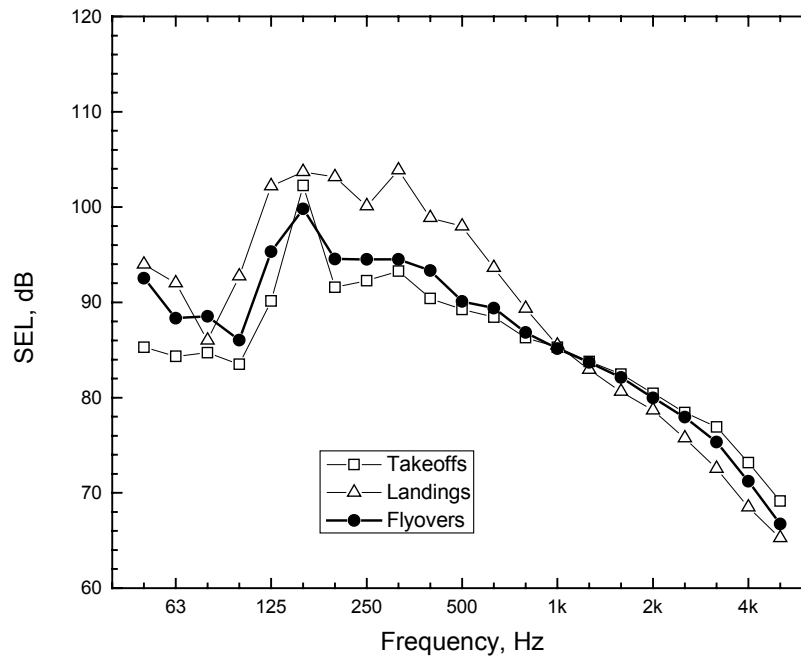


Figure 63. Comparison of average helicopter spectra for, takeoffs, landings and flyovers.

6.3 Helicopter source spectra

No measurements of helicopters were possible and so a helicopter aircraft noise spectrum was derived from published measurements of helicopter spectra for 16 types of helicopters [13]. The FAA measurements were made at a distance of 305 m and at the point corresponding to the maximum A-weighted level. That is, they are not integrated

over a complete passby as were our measurements. The data included 1/3 octave band levels and are normalised to the same value at 1000 Hz. The normalisation shift was first reversed [19] to produce absolute sound level spectra. The 7 dB was added to these maximum levels to approximate SEL values (based on observed differences between maximum levels and SEL values at the OATS). Seven of the helicopter spectrum types were found to be representative of Canadian helicopter operations [20]. The 7 spectra are shown in Figure 62.

The spectra shown in Figure 62 are for helicopters flying by the measurement point. Measurement results were also published for helicopters taking off and helicopters landing. The calculated average spectrum of the 7 types of helicopters and for each of these 3 conditions are given in Figure 63. The helicopters are most noisy when landing, while flyovers and landings have similar levels. The average ‘flyover’ spectrum from Figure 63 will be used as the representative helicopter noise spectrum shape.

6.4 Comparisons of new average spectra with other spectra

It is proposed to use the smaller Chapter 2 aircraft spectrum as the general ‘standard’ commercial jet aircraft source spectrum as explained above. Where more precise information on aircraft types is known, separate average spectra are available for smaller Chapter 2 aircraft, smaller Chapter 3 aircraft, propeller aircraft and helicopters. The four new average spectra are shown in Figure 64. There are obvious differences in the overall

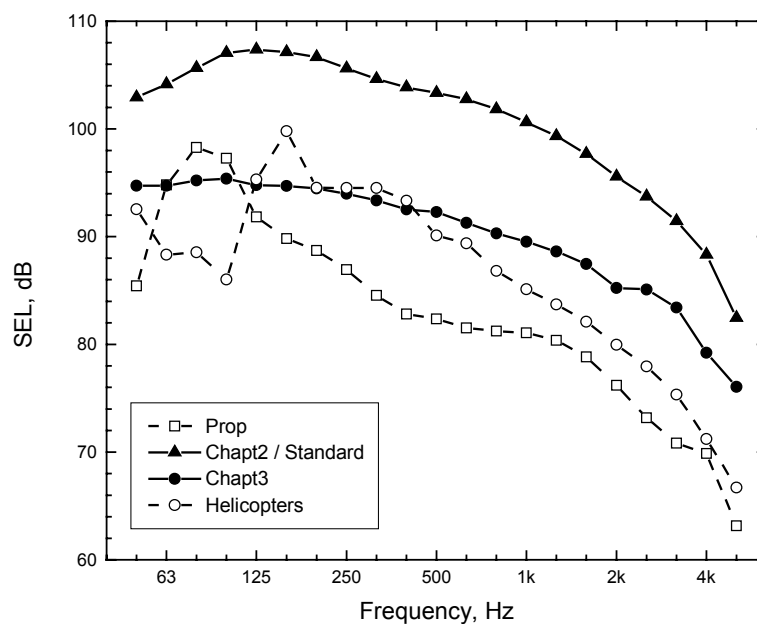


Figure 64. Comparison of 4 new average aircraft noise spectra.

noise levels as well as the details of the spectrum shape.

The new ‘standard’ aircraft noise spectrum is compared with the source spectrum in the OITC standard [16] and with the source spectrum in the earlier CMHC Guide [7] in Figure 65. The spectra have been normalised to coincide at 500 Hz so that the spectrum shapes can be more easily compared. The source spectrum in the OITC standard is intended to be representative of all types of outdoor noise. It is seen to have relatively higher levels at the lowest few frequency bands. The source spectrum from the CMHC

Guide is quite different because it represents much older aircraft types. It would significantly underestimate the low frequency levels of modern aircraft and over estimate high frequency levels. Also shown in Figure 65 is the average outdoor noise spectrum obtained from measurements at schools near Toronto (Pearson) Airport [21]. The shape is similar to the new measurements except that at higher frequencies levels are relatively lower. This is probably due to differences in air absorption related to variations in temperature humidity and distance to the flight track.

To further validate the procedure used to determine the helicopter source spectrum, the same process was carried out for DC9, F28 and A300 aircraft included in the FAA data. The published FAA spectra [13] were again un-normalised [19] and 7 dB was added to approximated SEL values. The DC9 and F28 spectra were then averaged and compared with the average of measurements at the OATS, i.e. the Chapter 2 spectrum. Similarly the published A300 spectrum [13] was un-normalised and compared with the average Chapter 3 spectrum obtained from measurements at the OATS. These comparisons are plotted in Figure 66. The two sets of data agree reasonably well except at low frequencies. The FAA spectra are more irregular, presumably because they are from a single measurement point and are not averages of a complete flyby. The low frequency differences may also relate to these differences in measurement procedure. The FAA data were obtained at the single measurement point where the overall A-weighted level was maximum. This is usually near the point of closest approach to the microphone position. However, low frequency levels are highest when the aircraft has flown past the measurement point. Thus it seems that the new results that integrate over complete flybys are more appropriate for predicting the total incident sound energy on a building exposed to the noise from passing aircraft. Using measurements from a single point can apparently underestimate low frequency levels by as much as 10 dB or more. The derived helicopter noise spectrum (shown in Figure 64) may similarly underestimate the incident low frequency sound energy. However, without further information on the directionality of helicopter noise and further details of the measurement procedure it is not possible to correct for this possible source of error. Integrated helicopter noise passby sound level measurements must be made and if possible sound insulation measurements included too.

The importance of the source spectrum differences can be assessed by calculating the expected differences in indoor sound levels for a particular construction exposed to different aircraft noise spectra with the same overall A-weighted level. The construction used was a simple 140 mm (2" by 6") wood stud wall with vinyl siding on OSB on the exterior, a single layer of 13 mm gypsum board on the interior, and with glass fibre thermal insulation in the cavity. The indoor sound levels were calculated for 6 different source spectra and with all other conditions unchanged. The 6 source spectra were: (1) the new 'standard' aircraft noise spectrum (smaller Chapter 2 aircraft), (2) the new smaller Chapter 3 aircraft source spectrum, (3) the new propeller aircraft source spectrum, (4) the new helicopter noise source spectrum, (5) the OITC standard source spectrum and (6) the older aircraft source spectrum from the CMHC guide.

The resulting calculated indoor sound levels are compared in Figure 67. This figure also includes the overall A-weighted level reductions for the 6 different source spectra. These

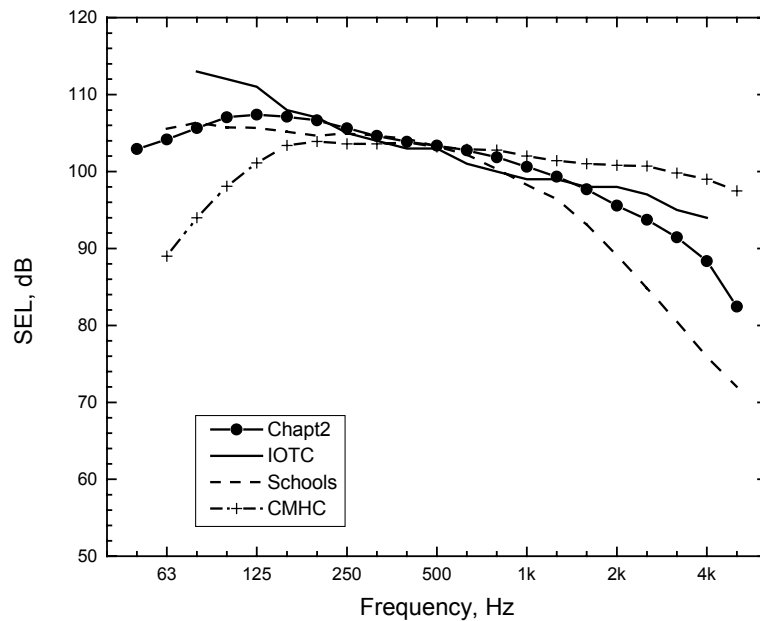


Figure 65. Comparison of new 'standard' aircraft (Chapt2) noise spectrum with the OITC source spectrum [16], the CMHC Guide spectrum[7] and with measurements at schools near Toronto airport [21].

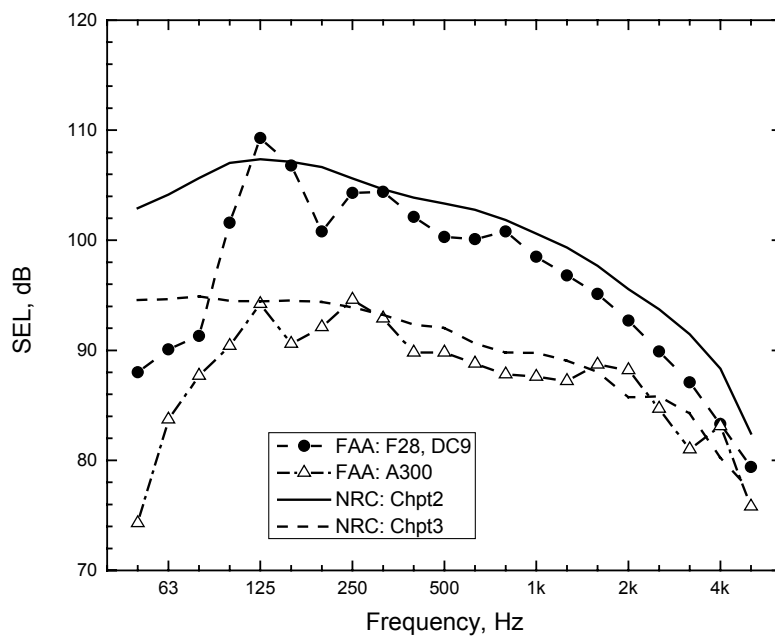


Figure 66. Comparison of FAA spectra with measured spectra at the OATS.

overall A-weighted level reductions varied from 23 to 33 dBA and using the older CMHC source spectrum was most different than the other results. Increasing low sound energy in the source spectrum tends to lead to reduced overall A-weighted level reductions. Thus, the Propeller, the Helicopter and the OITC source spectra are associated with lower overall A-weighted level reductions (higher indoor noise levels). The CMHC spectrum has much less low frequency sound energy and leads to higher overall A-weighted level reductions.

Small differences in the mix of Chapter 2 and Chapter 3 aircraft will have only small effects on the resulting indoor sound levels. However, for more different mixes of aircraft types, such as large numbers of helicopters or propeller aircraft, the effects of source spectrum would be larger and could change indoor levels by several decibels.

Thus for most medium and larger sized airports, where there is a mix of different aircraft types, using the new ‘standard’ aircraft source spectrum is probably adequate. For medium, sized airports similar to Ottawa where there is a mix of smaller Chapter 2 and Chapter 3 commercial jet aircraft, a mix of these two aircraft source spectra could be used but is not normally necessary. However, at more specialised airports where the aircraft activity is predominantly some other type of aircraft such as propeller aircraft or helicopters, it is more important to use a source spectrum shape that best approximates these particular aircraft types.

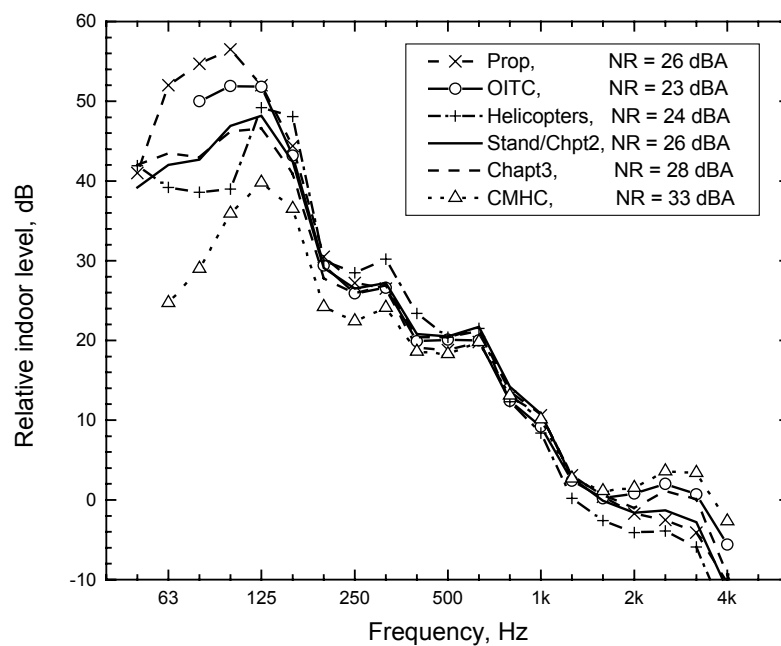


Figure 67. Calculated indoor sound levels for the same construction and varied aircraft noise source spectrum. The overall A-weighted noise reductions are included in the legend.

7. Sound Insulation Calculations for IBANA-Calc

As part of the IBANA project, software has been developed to facilitate the calculation of the effects of various sound insulation designs for buildings exposed to aircraft noise. The IBANA-Calc software calculates indoor sound levels for user-specified outdoor aircraft noise levels and for the combination of façade elements selected by the user from the program's database. This section explains the details of the calculations used in the software because many of the details have been derived from the analyses discussed in this report.

7.1 Basic sound insulation calculations

For sound propagation from aircraft sources, one can usually assume that the outdoor incident sound consists of approximately plane waves at some particular angle of incidence. The ASTM E966 [10] and ISO 140 part V [11] standards describe standardised procedures for these types of measurements. These procedures are based on the following equation relating the *transmission loss* to the area of the partition S in m^2 , the total absorption in the receiving room A in m^2 and the angle of incidence θ .

$$TL = L_1 - L_2 + 10 \log(4S \cos(\theta) / A), \text{ dB} \quad (7.1)$$

L_1 is the outdoor incident sound level and L_2 is the room average indoor received level. This assumes that the outdoor microphone is in the free field away from reflecting surfaces. For indoor transmission loss measurements between two rooms, the sound is more or less incident from all angles and when averaged over all $\cos(\theta)$ the equation approximately reduces to,

$$TL = L_1 - L_2 + 10 \log(S/A), \text{ dB} \quad (7.2)$$

Integrating the incident sound levels over complete aircraft flybys also averages over a range of angles of incidence. Although intermediate equations between (2.3 or 7.1) and (2.4 or 7.2) are sometimes suggested, the comparisons reported in this report suggest that equation (2.4 or 7.2) is most appropriate and was used in all calculations in this report and will be used in the IBANA-Calc software.

For this application L_1 should be measured in the free field away from all reflecting surfaces and L_2 should represent room average indoor sound levels. The ASTM and ISO measurements standards [10,11] suggest that it is also acceptable to measure the incident sound with a microphone mounted on the exterior façade of the building and assuming that this leads to a 6 dB increase in measured outdoor levels at all frequencies. However, the results in section 4.2 show that this assumption is not a very good approximation to what actually occurs and façade mounted microphones should not be used to obtain measurements of the incident aircraft noise.

7.2 NEF to Leq24 conversions

It is expected that outdoor aircraft noise levels in Canada will usually be derived from aircraft noise contours calculated using Transport Canada's NEF_1.7 program. However, these NEF values are converted to Leq24 values in the IBANA-Calc program. Thus all calculated indoor sound levels are in terms of Leq24 values.

The conversion between NEF and Leq24 values was based on previous analyses of the NEF_1.7 noise contour program [4]. Measured values of the day-night sound level Ldn and NEF_{meas} have been related as follows,

$$Ldn = NEF_{meas} + 35, \text{ dB} \quad (7.3)$$

and Leq24 values are approximately 1 dB less than Ldn values. Therefore,

$$Leq24 = NEF_{meas} + 34, \text{ dB} \quad (7.4)$$

NEF values from the NEF_1.7 program are thought to be different than one might measure due to the procedure for estimating excess ground attenuation and due to the larger number of operations for a peak planning day used in the NEF_1.7 calculations than for an average day.

Noise contours from the NEF_1.7 program and from the Integrated Noise Model (version 3) were compared [4] for the same aircraft operations and indicated some differences. These differences were assumed to be mostly due to different procedures for calculating the effects of excess ground attenuation. The output of the two programs was compared for 4 airports varying from small to large and these differences are shown in Table V.

	NEF_1.7 – INM differences				
NEF Range	20-25	25-30	30-35	35-40	Overall AVG
Windsor	4.50	4.80	4.10	3.20	
St John's	3.55	3.40	4.10	5.20	
Ottawa	3.20	3.80	3.55	4.35	
Montreal	3.65	3.70	3.20	3.60	
AVG	3.73	3.93	3.74	4.09	3.87

Table V. Differences between NEF values calculated by NEF_1.7 and INM programs by NEF range for four airports (from [4]).

The NEF values calculated by the NEF_1.7 program were on average 3.9 dBA higher than those calculated by the INM program. It was concluded that the ‘correct’ estimate of NEF was intermediate to those of the two programs and that the NEF_1.7 results were about 2 dB greater than expected measured values. Therefore,

$$NEF_{1.7} = NEF_{meas} + 2.0, \text{ dB} \quad (7.5)$$

Combining equations 7.4 and 7.6 gives,

$$Leq24 = NEF_{1.7} + 32, \text{ dB} \quad (7.6)$$

This relationship will be used in the IBANA-Calc software.

No correction is made to account for the larger number of operations on a peak planning day than on an average day. The use of a peak planning day corresponds to a 95th percentile day and so is representative of activities on busier days. It is assumed that the indoor levels should also be calculated for this condition.

7.3 Corrections to field conditions

The IBANA-Calc software includes 4 optional corrections to modify either the source spectrum or the transmission loss values of the specified façade construction.

- (a) Air absorption correction to source spectrum shape.

Higher frequency sounds can be significantly reduced by air absorption. The amount of attenuation varies with frequency, temperature, relative humidity and distance. Typically, the farther sounds propagate, the more attenuated will be the higher frequency components. The aircraft noise source spectra presented in Chapter 6 are representative of a distance of 240 m at 20 degrees C and 50% relative humidity. For other conditions the spectrum shape will change.

Although these effects will usually not have a large effect on the overall sound insulation rating, it is possible to correct for the effects of air absorption based on either ANSI S1.26 (1995) [14] or ISO 9613 [15]. The two standards give the same procedure for accounting for air absorption and this is included as an optional correction in the IBANA-Calc software.

(b) Vertical angle corrections to façade transmission loss.

Measurement standards [10, 11] suggest that the measured sound transmission loss will vary as the cosine of the angle of incidence. The measurement results discussed in Section 4.3 indicate that measured noise reductions at the test house did approximately vary with the cosine of the vertical angle of the passing aircraft.

An optional correction for the vertical angle of the passing aircraft is therefore included in the IBANA-Calc software. The correction is included normalized to a 60 degree vertical angle because at this angle field results are expected to best approximate lab results. The corrected noise reduction NR_c is determined from the uncorrected noise reduction NR by the following,

$$NR_c = NR + 10 \log \{ \cos(\theta) / \cos(60) \} , \text{ dB} \quad (7.7)$$

where θ is the vertical angle of the aircraft above horizontal in degrees.

These corrections are only made for frequencies below 1000 Hz because the measurement results did not indicate that this effect occurred at higher frequencies. For typical situations this correction will be quite small and the measurement results in section 4.3 suggest that there is a large uncertainty to it.

(c) Horizontal angular corrections to effective source levels.

There are differences in the incident sound energy from a passing aircraft due to the orientation of the façade relative to the aircraft flight track. These have been considered in Chapter 5 of this report. The optional correction included in the IBANA-Calc software simply relates the incident sound energy to the portion of the aircraft flyby that is visible at the façade with a small empirical correction for diffraction. That is, the incident sound energy is reduced when the complete aircraft flyby is not visible at the façade. This correction was seen to match measurements at a Vancouver Airport building and approximates the results at the OATS.

The effective incident sound level $L_i''(f)$ is calculated as follows,

$$L_i''(f) = L_i(f) + 10 \log \{ (\phi / 180) D(f) \} , \text{ dB} \quad (7.8)$$

Where ϕ is the horizontal angular view of the flyby and $0 \leq \phi \leq 180$.

The correction varies a little with frequency because some energy is diffracted around the vertical edge of the building. $D(f)$ accounts for this and can be thought of as increasing

the effective angular view. $D(f)$ increases the effective angular view to increase incident sound levels by 0.1 dB per 1/3 band relative to the highest frequency band.

For a wall that is perpendicular to the flight track, the horizontal angular view is 90 degrees and the basic correction is - 3 dB. That is, the effective $L_i''(f)$ is 3 dB less than for a complete 180 degree angular view. However, the $D(F)$ factor decreases the magnitude of this correction for lower frequencies. That is at 5000 Hz the correction is -3.0 dB but in the next band (4000 Hz) the correction is -2.9 dB, etc. At 50 Hz the angular view correction is reduced to about -1 dB for the 90 degree angular view case. $D(f)$ is limited so that the effective angular view, $\phi \times D(f)$, does not exceed 180 degrees.

(d) Ground reflection correction to effective source spectrum

Ground reflected sound destructively interferes with the direct incident sound at lower frequencies and for receiver positions relatively close to the ground. For the building façades of ground floor rooms, this significantly reduces the incident sound energy in the lowest frequency bands. Therefore an optional correction is included to create reduced effective incident levels as a function of frequency. Figure 68 illustrates the measured effect and a best fit curve to it.

The best fit equation to the variation with frequency for this bass attenuation B is given by,

$$B(f) = 15 \log \{ K / [(f/f_0)^2 + (f_0/f)^2] \}, \text{ dB} \quad (7.9)$$

A value of $K = 6.5$ is seen to work best and is used in the IBANA-Calc software.

The value of f_0 is determined from the height of the middle of the façade above ground level. It assumes a height of 1.2 m above the floor level of the ground floor room to be representative of sound incident on the particular façade. In calculating f_0 one must determine the path difference between the direct and ground reflected paths. However, this is not always the path difference when the aircraft is closest to the house. For simulated passbys at a distance of 240 m, as at the OATS, the minimum in the total incident sound was due to the combination of two interference minima at ± 64 degrees to the point of closest approach. As the distance to the flight track increases the interference patterns spread out and the minimum in the total incident sound is due to a single interference dip at a little lower frequency. For distances to the flight track of less than 920 m, the simulations in Appendix III suggest that a further correction is required to determine the effective distance to the flight track to calculate the correct minimum frequency for the ground reflection effect. This is described below.

If the aircraft height above the ground is H and the receiver height above the ground is h , and the horizontal distance to the flight track is d , we can calculate the direct and ground-reflected path lengths.

$$\text{The direct path,} \quad r_1 = \sqrt{\{(H-h)^2 + d^2\}} \quad (7.10)$$

$$\text{The reflected path,} \quad r_2 = \sqrt{\{(H+h)^2 + d^2\}} \quad (7.11)$$

The interference minimum occurs when the path difference is $\lambda/2$, where λ is the wavelength.

$$\text{Therefore,} \quad f_0 = c / \{2(r_2 - r_1)\} \quad (7.12)$$

For distances to the flight track d of between 200 and 920 m, the effective distance d' should be used which is obtained as follows,

$$d' = d \sqrt{(920/d)} \quad (7.13)$$

No correction for d is required at larger distances. The simulation calculations suggest that at closer distances, multiple interference effects occur and tend to average out reducing the importance of the ground reflection effect. Therefore the IBANA-Calc program does not include ground reflection corrections for locations within 200 m of the flight track.

As included in Figure 68, this gives an f_0 of about 89 Hz for the Ottawa Airport data and a best fit curve that is in reasonable agreement to the measured effect.

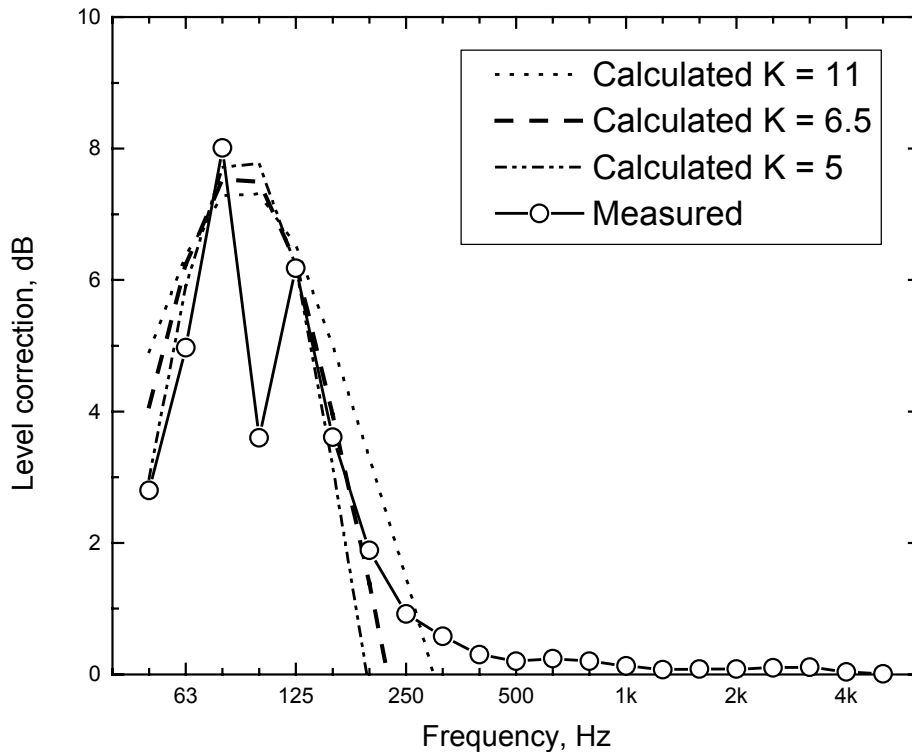


Figure 68. Measured and best fit approximations to expected increase in measured noise reductions due to the interference of direct and ground reflected incident sound.

8. Conclusions

This report has,

- compared overall sound insulation measurements in a number of constructions in a wood frame building exposed to aircraft noise with predictions from laboratory measurements,
- explored various factors influencing the difference between laboratory and field results,
- developed corrections to improve the agreement between laboratory and field results, and
- produced new aircraft noise spectrum shapes for different aircraft categories.

The comparisons of laboratory and field measurements of sound insulation have quantified the differences for a range of conditions typical of Canadian wood stud construction. The causes of the major differences have been identified and further explored as part of this work and corrections developed to improve the accuracy of future sound insulation calculations.

The most important factors leading to differences between laboratory and field results are:

- ground reflected sound,
- façade orientation to, and angular view of the aircraft flyby,
- variation of sound insulation with angle of incidence at principal resonances
- vertical angle of the aircraft,
- flanking paths in the building.

The Main Comparisons

The overall comparisons of sound insulation measurements were analysed in 3 groups. The first group considered cases with only one or two walls of the test house contributing to indoor sound levels. The second group included walls with windows and the third group included constructions with various vents.

(a) Walls

For these 4 constructions, the overall A-weighted Noise Reduction (NR) was predicted with a mean error of -6.4 dBA (varying from -8.7 to -4.3 dBA). When additional corrections were added to account for ground reflected sound and for flanking paths, the mean error was reduced to -3.1 dBA (varying from -5.4 to -1.1 dBA). Measured NR values were greater (better) than predicted values. For 3 of the 4 constructions the differences in NR values near the primary structural resonance frequency that produced a pronounced dip at 125 Hz in the laboratory results, would explain about a 3 dBA difference. The reduced incident sound energy incident on the approach façade of the test house could also explain differences of up to 3 dBA for tests where this wall transmitted significant sound energy.

(b) Windows

When windows were added to the walls, indoor sound levels were 2 to 4 dBA greater than for the cases of walls without windows. The cases with windows were more accurately predicted because indoor transmitted sound levels were dominated by mid-frequency sound and hence less influenced by the low frequency effects of ground reflections and low frequency aircraft directionality. The overall A-weighted NR values for the window cases were predicted with an average error of only 0.5 dBA (varying from -2.4 to +1.6 dBA).

(c) Vents

Roof vents, ridge vents and soffit vents have quite small effects while through-the-wall vents have quite large effects on measured sound insulation.

Separate roof vents and a roof ridge vent increased transmitted indoor sound levels by 0.7 to 1.9 dBA in the test house and these results were seen to vary with the vertical angle of the aircraft. Laboratory tests of the same vents showed that vents were less detrimental when there was adequate fibrous insulation in the attic space, when there was a double layer of gypsum board, and when there were a smaller number of roof vents. When resilient channels were added to the ceiling, the negative effects of roof vents increased slightly. For numbers of vents likely to be installed in houses and with R40 fibrous insulation in the attic space, the effect of roof vents is about a 1 dBA reduction in the overall A-weighted NR value.

Tests of through-the-wall vents, that connected the outside directly to indoor spaces, led to 8 and 9 dBA reductions in the overall A-weighted NR values. At mid-frequencies, they had an effective transmission loss of 0 dB. It is important that such vents include acoustical treatment and be located on the quiet side of the building to minimize transmitted sound.

Exploration of Details

Ground reflected sound decreased incident low frequency sound levels by up to 8 dB. Calculations, using simulated aircraft flybys, indicated how this effect would vary with the height and distance of the aircraft from the building façade and that the effects would be insignificant for receivers above the ground floor level.

Façade orientation affects sound insulation because it influences the angular view of the flyby and because incident and transmitted sound energy vary with the angle of incidence of the sound. Attempts to quantify these effects may be practically adequate but were less precise than desired because results were complicated by unexpectedly large effects of ground reflections, aircraft directionality and flanking paths.

Measurements of the effect of the vertical angle of the aircraft led to the expected small variations in measured NR values within the limits of the accuracy of the measurements.

Flanking paths in the wood frame building had large effects at higher frequencies but they did not result in large effects on the overall A-weighted indoor sound levels. They were assumed to be structural flanking paths and were seen to effectively bypass any benefits from using resilient channels to mount the gypsum boards on the walls of the test house.

Measurements of incident sound levels using façade mounted microphones as recommended in various standards were found to produce large errors of up to 12 dB.

Incident sound levels measured at the building façade are strongly influenced by ground reflections and diffraction effects that vary with the vertical angle of the aircraft.

New average spectrum shapes were derived for 4 aircraft categories. No helicopter noise measurements were obtained, so a helicopter spectrum shape was derived from published FAA data. These data, based on single point maximum levels may to underestimate the actual low frequency sound produced by a complete aircraft passby. The other new spectrum shapes were derived from measurements at Ottawa, Toronto and Vancouver airports. Use of inappropriate older spectrum shapes was demonstrated to produce errors of up to 10 dB in calculated NR values.

Corrections to the source spectrum shapes to account for air absorption can further adjust these new spectrum shapes. Other corrections for the effects of ground reflections, façade orientation and vertical angle of the aircraft were derived to improve the calculation of building sound insulation in the IBANA-Calc software.

Future Research

Some of the largest differences between laboratory and field sound insulation measurements are associated with the principal structural resonance of common wood stud walls and the mass-air-mass resonance in windows. These are important because these resonances limit the overall noise reduction, but the noise reduction at these resonances seems to vary significantly with the angle of the incident sound. Improving our understanding of these effects could improve the prediction accuracy by as much as 3 dBA.

Ground reflected sound was found to have large effects at the ground floor facades of the test house. These important effects need to be further experimentally explored for varied façade orientation and floor level.

Further experimental effort is required to better define the effects of façade orientation and vertical angle of the aircraft. This goal could be achieved using facades at higher floor levels to minimize the effects of ground reflections and in buildings with minimal flanking paths. It may also require a more detailed examination of individual aircraft events so that the directionality and particular angles of incidence for each aircraft event can be correctly considered.

Representative spectra for helicopters should be derived from recordings of complete passbys to correctly estimate low frequency sound levels. Because of the importance of the orientation of the façade to the aircraft, measurements of building sound insulation should be made with helicopter noise sources. These would better define the sound intrusion from these types of aircraft and would help to better understand the details of angle of incidence effects.

Sound insulation measurements should be made in high rise buildings because the combination of various angle of incidence effects and the influence of ground reflections are expected to be quite different. These expected differences need to be precisely verified.

The work should be expanded to road and rail noise sources. This is not just a question of acquiring new source spectra but also would require consideration of how the various

complicating factors such as façade orientation and ground reflections would influence sound insulation to these sources.

References

- [1] Bradley, J.S. and Birta, J.A., “Laboratory Measurements of the Sound Insulation of Building Façade Elements”, IRC Internal Report IR-818, October 2000.
- [2] Anon, ASTM E90 – 97, “Standard Test Method for Laboratory Measurement of Airborne Sound Transmission loss of Building Partitions and Elements”, Am. Soc. for Testing and Materials, Philadelphia.
- [3] Anon, ISO 140/III, “Laboratory Measurement of Airborne Sound Insulation of Building Elements – Part III: Laboratory Measurements of Airborne Sound Insulation of Building Elements”.
- [4] Bradley, J.S., “NEF Validation Study: (1) Issues Related to the Calculation of Airport Noise Contours”, IRC Contract Report A-1505.3, 1996.
- [5] Bradley, J.S., “NEF Validation Study: (2) Review of Aircraft Noise and its Effects”, IRC Contract Report A-1505.5, 1996.
- [6] Bradley, J.S., “NEF Validation Study: (3) Final Report”, IRC Contract Report A-1505.3, 1996.
- [7] Anon, “New Housing and Airport Noise”, Canada Mortgage and Housing (1981).
- [8] J.S. Bradley, “Insulating Buildings Against Aircraft Noise: A Review”, IRC Internal Report, IRC IR-760, March 1998.
- [9] Lin G-F., and Garrellick, J.M., “Sound Transmission Through Periodically Framed Parallel Plates”, J. Acoust. Soc. Am., Vol. 61, No. 4. pp. 1014-1018, (1961).
- [10] Anon, ASTM 966, “Standard Guide for Field Measurement of Airborne Sound Insulation of Building Facades and Facade Elements”, Am. Soc. for Testing and Materials, Philadelphia.
- [11] Anon, ISO 140/V, “Laboratory Measurement of Airborne Sound Insulation of Building Elements – Part V, Field Measurements of Airborne Sound Insulation of Façade Elements and Facades”.
- [12] J.S. Bradley, K.A. Lay and S.G. Norcross, “Measurement of the Sound Insulation of Buildings Near Vancouver Airport”, IRC Contract Report B3122.1, January 2000.
- [13] Anon, “Spectral Classes for FAA’s Integrated Noise Model Version 6.0”, Federal Aviation Administration, U.S. Department of Transportation, Letter Report December 1999 (DTS-34-FA065-LR1).
- [14] Anon, ANSI S1.26 1995, “Method for the calculation of the absorption of sound by the atmosphere”.
- [15] Anon, ISO 9613-1, “Attenuation of sound during propagation outdoors – Part 1 Calculation of the absorption of sound by the atmosphere”.
- [16] Anon, ASTM 1332, “Standard Classification for Determination of Outdoor-Indoor Transmission Class”, Am. Soc. for Testing and Materials, Philadelphia.
- [17] M.J. Crocker (ed.), “Encyclopedia of Acoustics, Vol. 1, p. 347, John Wiley, New York (1997).

- [18] S. Pietrzko and R. Hofmann, "Prediction of A-Weighted Aircraft Noise Based on Measured Directivity Patterns" *App. Acoustics*, 23 (29-44) 1988.
- [19] Amada Rapoza, Volpe National Transportation Systems Center, Cambridge, U.S.A. (personal communication).
- [20] Guy Héneault, Transport Canada, Ottawa, (personal communication).
- [21] Anon, "Sound Insulation and Aircraft Noise in Schools Near Lester B. Pearson International Airport", *Valcoustics Report*, (October 1991).

Appendix I . Measured Average NR for each Configuration

This appendix gives the average measured noise reductions (NR) for each of the measurement cases at the Ottawa Airport Test House (OATS). The details of the constructions for each measurement case were described in section 2.2. Table A1 gives the average measured noise reductions in decibels for each 1/3 octave frequency band from 50 to 5000 Hz. The noise reductions are relative to the outdoor incident aircraft noise as measured in the free field at the outdoor microphone. That is, they are the differences between the average levels in each room and the corresponding outdoor sound levels. The upper half of the table is for room A and the lower half for room B. (Rooms A and B are identified in Figure 1 of this report). Table A1 also includes the average vertical angle of the passing aircraft for each measurement case.

		Frequency, Hz																				
Case	Vert. ang.	50	63	80	100	125	160	200	250	315	400	500	630	800	1k	1.25k	1.6k	2k	2.5k	3.15k	4k	5k
		Outdoor-Room A																				
1	54.8	14.5	18.7	18.4	19.7	17.5	20.9	26.5	27.8	27.4	27.7	28.8	30.5	34.4	37.5	39.0	42.0	43.5	44.3	45.9	46.8	45.4
2	57.4	15.2	22.2	23.6	20.8	23.2	24.2	29.1	28.2	29.3	29.9	31.1	30.3	34.4	36.9	36.9	39.8	41.2	43.3	44.7	46.2	44.6
3	56.7	13.5	20.8	17.7	16.0	16.2	20.1	25.3	27.1	27.0	27.1	28.2	28.4	32.3	34.9	35.1	39.0	39.5	41.1	42.4	42.0	39.3
5	44.4	14.2	18.1	19.5	21.4	25.5	26.6	30.5	32.0	30.8	29.4	30.8	32.1	35.3	38.2	39.9	43.7	44.1	44.0	45.1	46.1	44.2
6	49.1	14.6	19.0	18.9	21.1	24.5	25.2	29.9	31.4	30.1	28.4	30.4	31.3	34.6	37.3	38.4	42.3	42.2	42.3	44.1	42.2	39.4
7	40.8	11.7	17.2	17.2	21.4	25.2	24.9	29.4	30.8	29.1	28.3	30.0	31.9	35.3	37.5	38.6	42.6	43.7	43.2	44.9	46.8	45.8
8	57.8	13.2	17.4	17.1	19.5	23.1	23.1	28.8	30.4	28.5	27.7	30.6	30.5	33.6	37.0	37.0	40.8	40.3	41.6	41.5	36.2	27.8
9	44.2	12.6	17.5	18.3	20.3	24.0	24.0	26.0	23.1	20.0	20.2	23.3	24.1	21.1	25.3	27.9	31.9	31.2	30.7	32.7	31.2	29.3
10	51.0	16.2	18.0	19.2	21.7	19.5	20.7	21.6	24.6	21.0	20.8	24.5	27.7	30.7	33.9	35.4	36.6	36.1	36.8	36.9	31.3	26.8
11	56.7	16.5	20.2	23.3	21.8	24.8	24.3	26.4	24.5	27.5	24.2	26.6	26.9	29.2	31.5	33.4	35.5	35.3	37.0	36.8	31.1	27.1
12	53.2	15.3	21.4	18.9	19.6	22.3	23.2	25.0	22.2	23.3	22.0	24.9	25.5	27.1	29.0	31.3	32.5	32.5	34.8	35.0	28.6	24.4
		Outdoor-Room B																				
1	54.8	15.6	22.4	22.5	23.8	24.6	29.5	31.9	32.2	32.0	31.2	33.0	34.9	38.1	39.4	40.2	44.0	45.4	47.4	48.5	49.7	46.9
2	57.4	17.6	20.4	23.2	19.7	21.5	25.2	27.3	29.7	29.7	30.4	31.3	32.3	36.6	38.1	39.2	43.4	43.6	45.8	46.6	47.7	45.9
3	56.7	16.5	23.4	22.2	21.3	21.5	25.2	27.4	29.8	29.4	30.0	31.0	32.4	35.9	37.3	38.8	43.2	43.1	44.7	45.3	45.1	42.4
5	44.4	17.4	20.2	24.5	22.5	26.1	28.4	31.3	32.8	32.2	31.5	32.1	33.8	37.3	40.4	40.9	43.5	44.7	45.6	46.4	46.9	46.0
6	49.1	15.7	19.2	22.3	21.3	25.2	26.4	29.9	32.0	30.7	29.9	30.7	32.1	35.9	38.1	38.4	41.7	42.7	43.1	44.7	42.7	40.7
7	40.8	16.0	20.5	23.2	21.5	24.4	26.6	30.5	31.7	31.3	30.9	31.3	33.5	36.8	39.8	40.0	43.1	44.3	44.7	46.3	48.0	47.4
8	57.8	15.8	18.3	21.0	22.9	26.9	26.6	29.9	31.9	30.3	30.2	31.4	32.3	35.8	37.1	38.1	41.9	41.5	43.4	43.0	38.2	30.1
9	44.2	16.2	20.3	21.8	21.3	25.1	25.8	28.4	30.7	26.3	27.5	25.0	24.9	25.5	24.2	25.9	29.2	32.0	33.8	34.5	33.0	31.9
10	51.0	15.2	17.8	22.3	25.5	25.9	26.6	27.6	25.7	28.9	26.9	27.9	30.6	33.2	34.8	36.2	37.1	38.7	40.5	38.7	34.7	29.9
11	56.7	16.1	18.5	22.2	20.8	26.8	26.1	26.6	24.7	26.4	23.2	25.7	26.7	30.3	32.6	34.7	36.4	36.9	38.3	37.3	31.9	27.9
12	53.2	16.2	20.8	22.7	22.2	26.3	26.8	27.0	25.1	28.2	25.1	26.8	27.7	30.1	32.0	33.9	35.1	36.4	38.1	37.3	31.5	27.6

Table A1. Average measured noise reductions in decibels between the outdoor (free field) microphone and the average of the 3 microphones in each room for room A (upper) and room B (lower) for the 1/3 octave frequency bands from 50 to 5k Hz. The average vertical angles, in degrees, of the passing aircraft are given in the second column.

Appendix II . The Effect of Aircraft Directionality on Sound Insulation Measurements

The Swiss laboratory EMPA has made a considerable effort to measure the horizontal directionality of many modern aircraft types [18]. Their data were used to calculate an average aircraft directionality and to estimate its effect on sound transmitted into buildings.

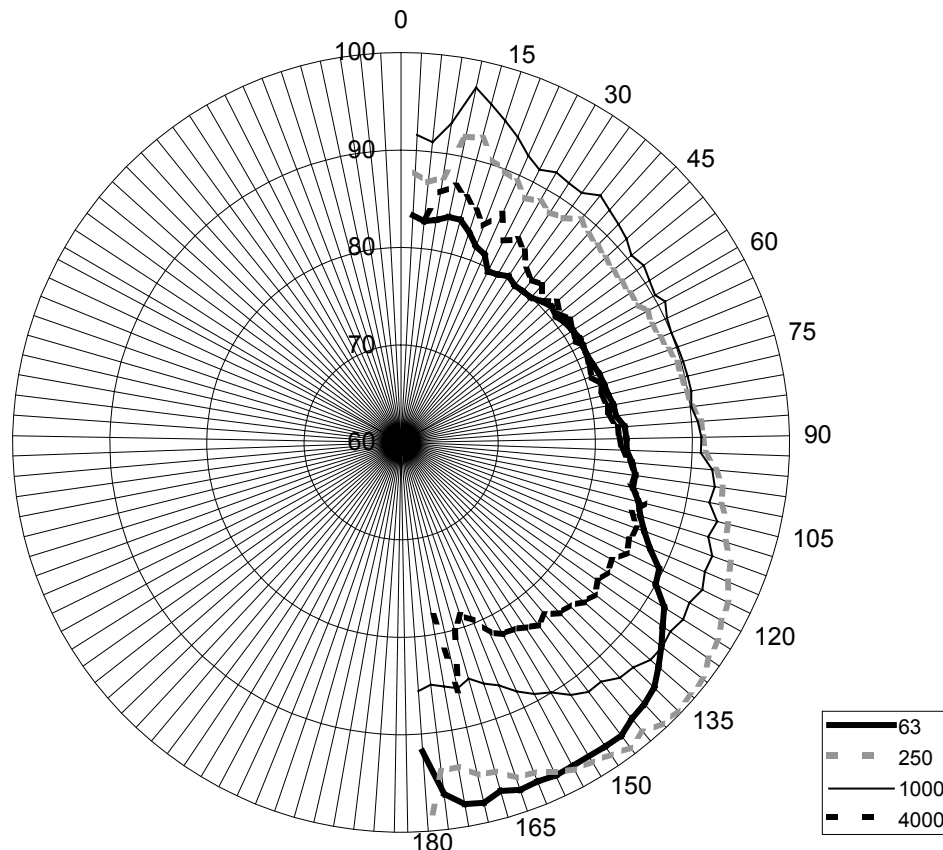


Figure AII-1. Measured directionality at 4 octave band frequencies for a departing B737 aircraft (from EMPA data).

Figure AII-1 illustrates examples of the measured aircraft directionality for a departing B737 aircraft. The sound energy radiated by the aircraft is seen to vary considerably with the horizontal direction. There is a tendency for sound levels to be greatest in directions between 120 and 165 degrees from straight ahead at low- to mid-frequencies. In this and following plots, 0 degrees corresponds to straight ahead of the aircraft and 180 degrees to directly behind it. For this example, sound levels in the 63 Hz octave band are about 18 dB greater for angles of 150 to 165 degrees than for angles of 20 to 40 degrees. This general pattern explains the common experience of the apparently louder and deeper pitched roar of a jet aircraft after it has passed the listener.

The directional characteristics vary between aircraft types. More modern Chapter 3 aircraft tend to be more omni-directional than the older Chapter 2 types. To help to better understand the different characteristics of aircraft noise incident on the different facades

of a building, an average directional characteristic was calculated from the measured EMPA data. Directional data from the following aircraft types were used in the calculations: MD11, MD80, A310, A320, B767, B757, B747, B737, and B727.

The EMPA data for these 9 aircraft types was available at octave band frequencies from 31 to 4000 Hz in 3 degree increments. These data were first normalised so that all aircraft had the same average sound level (of 0 dB) in each frequency band. The energy averages of these data for all aircraft types were then calculated as a function of angle. To create information at the same 1/3 octave frequencies as the sound insulation data, values were interpolated between the measured octave band values. Finally, 5th order polynomials were fitted to the average data versus angle in each 1/3 octave band. These 5th order polynomial regression equations can be used to describe an average aircraft directionality. Table AII-1 below gives the regression coefficients of these equations.

Freq	X ⁵	X ⁴	X ³	X ²	X	constant
50	-1.954E-09	7.421E-07	-1.093E-04	9.531E-03	-4.687E-01	2.181
63	-1.071E-09	3.585E-07	-4.944E-05	5.325E-03	-3.302E-01	1.059
80	-4.729E-10	7.828E-08	-3.468E-06	1.992E-03	-2.242E-01	0.7689
100	1.439E-10	-2.104E-07	4.389E-05	-1.442E-03	-1.150E-01	0.4697
125	7.425E-10	-4.906E-07	8.986E-05	-4.775E-03	-9.012E-03	0.1793
160	8.135E-10	-4.806E-07	8.161E-05	-3.915E-03	-3.264E-02	0.8605
200	8.866E-10	-4.704E-07	7.311E-05	-3.028E-03	-5.699E-02	1.562
250	9.576E-10	-4.604E-07	6.485E-05	-2.167E-03	-8.062E-02	2.244
315	1.324E-09	-6.295E-07	9.206E-05	-4.056E-03	-2.975E-02	2.201
400	1.702E-09	-8.038E-07	1.201E-04	-6.002E-03	2.266E-02	2.158
500	2.069E-09	-9.729E-07	1.473E-04	-7.891E-03	7.353E-02	2.116
630	3.268E-09	-1.486E-06	2.270E-04	-1.334E-02	2.213E-01	1.343
800	4.504E-09	-2.015E-06	3.093E-04	-1.895E-02	3.735E-01	0.5472
1000	2.897E-09	-1.407E-06	2.305E-04	-1.496E-02	3.049E-01	1.019
1250	4.054E-09	-1.893E-06	3.044E-04	-1.986E-02	4.336E-01	0.2353
1600	5.245E-09	-2.393E-06	3.806E-04	-2.491E-02	5.663E-01	-0.5726
2000	6.402E-09	-2.879E-06	4.545E-04	-2.982E-02	6.951E-01	-1.357
2500	7.009E-09	-3.140E-06	4.974E-04	-3.297E-02	7.815E-01	-1.791
3150	8.573E-09	-3.794E-06	5.979E-04	-3.971E-02	9.559E-01	-2.805
4000	5.199E-09	-2.541E-06	4.345E-04	-3.075E-02	7.554E-01	-1.227

Table AII-1. Regression coefficients for 5th order polynomials fitted to the average directional characteristics of modern jet aircraft.

The normalised measured average aircraft directional data and the calculated 5th order polynomial fits are shown in Figures AII-2 to AII-8. These plots also illustrate the standard deviations about each mean value to illustrate the magnitude of the variations between aircraft types. The plots are given for only the octave frequencies from 63 to 4000 Hz.

The regression lines are seen to be good fits to the average measured data with most points agreeing within a fraction of a decibel. However, the standard deviations about the measured data indicate that there are significant differences among the 9 aircraft types. Standard deviation values vary from about 1 to 6 dB but the average value in each frequency band is less than 3 dB.

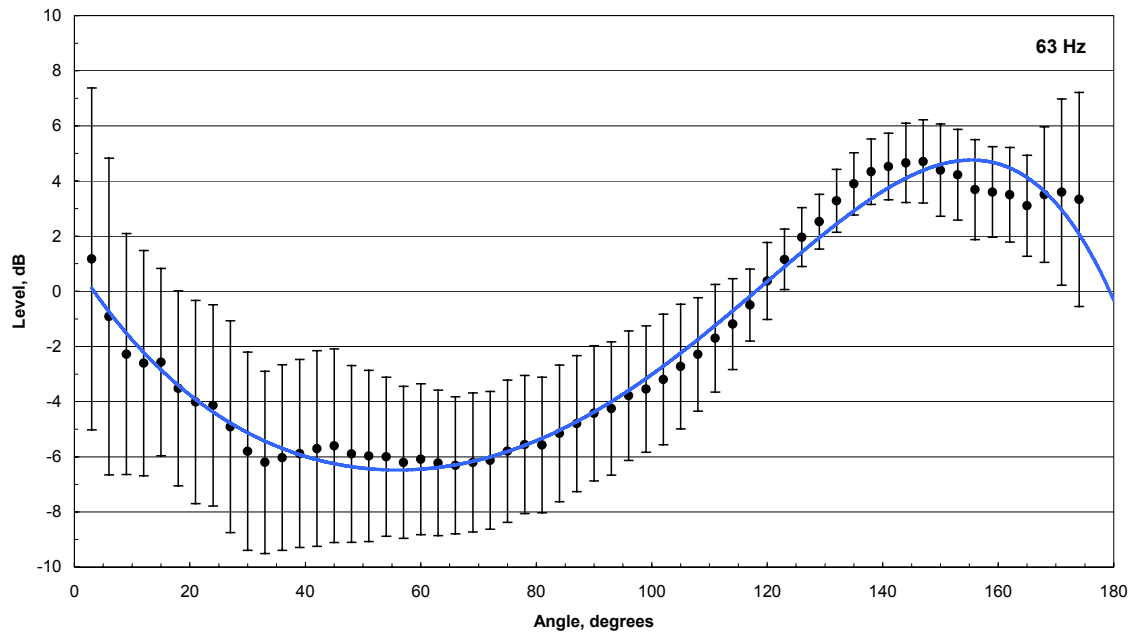


Figure AII-2. Normalised average aircraft noise levels (solid circle symbols) versus horizontal angle, standard deviations about these averages and the best fit 5th order polynomial line (0 degrees = straight ahead of the aircraft).

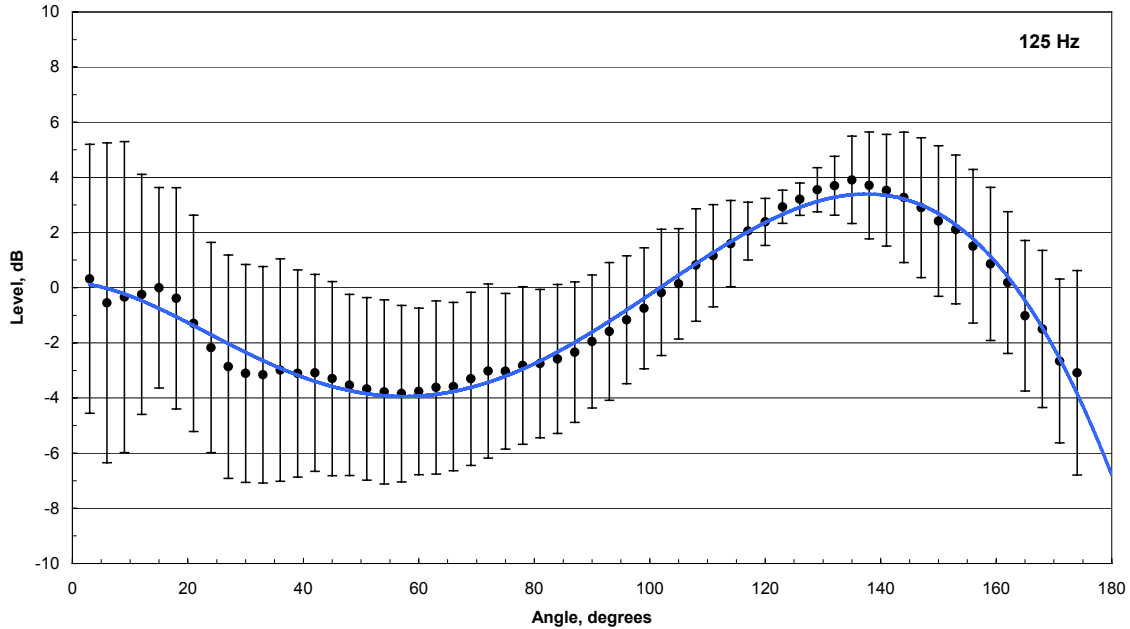


Figure AII-3. Normalised average aircraft noise levels (solid circle symbols) versus horizontal angle, standard deviations about these averages and the best fit 5th order polynomial line (0 degrees = straight ahead of the aircraft).

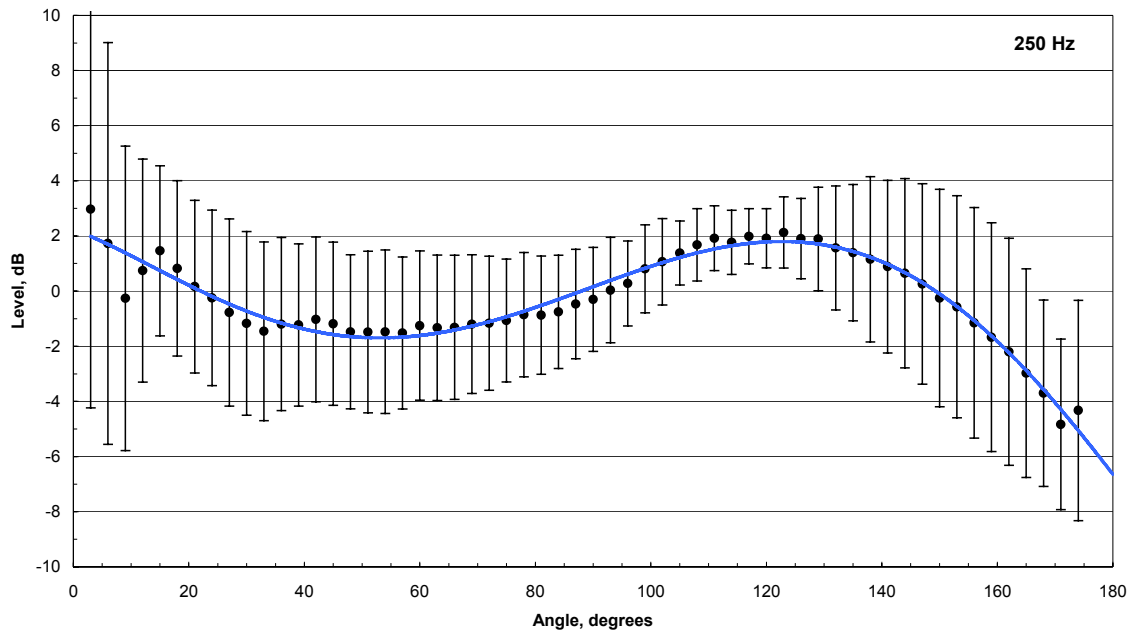


Figure AII-4. Normalised average aircraft noise levels (solid circle symbols) versus horizontal angle, standard deviations about these averages and the best fit 5th order polynomial line (0 degrees = straight ahead of the aircraft).

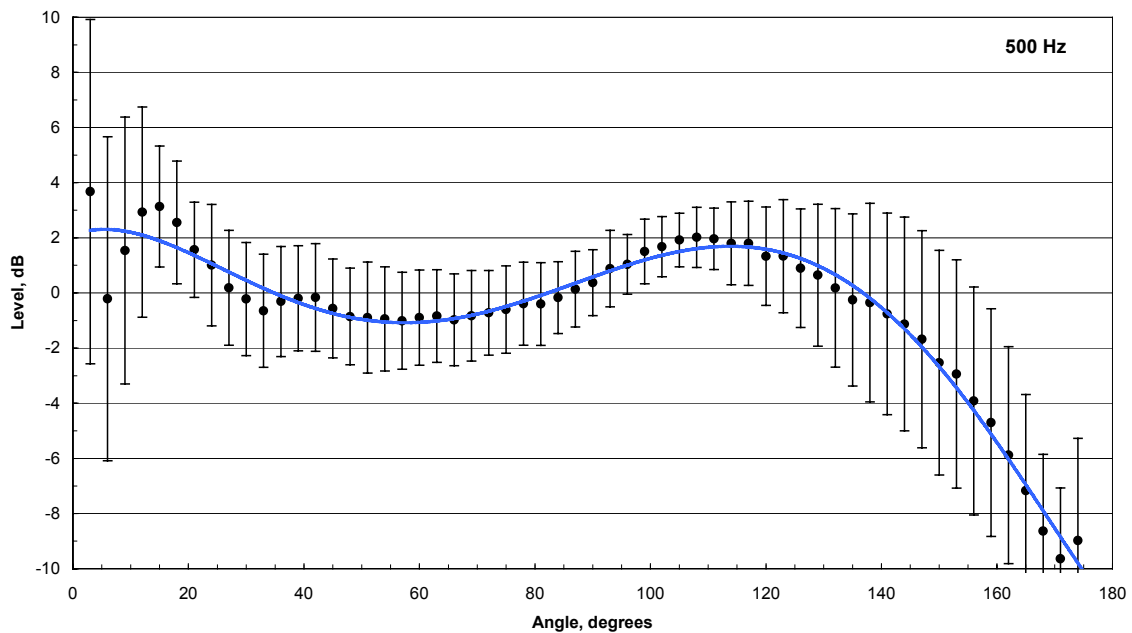


Figure AII-5. Normalised average aircraft noise levels (solid circle symbols) versus horizontal angle, standard deviations about these averages and the best fit 5th order polynomial line (0 degrees = straight ahead of the aircraft).

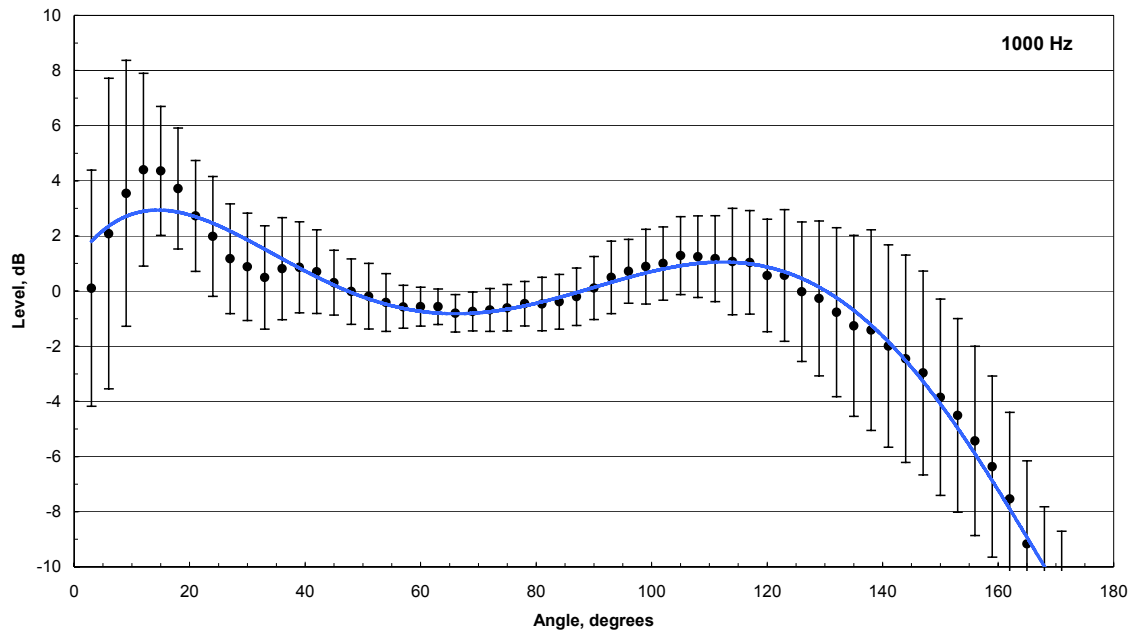


Figure AII-6. Normalised average aircraft noise levels (solid circle symbols) versus horizontal angle, standard deviations about these averages and the best fit 5th order polynomial line (0 degrees = straight ahead of the aircraft).

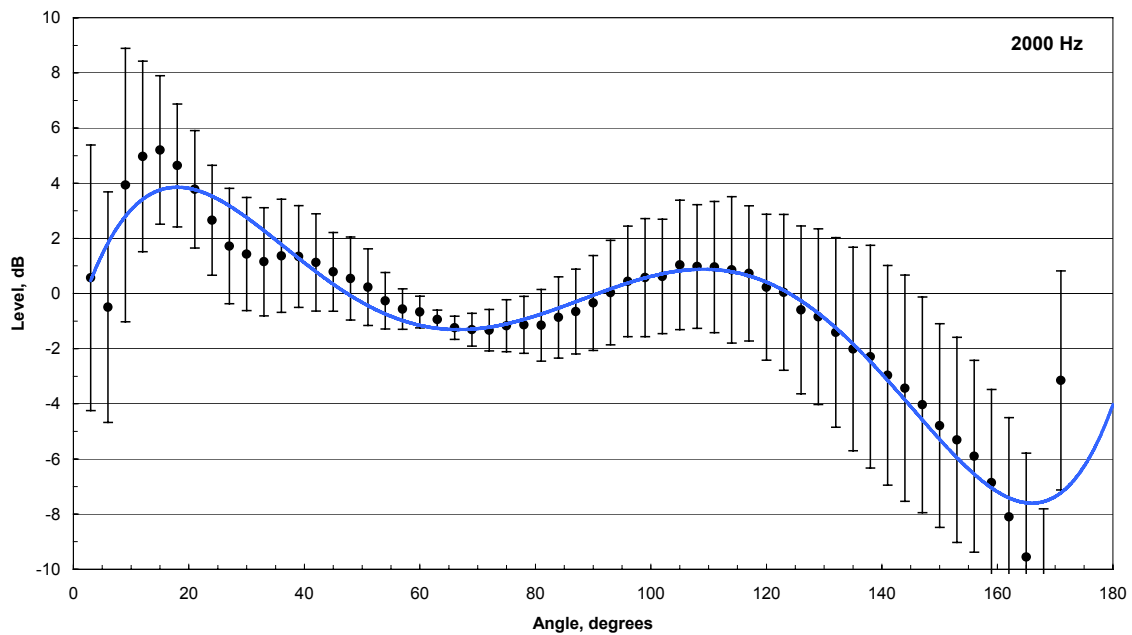


Figure AII-7. Normalised average aircraft noise levels (solid circle symbols) versus horizontal angle, standard deviations about these averages and the best fit 5th order polynomial line (0 degrees = straight ahead of the aircraft).

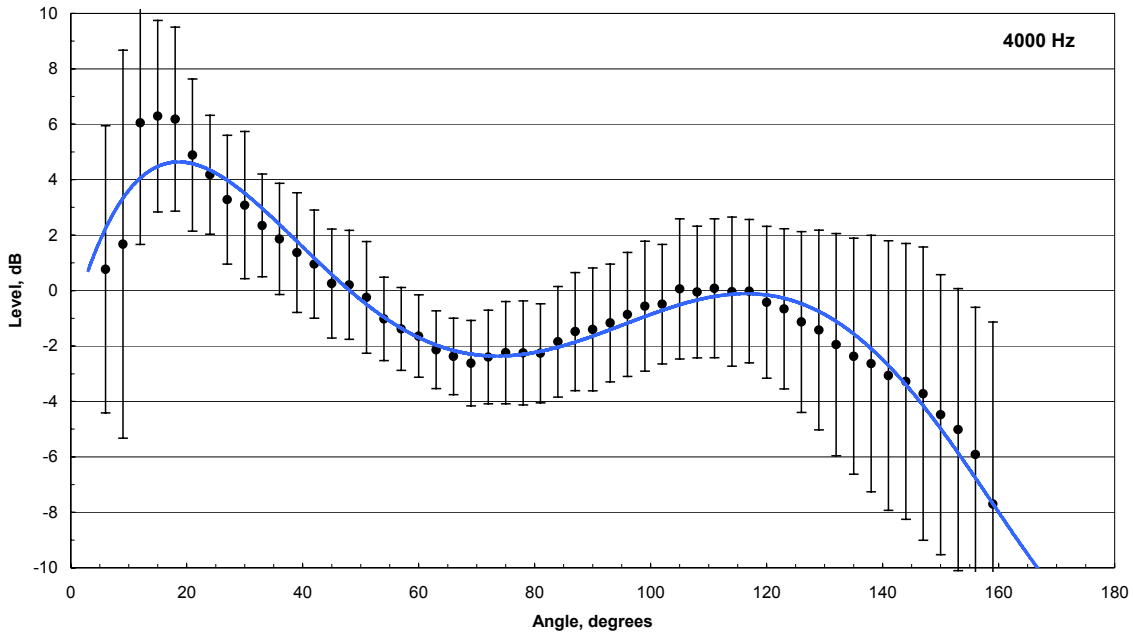


Figure AII-8. Normalised average aircraft noise levels (solid circle symbols) versus horizontal angle, standard deviations about these averages and the best fit 5th order polynomial line (0 degrees = straight ahead of the aircraft).

Although these results are a good estimate of average aircraft directional characteristics, one must be aware that the large standard deviations indicate that each aircraft type will exhibit significant differences.

As an aircraft flies by a point, the sound level will first vary with the distance to the aircraft at each instant in time. This variation with time will be further modified by the directionality of the aircraft noise. In addition to these two factors, the incident energy at a particular façade is related to the cosine of the angle of incidence of the sound energy, which also varies with time as the aircraft passes. This is the angle between the normal to the façade surface and the direction to the aircraft. The variation with time of the incident sound intensity can then be calculated as follows,

$$L_i(t) = 10 \log\{Q(f) \cos(\theta) / r^2\}, \text{ dB} \quad (\text{AII.1})$$

Where, $Q(f)$ is the directivity factor of the aircraft at frequency f ,

θ is the angle of incidence to the façade,

r is the distance from the façade to the aircraft in m.

Equation AII.1 was used to calculate passby time histories of the incident intensity at various facades. These included a façade facing the passing aircraft, i.e. parallel to the aircraft flight track. This was intended to approximate conditions at the facing façade of the OATS. Figure AII-9 shows calculated passby time histories at a facing façade for representative frequencies of 63, 500 and 4000 Hz. For comparison, the plots also show a simple $1/r^2$ variation, i.e. excluding aircraft directionality. The results in Figure AII-

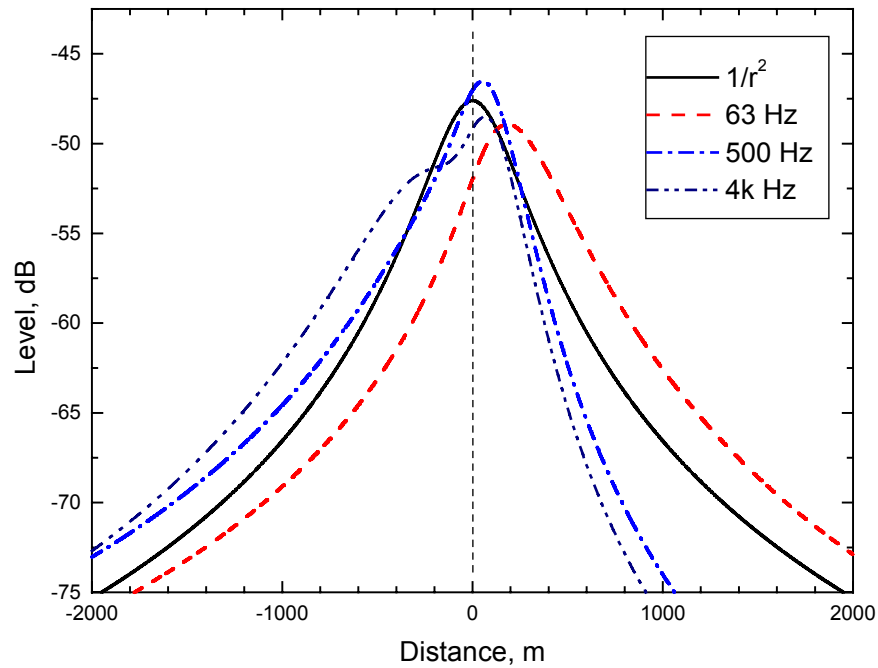


Figure AII-9. Calculated variation of incident sound intensity for a façade facing the passing aircraft. (receiver 240 m from flight track).

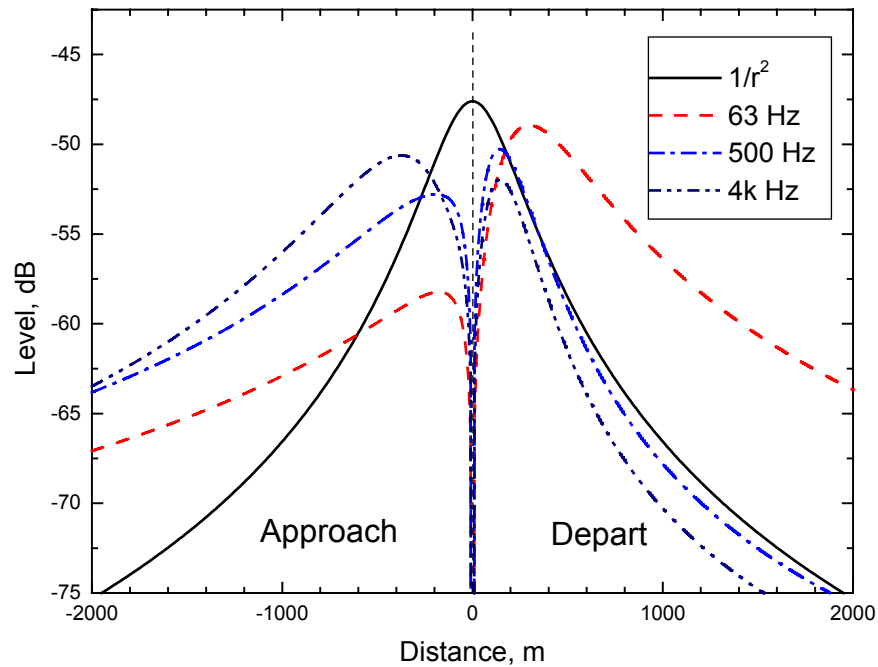


Figure AII-10. Calculated variation of incident sound intensity for façades perpendicular to the passing aircraft. The left half of the graph represents a façade to which aircraft are approaching and the right half a façade from which they are departing. (receiver 240 m from flight track).

9 show that the aircraft noise levels peak after the mid-point of the passby as expected from the directivity measurements. The effect is most noticeable at lower frequencies.

The calculated variations in incident intensity at façades that are perpendicular to the aircraft flight track are illustrated in Figure AII-10. The left side of the graph represents a façade to which aircraft are approaching and the right side a façade from which they are departing. The results in this graph are different than those in Figure AII-9 because the variation with the cosine of the angle of incidence depends on an angle of incidence that is different by 90 degrees between the facing and perpendicular façade cases. For the two perpendicular façades, the variation with time is quite different to the simple $1/r^2$ effect and there is not a peak when the aircraft is near the mid-point of the flight track.

By summing all of the incident energy over complete aircraft passbys, these calculations were extended to estimate the total incident sound energy at each façade. The differences between the two perpendicular façades and the facing façade are illustrated in Figure AII-11. Each of the perpendicular façades is exposed to only half of the complete aircraft flyby, which would suggest that the incident intensities would be 3 dB less than for the facing façade. However, the directionality of the aircraft further modifies this and the actual differences seen in Figure AII-11 vary from -7 to +1 dB. Thus, the expected incident sound energy is expected to vary with the orientation of the façade to the aircraft flight track as well as with the directionality of the noise from the particular aircraft. These calculations give a first estimate of the likely differences in incident aircraft noise at different façades. However, they do not include the effects of ground reflections that may also vary with façade orientation. They also do not consider differences between aircraft types nor differences in flanking paths from the different building façades.

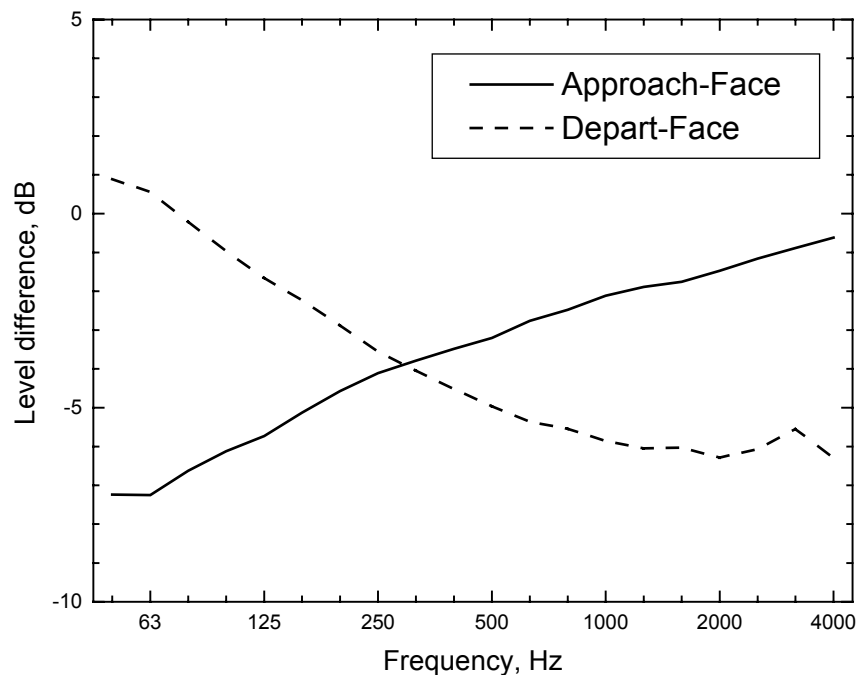


Figure AII-11. Variation of the total incident sound intensity with frequency at the two perpendicular façades relative to the facing façade.

Appendix III. Interference between Direct and Ground Reflected Aircraft Noise

This appendix summarises the results of calculations that were performed to indicate the effects of ground reflected sound on aircraft noise levels incident on a building façade. The calculations were for an aircraft source travelling on a horizontal path at a particular height and distance from a measurement point. The measurement point was a specified height above the ground.

The simplest calculations assumed an omni-directional source with a perfectly reflecting ground surface. Then the directional characteristics of the average aircraft were added to the source. Next the effect of a more realistic ground absorption was considered. The effects of the combination of direct and ground reflected sound were then examined for varied receiver height and for varied vertical angle of the aircraft at different distances from the flight track to the receiver. Results are illustrated for situations similar to those measured.

To perform the calculations the source was moved along the flight path in 10 m steps from a point 1000 m before the measurement point to a point 1000 m past the measurement point. For each increment the combined RMS pressure of the direct and ground reflected sound was calculated as follows,

$$P = \left\{ \frac{1}{r_d} + \frac{1}{r_r} \cos[(r_r - r_d)2\pi / \lambda] \right\} \quad (\text{AIII.1})$$

where r_d is the direct path length, m

r_r is the ground reflected path length, m

λ is the wavelength, m

The squared pressure values at each increment were then summed over all positions of the source to calculate the total incident sound energy resulting from the particular combination of direct and ground reflected sound.

The combination of direct and ground reflected sound leads to quite complex interference patterns as the source moves past the receiver. At some points and at some frequencies the direct and ground reflected sounds add in phase to create up to 6 dB increases relative to the direct sound alone. At other points and/or other frequencies the combination can lead to large reductions in the total sound level relative to the level of the direct sound only. Figures AIII-1 and AIII-2 illustrate some detailed passby time histories that illustrate some of these complex interference effects.

Figure AIII-1 shows results for the case where the receiver was 240 m from the flight track and Figure AIII-2 shows the case of the receiver at 480 m from the flight track. The OATS was 240 m from the nominal flight track. In each case the receiver was 1.65 m above the ground and the source passed the receiver at a vertical angle of 55 degrees. For comparison each plot also includes the simple $1/r^2$ variation expected for the direct sound from an omni-directional source. At some points the calculated combined effects of direct sound and ground reflections are up to 6 dB greater than the $1/r^2$ results but at other

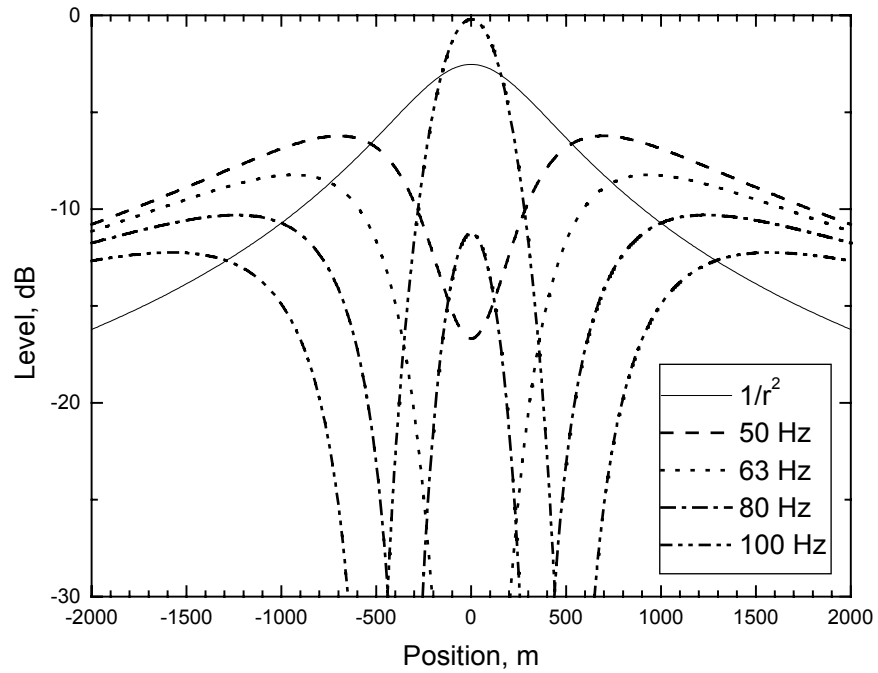


Figure AIII-1. Calculated passby time histories for an omni-directional source passing over a perfectly reflecting ground surface 240 m from the flight track at four different frequencies.

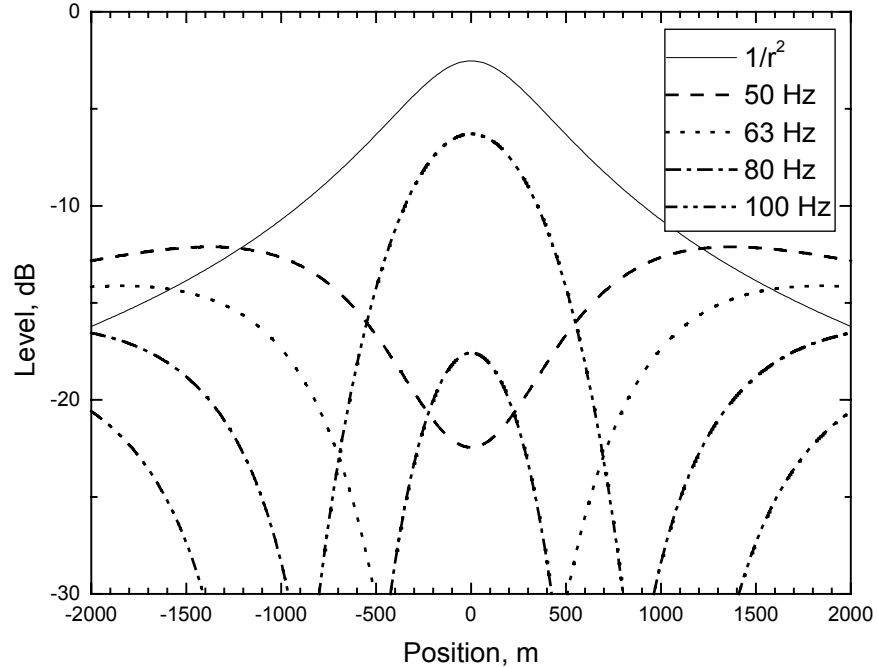


Figure AIII-2. Calculated passby time histories for an omni-directional source passing over a perfectly reflecting ground surface 480 m from the flight track at four different frequencies.

points calculated levels are much reduced below this result. In Figure AIII-1, the 50 Hz result indicates a minimum rather than a maximum at the centre of the passby. At 63 Hz this dip gets much larger. At 80 Hz the central minimum has split into two separate minima with a small peak in between. At 100 Hz this central maximum has become larger than the $1/r^2$ result. At higher frequencies, the interference patterns get more complex so that there are many peaks and minima.

Figure AIII-2 shows similar passby time histories calculated for a receiver 480 m from the flight track. The receiver height (1.65 m) and the vertical elevation of the source (55 degrees) were the same as in the previous results. The calculated passby time histories are similar to those in Figure AIII-1 except that they are more spread out in time. This results in greater overall reductions in passby levels over the key central portion of the passby.

Many complex time history plots could be produced but to simplify the demonstration of the effects of key parameters only the energy sums over complete passbys will be given. These are plotted in terms of sound levels relative to those expected for only the direct sound with no ground reflection.

Figure AIII-3 shows such summed relative levels for both an omni-directional source and for a source with the directionality of the average aircraft calculated in Appendix II. The effect of the source directionality is seen to be quite small. All other calculations illustrated below will include only sources with this average aircraft directionality.

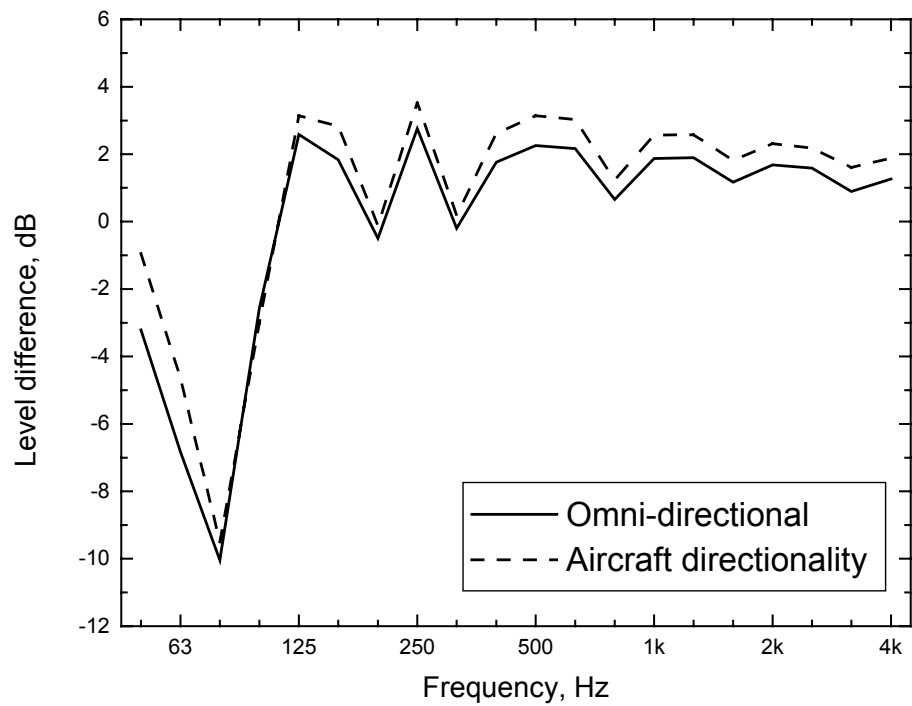


Figure AIII-3. Summed relative levels over complete passbys for a receiver 1.65 m above the ground and 240 m from the flight track and for a perfectly reflecting ground surface. For both the omni-directional and the average aircraft directionality sources, the vertical elevation was 55 degrees.

The reflection coefficients of an absorptive ground were approximately estimated from published impedance data for ground surfaces [17]. For plane waves the reflection coefficient, R_p , relates to the angle of incidence ϕ as follows,

$$R_p = (Z_s \sin \phi - 1) / (Z_s \sin \phi + 1) \quad (\text{AIII.1})$$

$$\text{If, } Z_s = R + iX, \text{ then magnitude of } R_p \text{ is given by,} \quad (\text{AIII.2})$$

$$R_p = \sqrt{[(R \sin \phi - 1)^2 + (X \sin \phi)^2]} / \sqrt{[(R \sin \phi + 1)^2 + (X \sin \phi)^2]} \quad (\text{AIII.3})$$

This led to values of R_p varying from about 0.9 at 50 Hz to 0.2 at 5000 Hz which are thought to be reasonable estimates for typical ground surfaces.

Further calculations were performed by multiplying the ground reflected term in equation AIII-1 by these R_p values. Figure AIII-4 compares results with a perfectly reflecting ground surface with those using the above estimates of the reflection coefficients of a typical ground surface. The addition of ground absorption reduces the interference minimum at 80 Hz a little and reduces the increased levels at mid and higher frequencies.

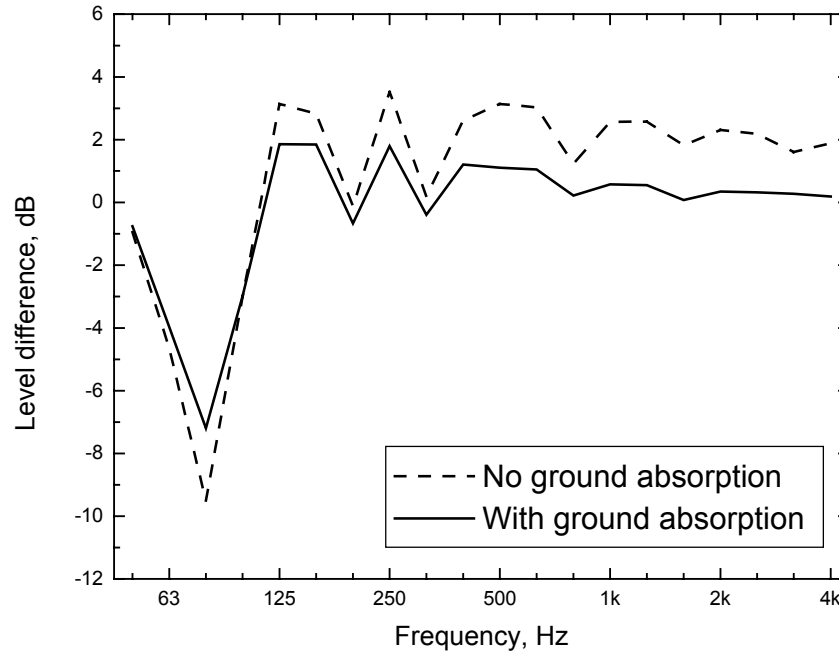


Figure AIII-4. Comparison of summed relative levels over complete passbys relative to the direct sound only for a receiver 1.65 m above the ground and 240 m from the flight track. The source included the average aircraft directionality and was at a vertical elevation of 55 degrees.

Receiver height was shown to have a larger effect on the calculated results. Figure AIII-5 compares three receiver heights: 1.65, 2.13 and 4.35 m. These correspond to the average façade height at the OATS (1.65 m), the height of the façade microphone for the measurements at houses near Toronto airport (2.13 m) and a height typical of the middle of the façade of a second floor room (4.35 m).

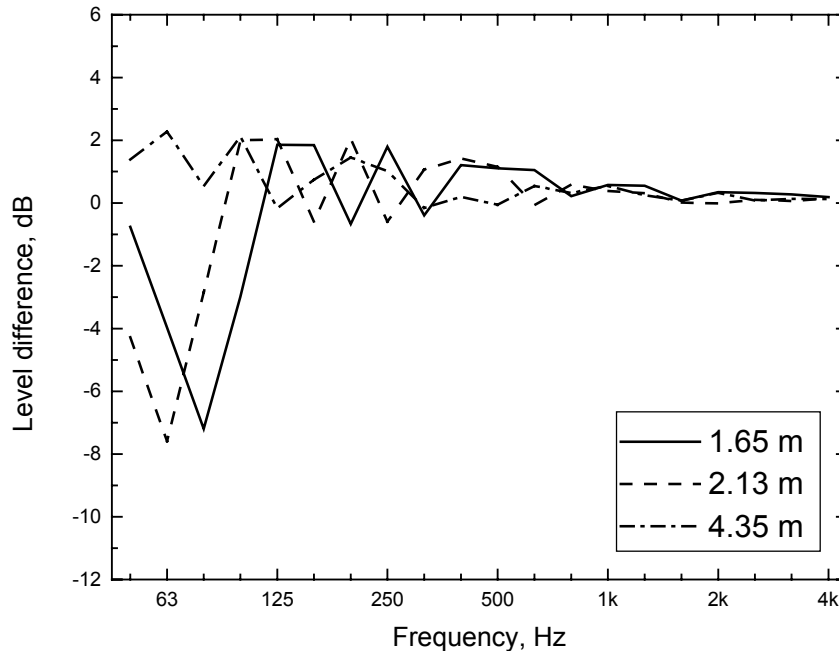


Figure AIII-5. Comparison of summed relative levels over complete passbys for a varied receiver height located 240 m from the flight track with an absorbing ground surface. The source included the average aircraft directionality and was at a vertical elevation of 55 degrees.

Increasing the receiver height from 1.65 m to 2.13 m is seen to shift the interference minimum from 80 to 63 Hz. However, when the receiver is moved to 4.35 m, representative of a second floor façade, the interference minimum has presumably shifted to a very low frequency and there is very little overall effect of ground reflected sound. Thus while ground reflections may reduce the incident low frequency sound energy at first floor façades, the effect of ground reflections is very small at higher floors.

The vertical height of the source and the distance from the receiver to the flight track both affect the calculated results as illustrated in Figures AIII-6 and AIII-7. In Figure AIII-6 for a receiver 240 m from the flight track, the 55 degree vertical elevation of the source leads to an interference minimum at 80 Hz. This is the average vertical angle of aircraft measured at the OATS and this calculated result is in reasonable agreement with estimates of the effect of ground reflections in Section 3.1.2. The frequency of the interference minimum is seen to systematically shift with variations in the vertical angle of the source.

Similar variations in the frequency of the interference minima are seen for the results in Figure AIII-7 where the receiver was 480 m from the flight track. However, for these results, the depth of the minimum is much greater. As was illustrated in Figure AIII-2, the greater distance to the flight track spreads out the interference pattern and leads to the greater overall reductions seen in Figure AIII-7.

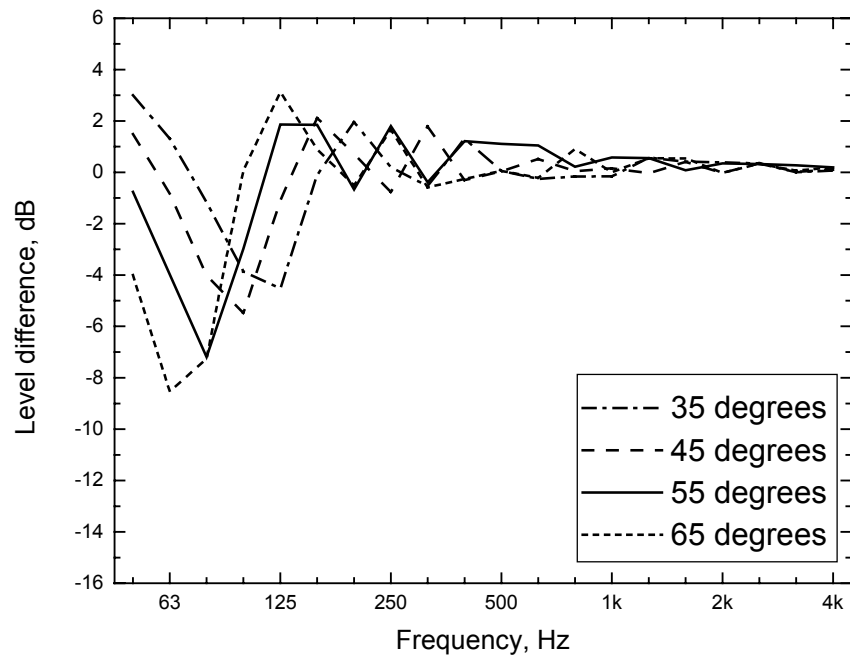


Figure AIII-6. Comparison of summed relative levels over complete passbys for varied vertical angle of the aircraft source. The receiver was 1.65 m above ground and located 240 m from the flight track with an absorbing ground surface. The source included the average aircraft directionality.

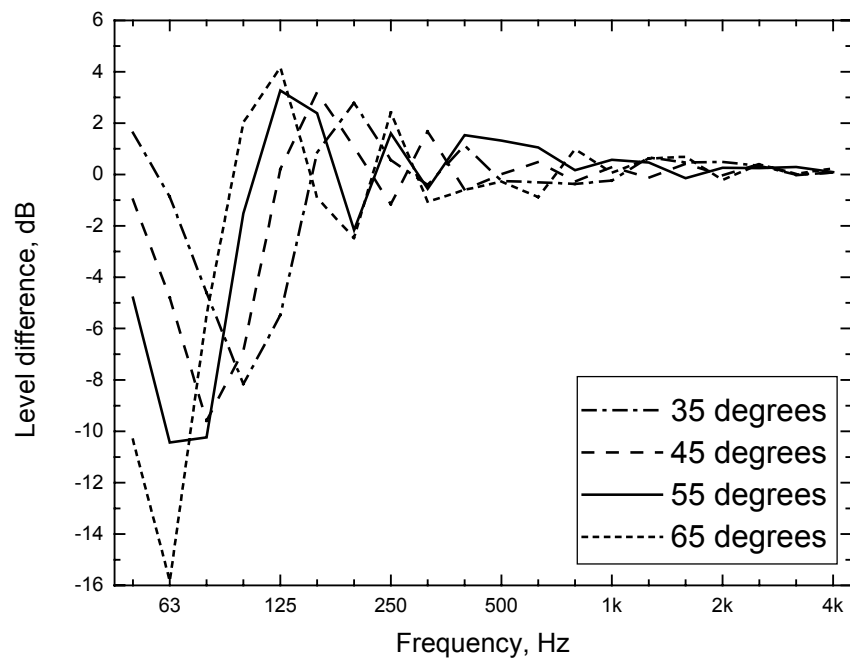


Figure AIII-7. Comparison of summed relative levels over complete passbys for varied vertical angle of the aircraft source. The receiver was 1.65 m above ground and located 480 m from the flight track with an absorbing ground surface. The source included the average aircraft directionality.

These calculations can only approximate actual measurement conditions. However, they are thought to correctly illustrate the effects of the key parameters. Differences between these calculations and measurement results would occur due to, differences in the directionality of particular aircraft and due differences in the reflecting properties of the actual ground surface. The calculations assumed simple coherent combinations of the direct and ground reflected sounds. In reality turbulence in the atmosphere causes random variations in the phase of the two sounds that will vary with frequency and with the distance to the sound source. It would also presumably vary from day to day according to weather conditions. Such turbulence could reduce the magnitude of the various interference effects but it is difficult to estimate how large these reductions would be.